UNIVERSITY OF PÉCS

Biological Doctoral School

Characterization of the Vestibular NADPH Oxidase Enzyme Complex

PhD Thesis

PÉTER KISS

PÉCS, 2009

UNIVERSITY OF PÉCS

Biological Doctoral School

Characterization of the Vestibular NADPH Oxidase Enzyme Complex

PhD Thesis

PÉTER KISS

Supervisors:
Dr. Joseph Zabner M.D.
Dr. Kerepesi Ildikó, PhD

PÉCS, 2009

1. Table of Contents

2. Glossary and Abbreviations

AD	Activation domain
ABR	Auditory-evoked brainstem responses
AIR	Autoinhibitory region
BAC	Bacterial artificial clone
CBA	Chicken β-actin promoter
cDNA	Complementary deoxyribonucleic acid
CSF	Cerebrospinal fluid
CGD	Chronic granulomatous disease
cM	Centi Morgan
CMV	Cytomegalovirus
COOH	Carboxyl group
CYBA	Cytochrome b558 subunit alpha
CYBB	Cytochrome b558 subunit beta
CYPs	Cytochrome P-450 enzymes
DUOXA1 and DUOXA2	DOUX maturation factors 1 and 2
DUOX	Dual Oxidase
EBV	Epstein-Barr virus
ED	Embryonic day
EDS	Energy Dispersive Spectroscopy
EPO	Eosinophil peroxidase
EST	Expressed Sequence Tag
FAD/FMN	Flavin adenine dinucleotide/ Flavin mononucleotide
GFP	Green fluorescence protein
Gfer	Growth factor erv1-like
hslt	Head slant
HPLC	High performance liquid chromatography
IgG	Immunoglobulin G
kDa	Kilo daltons
LPO	Lactoperoxidase
Mox-1	Mitogenic oxidase 1
mRNA	Messenger ribonucleic acid
MPO	Myeloperoxidase
NOS	Nitric oxide synthase
NOX	NADPH oxidase
NOH-1	NADPH oxidase homologue 1
NOXA1	NOX Activator 1

NOXO1	NOX Organizer 1
PAC	P1 artificial clone
PHOX	Phagocyte NADPH oxidase
PMA	Phorbol 12-myristate 13-acetate
PX	Phox domains
PB1	Phox and Bem1 domain
PCR	Polymerase chain reaction
P	Postnatal day
PRR	Proline-rich region
PKC	Protein Kinase C
RNS	Reactive nitrogen species
ROS	Reactive oxygen species
RSS	Reactive sulfur species
SDS-PAGE	Sodium dodecyl sulfate polyacrylamide gel electrophoresis
sPLA2	Secretory phospholipase A2
SH3	Src homology 3 domain
SOD	Superoxide dismutase
TPO	Thyroid peroxidase
TPR	Tetratricopeptide repeat
Tbl3	Transducin (beta)-like 3
XPS	X-ray photoelectron spectroscopy

3. Introduction

3.1 Reactive oxygen species

3.1.1 Reactive oxygen species in biology

The presence of reactive oxygen species (ROS) in biological materials was discovered more than 50 years ago [1]. Soon thereafter, Denham Harman hypothesized that oxygen radicals can be formed as by-products of enzymatic reactions in vivo. In 1956, he described free radicals as a Pandora's box of evils that may account for gross cellular damage, mutagenesis, cancer, and, last but not least, the degenerative process of biological aging [2, 3]. ROS have historically been viewed as a harmful but unavoidable consequence of an aerobic lifestyle. Considerable interest in ROS comes from related pathologies including atherosclerosis, hypertension, ischemia-reperfusion injury, inflammation, cystic fibrosis, cancer, type-2 diabetes, Parkinson's disease, Alzheimer's disease, and other neurodegenerative diseases. Defining the aspect of aging lies in the progressive vicious cycle in which oxidative stress plays a major role. Oxidative stress arises from a significant increase in concentrations of ROS and reactive nitrogen species (RNS) to the level that is toxic to biomolecules, including DNA, proteins, and lipids. Oxidative stress can be viewed as an imbalance of normal "ROS/RNS homeostasis" leading to the accumulation of oxidative damage in cell constituents. It can be called homeostasis, because certain types of ROS (such as H_2O_2) and RNS (particularly nitric oxide, •NO) are membrane permeable and diffusing species. These can be produced at non-harmful (optimum) levels under specific physiological conditions, thus playing physiological signaling roles. In a healthy cell, excessively harmful ROS/RNS are decomposed by protective antioxidant machinery, through detoxification reactions. Superoxide dismutase (SOD) and catalase are the two best known enzymes which can convert and neutralize $O_2•^-$ and H_2O_2, respectively. SOD can convert two superoxide anions into a molecule of hydrogen peroxide and one oxygen, while catalase catalyzes the

decomposition of hydrogen peroxide into water and oxygen. Glutathione-based systems, including glutathione S-transferase and the thioredoxin system, including peroxiredoxins, constitute the major redox buffer in the cytosol [4]. Small molecule antioxidants such as α-tocopherol (predominant form of Vitamin E) [5]; β-carotene, flavonoids, melatonin [6], and water-soluble ascorbic acid [7], uric acid and bilirubin in liver also belong to the major antioxidant defense of cells [4]. An important example of such regulation is apoptosis, which is a continuing process in the normal ontogenesis and life of organisms. Therefore, only excessive ROS or RNS production and/or decrease in detoxification mechanisms lead to oxidative stress and pathological conditions. The time scales of these processes are important. Elevated ROS (RNS) levels over short periods (less than minutes) can manage to initiate protein expression and other regulations, yet they cannot be completed within this short timing. Thus the functional responses, acting on detoxification as well as on the pro-oxidant side, require longer time, over a period of hours or days. On a time scale of years, modest but ongoing oxidative stress may play a significant role in aging. On the other hand, ROS/RNS are also involved in a variety of beneficial physiological events, such as host defense, synthesis of bioactive compounds, and signal transduction. The most relevant radicals in biological regulation are superoxide and nitric oxide. These radicals are formed by two groups of enzymes, the NAD(P)H oxidase (NOX) and Nitric oxide synthase (NOS) isoforms, respectively. Many regulatory effects are mediated by hydrogen peroxide and other ROS that are chemically derived from superoxide [8, 9].

Reactive oxygen species (ROS) include radical species (a free, i.e. unpaired, electron-containing species), such as primary superoxide ($O_2^{\bullet -}$, and its conjugated acid—hydroperoxyl radical, $HO_2^{\bullet}$), hydroxyl radical ($^{\bullet}OH$), carbonate radical $CO_3^{\bullet -}$, peroxyl radical ($RO_2^{\bullet}$), and alkoxyl radical ($RO^{\bullet}$). Also, some non-radical species are ascribed to ROS, namely hydrogen peroxide (H_2O_2), ozone (O_3), hypochlorus acid (HOCl), fatty acid hydroperoxides (FAOOH), reactive aldehydes, singlet oxygen ($^1O_2^*$) and other compounds. Similarly, RNS include radical species such as primary nitric oxide ($^{\bullet}NO$), nitrogen dioxide ($^{\bullet}NO_2$), as well as non-radical peroxynitrite

$OONO^-$ (and its conjugated acid HOONO, *N*-nitrosoamines, *S*-nitrosothiols, nitrosated fatty acids, and other compounds. Perhaps a group of reactive sulfur species (RSS) deserves its own definition as well. Those reactive oxygen species that are primarily produced by the NADPH oxidase enzyme family are listed below:

3.1.2 Reactive oxygen species produced by NADPH oxidases

3.1.2.1 Superoxide

Triplet oxygen ($^3O_2$) (oxygen molecule, whose outermost pair of electrons have parallel spins) can be transformed into a reactive state if it accepts a single electron. This process of accepting an electron is called reduction, and in this case, is "monovalent" reduction because only one electron is involved. The molecule that gave up the electron is oxidized. The result of monovalent reduction of triplet oxygen is called superoxide, abbreviated $O_2^{\bullet -}$. Superoxide is a radical. It is usually shown with a negative sign, indicating that it carries a negative charge of -1 (due to the extra electron, e-, it gained).

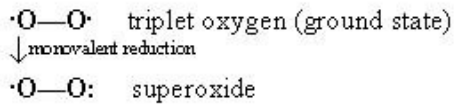

This reaction can also be written in this form:

$$^3O_2 + 1e^- \rightarrow \mathbf{O_2^{\bullet -}} \qquad (\textbf{Superoxide})$$

Superoxide can act both as an oxidant (by accepting electrons) or as a reductant (by donating electrons). However, superoxide is not particularly reactive in biological systems and does not by itself cause much oxidative damage. It is a precursor to other oxidizing agents, including singlet oxygen, peroxynitrite, and other highly reactive molecules. However, superoxide is not all distructive for the host, in fact it is necessary for health. For example, certain cells in the human body produce superoxide (and the reactive molecules derived from it) as an antibiotic "weapon" used to kill invading

microorganisms [10]. Superoxide also acts as a signaling molecule needed to regulate cellular processes [8].

Under biological conditions, the main reaction of superoxide is to react with itself to produce hydrogen peroxide and oxygen, a reaction known as "dismutation". Superoxide dismutation can be spontaneous, or catalyzed by the enzyme superoxide dismutase ("SOD").

$2\ O_2{\bullet}^- + 2H^+ \rightarrow \mathbf{H_2O_2} + {}^3O_2$ (**Hydrogen Peroxide**)

Superoxide is also important in the production of highly reactive hydroxyl radical (HO•). In this process, superoxide actually acts as a reducing agent, not as an oxidizing agent. This is because superoxide donates one electron to reduce the metal ions (ferric iron or Fe^{3+} in the example below) that act as the catalyst to convert hydrogen peroxide (H_2O_2) into the hydroxyl radical (HO•).

$O_2{\bullet}^- + Fe^{3+} \rightarrow {}^3O_2 + \mathbf{Fe^{2+}}$ (**Ferrous iron)**

The reduced metal (ferrous iron or Fe^{2+} in this example) then catalyzes the breaking of the oxygen-oxygen bond of hydrogen peroxide to produce a hydroxyl radical (HO•) and a hydroxide ion (HO^-):

$Fe^{2+} + H_2O_2 \rightarrow Fe^{3+} + OH^- + \mathbf{{\bullet}OH}$ (**Hydroxyl Radical**)

Superoxide can react with the hydroxyl radical (HO•) to form singlet oxygen ($^1O_2$*) (not a radical but reactive nonetheless):

$O_2{\bullet}^- + {\bullet}OH \rightarrow \mathbf{{}^1O_2{*}} + OH^-$ **(Singlet oxygen**)

Superoxide can also react with nitric oxide (NO•) (also a radical) to produce peroxynitrite ($OONO^-$), another highly reactive oxidizing molecule.

$O_2{\bullet}^- + NO{\bullet} \rightarrow \mathbf{OONO^-}$ **(Peroxynitrite**)

3.1.2.2 Hydrogen peroxide

Superoxide ($O_2{\bullet}^-$) can undergo monovalent reduction to produce **peroxide** (O_2^{2-}), an activated form of oxygen that carries a negative charge of -2. Usually peroxide is termed "hydrogen peroxide" (H_2O_2) since in biological

systems the negative charge of -2 is neutralized by two protons (two hydrogen atoms, each with a positive charge).

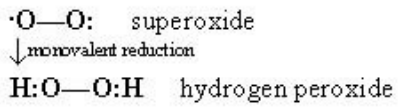

Hydrogen peroxide is important in biological systems because it can pass readily through cell membranes and cannot be excluded from cells. Hydrogen peroxide is actually necessary for the function of many enzymes, and thus is required (like oxygen itself) for health. One striking example is its role in neutrophils; the enzyme myeloperoxidase, which catalyzes the reaction of hydrogen peroxide (made from superoxide anions) with chloride ions to produce the strongly antiseptic hypochlorite ion (OCl^-)

$H_2O_2 + Cl^- \rightarrow$ **HOCl** + OH **(Hypochlorus acid)**

$HOCl \rightarrow H^+ +$ **OCl^-** **(Hypochlorite ion)**

Hydrogen peroxide is not as reactive as a product it can form, the hydroxyl radical. Hydrogen peroxide, in the presence of metal ions, is converted to a hydroxyl radical (HO•) and a hydroxide ion (HO^-). The metal ion is required for the breaking of the oxygen-oxygen bond of peroxide. This reaction is called the **Fenton reaction**:

$Fe^{2+} + H_2O_2 \rightarrow Fe^{3+} + OH +$ **•OH** **(Hydroxyl Radical)**

3.1.2 The source of free radicals

There are both endogenous and exogenous sources of free radicals (Table 1). The formation of ROS is a normal consequence of endogenous essential biochemical reactions. The endogenous free radicals include those that are produced and act intracellular, as well as those that are generated within the cell and released to the surrounding area [11-13] .They are derived from normal cellular metabolism and oxidative burst produced, for example, when phagocytic cells destroy invading microorganisms such as bacteria and viruses [13]. Some of the reactions include the auto-oxidation and consequent inactivation of small molecules, such as reduced flavins and thiols. Other reactions involve the activity of certain oxidases, cyclooxygenases, lipoxygenases, dehydrogenases, and peroxidases. Oxidases, and the electron transport chain that is coupled to oxidative phosphorylation, are primary and continuous sources of ROS. As shown in (Table 1), the sites of generation of these toxic molecules encompass all cellular constituents, including the plasma membrane, mitochondria, lysosomes, peroxisomes, nucleus, endoplasmic reticulum, and other sites within the cytosol. The exogenous sources of free radicals include tobacco smoke, air pollutants, organic solvents, anesthetics, pesticides, radiation, and high oxygen environment (Table 1). Under normal circumstances, there is a good balance between the generation of ROS and the antioxidant defense systems that destroy them. When increased ROS levels are present in the face of a deficiency of antioxidant substances in the body, the situation is referred to as oxidative stress, which has been associated with increase in age, [12, 14] and various chronic diseases.

Table 1. Sources of Reactive Oxygen Species

Endogenous (Cellular Sites)	Exogenous
Mitochondria Endoplasmic reticulum Peroxisomes Membrane lipid bilayers Lysosomes Specific enzymes (I.e. NADPH oxidases, NO synthase)	Tobacco smoke Industrial pollutants Pesticides Drugs Radiation High oxygen environment Anesthetics Organic solvents

3.1.2.1 Endogenous free radicals

3.1.2.1.1 Mitochondrial sources of free radicals

The classic textbook sentence declares the mitochondria as the major ROS source. It can indeed be valid in tissues in which mitochondria represent a substantial mass percentage of the cell, such as in heart or brain. Mitochondrial electron transport generates superoxide ($O_2^{\bullet -}$) as an inevitable by-product and primary ROS [15-18].

Reactive oxygen species (ROS) production can occur in low (physiological) oxygen concentration and in hypoxia. An apparent paradox exists in ROS production during ischemia. Whereas in heart, lung, and skeletal muscle, or even in aging, mitochondria increase their ROS production; while in other tissues, e.g. in neurons, the production is suppressed [19]. The explanation of ROS elevation under hypoxia seems to be less trivial than their increase after reoxygenation. However, the principles, which could be applied, are unknown.

Another physiologically important, readily diffusing and freely permeable radical, •NO is formed not only by the three isoforms of nitric oxide synthase (NOS), but also by a specific form of mitochondrial NOS (mtNOS) in liver, brain, thymus, and heart [20]. Non-mitochondrial NOS are represented by the constitutively expressed neuronal NOS and endothelial NOS; as well as by inducible NOS, expressed during inflammation.

3.1.2.2 Extramitochondrial ROS sources

3.1.2.2.1 Cytochrome P-450 enzymes

Non-specific monooxygenases, cytochrome P-450 enzymes (CYPs), are membrane bound terminal oxidases present mainly in endoplasmic reticulum as components of a multi-enzyme system, which also includes FAD/FMN-containing NADPH-cytochrome P450 reductase and cytochrome *b*5. Various enzymes of a large CYP superfamily, encompassing more than 30 genes [21], provide substrate oxidation reactions (oxidation, peroxidation, and/or reduction in O_2 and NADPH-dependent manner) of a structurally diverse

group of xenobiotics and endogenous substances, including cholesterol, steroids, arachidonic acid, converting the latter to biologically active eicosanoids.

Active CYPs produce ROS, namely $O_2\bullet^-$ and H_2O_2. CYPs must be considered as a significant ROS source and source of intracellular signals, not only via participation in metabolic pathways, but also via ROS-mediated signaling.

3.1.2.2.2 Peroxisomes

Peroxisomes can produce ROS internally, but their primary function is to consume cytosolic H_2O_2 and play an important antioxidant role. In liver 20% of total O_2 consumption is accounted for by peroxisomal oxidase activity and ~35% H_2O_2- production [22]. A net source of ROS, for example in liver, is the difference between the H_2O_2 synthesized and concurrently degraded by catalase and the glutathione peroxidases family enzymes. Excessive •OH produced by Fenton reaction is able to initiate lipid peroxidation of peroxisomal membrane, resulting in its disintegration and release of peroxisomal content into the cytosol.

3.1.2.2.3 NADPH oxidases

The major extramitochondrial ROS source is represented by the “oxidative burst” of activated inflammatory cells, macrophages and neutrophils [23] or endothelial cells [24]. The phagocyte NADPH oxidase was the first identified example of a system that generates ROS not as a byproduct but as its primary product. The discovery of other members of the NOX family demonstrated that enzymes with primary function of ROS generation are not limited to phagocytes. In fact, ROS-generating enzymes are found in virtually every tissue.

3.2 The NADPH oxidase enzyme family

3.2.1 Historical overview of ROS-generating NADPH oxidases

The first identified and best-studied NOX enzyme is $gp91^{phox}$, which also designated NOX2. $gp91^{phox}$ is the catalytic component of a multi-subunit enzyme complex, the phagocyte NADPH oxidase (PHOX). In the last several decades, the research of PHOX has spectacularly combined and intimately linked clinical research with biochemical and molecular biological studies.

In 1933 Baldridge and Gerrard described an "extra respiration of phagocytes" meaning large increase of oxygen consumption of the cells when phagocytosing bacteria [25]. However, it was also demonstrated later that the "respiratory burst" of phagocytes was not due to an increased mitochondrial metabolism, since cyanide and azide did not have any effect on it [26]. It was subsequently found to be essential for the efficient killing of microbes that were adequately engulfed, but not killed, in the absence of oxygen [27] (Figure 1).

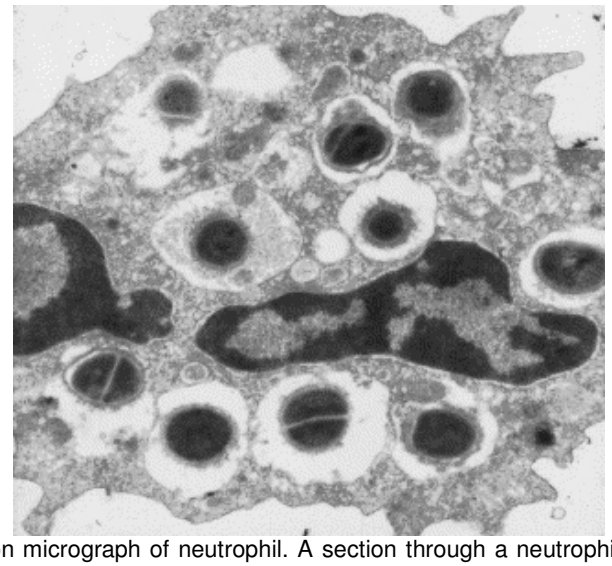

Figure 1. Electron micrograph of neutrophil. A section through a neutrophil (about 10 μm in diameter) containing 10 S. aureus within phagocytic vacuoles taken after about 30 seconds after mixing the cells and bacteria. Granules can be seen in the cytoplasm and degranulating into the vacuoles in which granule contents can also be seen. (Cross A.R., Segal, A.W. Biochim Biophys Acta. 2004;1657(1):1-22. [30])

In 1957 Brendes et al. recognized a new and relatively rare syndrome in young boys who suffered from recurrent, pyogenic infections that was accompanied with granulomatous reaction, lymphadenopathy, and hypergammaglobulinemia [28]. It was called “fatal chronic granulomatous disease of childhood” because it led to the death of young patients. As therapy evolved [29], the name shortened to chronic granulomatous disease (CGD). For a long time, observations of Bridges et al. were not linked to another milestone discovery in the PHOX field: Until 1967 when Baehner and Nathan recognized that the “respiratory burst” was absent in the phagocytes of CGD patients [30].

In 1973, Babior et al. [31] reported that the initial product of the respiratory burst oxidase was superoxide and not hydrogen peroxide. Mills et al. showed that phagocytes from CGD patients have diminished bactericidal capacity, although many functions of the phagocyte were functional and showed normal chemotaxis, phagocytosis, and degranulation [32].

The identification of the oxidase, the source of ROS production in phagocytes, was proven to be extremely difficult; mainly because of its instability, particularly its exquisite sensitivity to salts, which prevented most chromatographic separations [33]. Segal et al. demonstrated that a b-type cytochrome was missing in the leukocytes of CGD patients with X chromosome linked disease that is the most common form of CGD [34, 35], and named cytochrome b_{558} based on its absorbance near 558 nm. Eventually, with the help of molecular biology techniques and X-linked CGD cases the catalytic subunit of the phagocyte NADPH oxidase was identified by Royer-Pokora and colleagues [36]. The $gp91^{phox}$ gene was identified using positional cloning method [36, 37]. Later, Teahan at al. completed the cloning of the N-terminus where 43 amino acids were missing from the first clone.

Soon, it became clear that $gp91^{phox}$ was not the only component of cytochrome b_{558}. A 22 kDa protein ($p22^{phox}$) was co-purified with $gp91^{phox}$, and both subunits were shown to be missing in X-linked CGD patents [38, 39] indicating, that $p22^{phox}$ is unstable in the absence of $gp91^{phox}$. The smaller and larger proteins were then called the α and β subunits, respectively, and subsequently $p22^{phox}$ and $gp91^{phox}$ [40-42] The genes of $p22^{phox}$ and $gp91^{phox}$ were named *CYBA* and *CYBB,* respectively, as they encode the α and the β

subunits of cytochrome b558. After identification of $p22^{phox}$, CGD patients with mutations in *CYBA/$p22^{phox}$* (chromosome 16) were rapidly identified [43, 44].

The demonstration that flavocytochrome was absent in only two-thirds of CGD patients led to the identification of other forms of the disease [45] that were inherited in an autosomal recessive manner. Most patients with the autosomal pattern of inheritance of CGD usually posses a normal flavocytochrome b558 and $p22^{phox}$, indicating that other component or components of the PHOX system were missing. The development of new methods made possible the identification of the unknown components of PHOX [46-48]. The $p67^{phox}$ and $p47^{phox}$ phosphoproteins were shown to be missing in most cases of autosomal recessive CGD, and were named after their molecular mass (67 kDa and 47 kDa, respectively) [49-52]. Two, small GTP-binding proteins were also shown to be involved in the regulation of PHOX activity Rac1 and Rac2 [53-57]. Although, Rac2 is the predominant form in human neutrophils, the Rac isotype involved in PHOX activation can be either Rac1 or Rac2 depending on the cell type and species [58]).

In 1993, Wientjes et al. described a third, PHOX-specific cytosolic subunit, $p40^{phox}$ [59, 60]. It is strongly homologous with $p47^{phox}$, and also regulates the activity of the oxidase. *In vitro*, in the absence of $p47^{phox}$, $p40^{phox}$ could elicit a small amount of oxidase activity (~5%), possibly by increasing the affinity of $p67^{phox}$ and/or Rac2 binding to flavocytochrome b558 [61]. However, CGD patients with $p40^{phox}$ deficiency have not been described.

In parallel, some reports suggested that other cell types than phagocytes and B-lymphocytes, such as fibroblasts, that do not express $gp91^{phox}$, also produce superoxide. The use of inhibitors indicated that the actual source might be via a PHOX-like system. However, the molecular identity of the oxidase(s) in question remained obscure. That was fundamentally changed by the Human Genome Project. At the end of 1990s', the Project sequenced and made available sequences encoding portions of new $gp91^{phox}$ homologues. In 1999, a $gp91^{phox}$ homologue was recognized by two groups and the corresponding cDNA sequences were cloned [62, 63]. The novel oxidase was first entitled Mitogenic oxidase 1 (Mox-1)[62] or NADPH oxidase homologue 1 (NOH-1)[63]. Latter, the name of agreement became NADPH oxidase 1 (NOX1), and $gp91^{phox}$ got NOX2 as an alias

(approved by the HUGO Nomenclature Committee). The identification of NOX1 was quickly followed by the cloning of NOX3 [64-66], NOX4 [67, 68], and NOX5 [69]. The discovery of the two DUOX (Dual Oxidase) proteins (originally called thyroid oxidase) depended less on the Human Genome Project. Two groups using different methods identified them from thyroid gland. Purification and partial sequencing of the DUOX2 enzyme was followed by RACE polymerase chain reaction (PCR) [70] or low temperature hybridization of a thyroid cDNA phage library with a $gp91^{phox}$ probe [70, 71].

The identification of the NOX/DUOX proteins did always allow an immediate demonstration of their biochemical function. Indeed, the closest $gp91^{phox}$ homologues are either inactive (e.g. NOX1) or produce minimal amount of superoxide (e.g. NOX3) when transfected alone in various cell types. In order to verify superoxide production by NOX1 and NOX3, these proteins had to be in the presence of $p22^{phox}$, $p47^{phox}$ and $p67^{phox}$. As the latter two subunits are restricted mainly to phagocytes, an intensive search for their homologues led to the cloning of a $p47^{phox}$ homologue NOXO1 (NOX Organizer 1), and a $p67^{phox}$ homologue NOXA1 (NOX Activator 1). *In vitro,* these proteins can activate both NOX1 and NOX3 [72-75]. Similarly, heterologous expression of DUOX enzymes is only successfully achieved since the identification of the DOUX maturation factors 1 and 2 (DUOXA1 and DUOXA2, respectively) [76].

3.2.2 Nox family enzymes in mammals

The NOX family NADPH oxidases are proteins that transfer electrons across biological membranes. In general, the electron acceptor is oxygen and the product of the electron transfer reaction is superoxide. The biological function of NOX enzymes is therefore the generation of reactive oxygen species. NOX proteins are found in virtually every tissue; however, different members have differing tissue distribution, suggesting distinct physiological functions. Table 2. summarizes the tissue distribution of the NADPH oxidase family members.

Table 2. Tissue distribution of NOX enzymes in human

	High-Level Expression	Intermediate- to Low-Level Expression
NOX1	Colon	Smooth muscle, endothelium, uterus, placenta, prostate, osteoclasts, retinal pericytes
NOX2	Phagocytes	B lymphocytes, neurons, cardiomyocytes, skeletal muscle, hepatocytes, endothelium, hematopoietic stem cells, smooth muscle
NOX3	Inner ear	Fetal kidney, fetal spleen, skull bone, brain
NOX4	Kidney, blood vessels	Osteoclasts, endothelium, smooth muscle, hematopoietic stem cells, fibroblasts, keratinocytes, melanoma cells, neurons
NOX5	Lymphoid tissue, testis	Endothelium, smooth muscle, pancreas, placenta, ovary, uterus, stomach, various fetal tissues
DUOX1	Thyroid	Airway epithelia, tongue epithelium, cerebellum, testis
DUOX2	Thyroid	Salivary and rectal glands, gastrointestinal epithelia, airway epithelia, uterus, gall bladder, pancreatic islets

We presently know seven members of the NOX family in mammals: NOX1, NOX2, NOX3, NOX4, NOX5, DUOX1, and DUOX2. Human express all seven NOX family NADPH oxidases [9, 77]. Figure 2. shows the relationship between NOX family members in human.

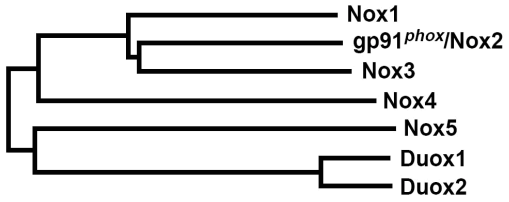

Figure 2. Phylogenetic tree of human NOX family oxidases. The phylogenetic tree constructed on the basis of the gp91phox-related domains of human NOX1–5 and DUOX1-2.

In accordance with this preserved function, there are conserved structural properties of NOX enzymes that are common to all family members. Starting from the COOH terminus, these conserved structural features include *1*) an NADPH-binding site at the very end of the COOH terminus, *2*) a FAD-binding region in proximity of the most COOH-terminal transmembrane domain, *3*) six

conserved transmembrane domains, and *4*) four highly conserved heme-binding histidines, two in the third and two in the fifth transmembrane domain in the NOXs (Figure 3).

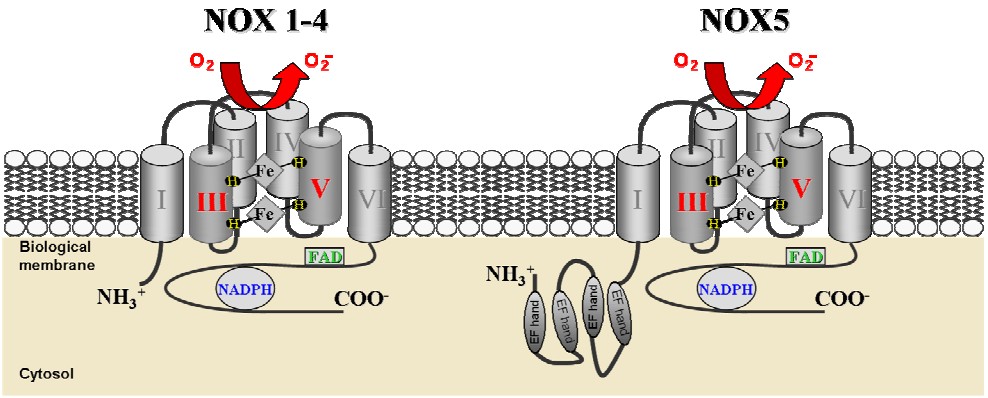

Figure 3. Proposed structure of the core region of NADPH oxidase 1-5 enzymes.

Given the additional NH2-terminal transmembrane domain, the histidines are in the fourth and sixth transmembrane domains in DUOX proteins (Figure 4). There are additional features, such as EF hands in NOX5 and DUOXs; while an additional N-terminal transmembrane domain and a peroxidase homology domain are limited to DUOXs.

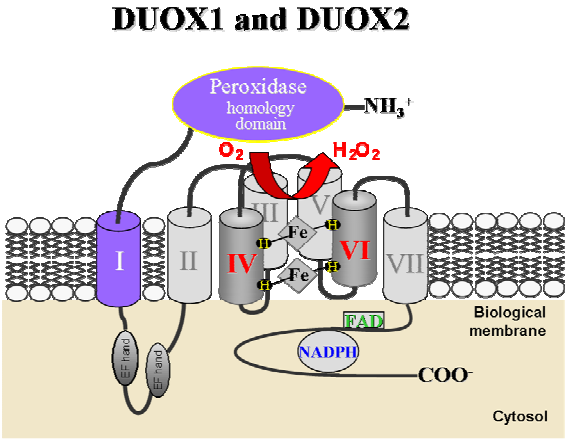

Figure 4. Proposed structure of the core region of Dual oxidase 1 and 2 enzymes.

As opposed to the conserved elements of electron transport, it appears now that activation mechanisms of NOX/DUOX enzymes are quite divergent.

2.2.2.1 NOX2, also known as gp91^{phox}, is the historical prototype of NADPH oxidases. Here I focus on the properties of NOX2 that allow a better understanding of other NOX isoforms, particularly of NOX3.

No crystal structure of gp91^{phox} is available yet, nevertheless, the transmembrane topology of gp91^{phox} is well studied and understood. NOX2 has six transmembrane domains and its COOH terminus and NH_2 terminus are facing the cytoplasm (Figure 3).

NOX2 is a heavily glycosylated protein in humans, which appears as a broad smear on SDS-PAGE (~85-100 kDa) reflecting the heterogeneity of glycosylation of the N-linked glycoprotein with a 65 kDa protein core [78].

NOX2 maturation is tightly correlated with heterodimerization of gp91^{phox} and p22^{phox} during flavocytochrome b biosynthesis (Figure 5) [79, 80]. During synthesis of flavocytochrome b558, heme insertion into NOX2 is required before heterodimer formation, which in turn precedes glycosylation. Although the human neutrophil flavocytochrome b558 is heavily glycosylated, this appears to vary among phagocytes and among species. For example in mouse, NOX2 has a molecular mass very close to the calculated one of the polypeptide chain (65.3 kDa) due to absent or minimal glycosylation. Glycosylation is not a requirement for NOX2 catalytic function *in vitro* [81].

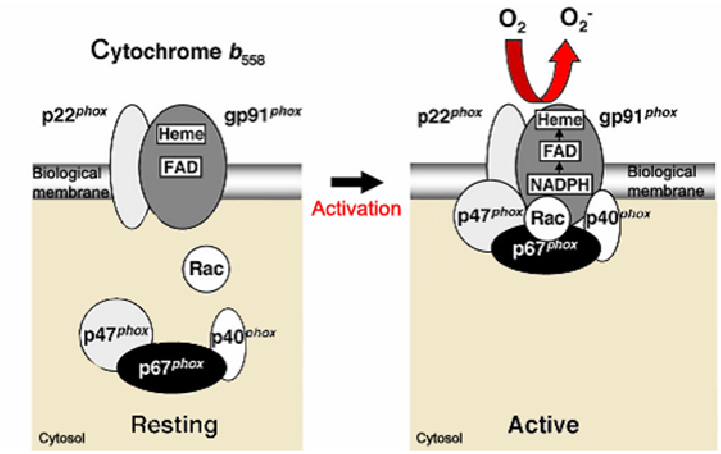

Figure 5. Schematic representation of the formation of fully assembled and active phagocyte NADPH oxidase gp91^{phox}/NOX2 complex.

The activation of NOX2 occurs through a complex series of protein/protein interactions (Figure 6A) [79, 80, 82-84]. NOX2 constitutively associates with $p22^{phox}$ and is unstable in the absence of $p22^{phox}$. Indeed, phagocytes from $p22^{phox}$-deficient patients have no detectable NOX2 protein [43, 44, 85]. Activation of NOX2 requires translocation of cytosolic factors to the NOX2/$p22^{phox}$ complex (Figure 5). Phosphorylation of $p47^{phox}$ leads to a conformational change allowing its interaction with $p22^{phox}$ [82, 86]. The binding of $p47^{phox}$ to $p22^{phox}$ is thought to organize the translocation of other cytosolic factors, hence its designation as "organizer subunit." The localization of $p47^{phox}$ to the membrane brings the "activator subunit" $p67^{phox}$ into contact with NOX2 [87] and also brings the small subunit $p40^{phox}$ to the complex. Finally, the small GTPase Rac interacts with NOX2 [88] and $p67^{phox}$ [89, 90]. Once assembled, the complex is active and generates superoxide by transferring an electron from NADPH in the cytosol to oxygen on the luminal or extracellular space.

NOX2 can be regarded as a transmembrane redox chain that connects the electron donor (Figure 3), NADPH on the cytosolic side of the membrane with the electron acceptor, oxygen on the outer side of the membrane [91, 92]. In the first step, electrons are transferred from NADPH to FAD, a process that is regulated by the activation domain (AD) of $p67^{phox}$ [93]. NOX2 is selective for NADPH over NADH as a substrate, with *K*m values of 40–45 μM versus 2.5 mM, respectively [94]. In the second step, a single electron is transferred from the reduced flavin $FADH_2$ to the iron center of the inner heme. Since the iron of the heme can only accept one electron, the inner heme must donate its electron to the outer heme before the second electron can be accepted from the now partially reduced flavin, FADH. The force for the transfer of the second electron, while smaller (31 vs. 79 mV), is still energetically favorable. However, the transfer of the electron from the inner heme to the outer heme is actually against the electromotive force between these two groups. To create an energetically favorable state, oxygen must be bound to the outer heme to accept the electron [10, 91, 95]. NOX2 was first described in neutrophils and macrophages and is often referred to as the phagocyte NADPH oxidase. NOX2 is still widely considered to have a very limited, essentially phagocyte-specific tissue expression (e.g., Ref. [84]), however, there is increasing

evidence at both the message and the protein level for expression of NOX2 in nonphagocytic cells, including neurons [96], cardiomyocytes [97], skeletal muscle myocytes [98], hepatocytes [99], endothelial cells [100-102], and hematopoietic stem cells [103]. In phagocytes, NOX2 localizes to both intracellular and plasma membranes in close association with the membrane protein $p22^{phox}$ [104, 105]. In resting neutrophils, most of the NOX2 localizes to intracellular compartments, in particular secondary (i.e., specific) granules [104, 106, 107] and tertiary (i.e., gelatinase-containing) granules [108]. Upon phagocyte stimulation, there is a translocation of NOX2 to the surface as the granules fuse with the phagosomal or the plasma membrane [104, 109, 110]. This fusion is thought to be a key event for the microbicidal activity of NOX2. However, NOX2 can also be activated within the granules without a need for fusion with surface membranes [111, 112]. The resulting intracellular ROS generation might be involved in signaling functions of NOX2 [107].

2.2.2.2 NOX1 was the first recognized homolog of NOX2 [62, 63]. *NOX1* and *NOX2* genes appear to be the result of a relatively recent gene duplication, as the number and the length of the exons is virtually identical between the two genes [72]. Similarly, at the protein level, there is a high degree of sequence identity (~56%) between NOX1 and NOX2 [62, 63, 113, 114]. The human and mouse *NOX1* gene is located on the X chromosome. An alternatively spliced form of NOX1 lacks exon 11 [63, 115, 116]. The message for NOX1 is most highly expressed in colon epithelium [62, 72, 117] ; however, it is also expressed in a variety of other cell types, including vascular smooth muscle cells [62, 118], endothelial cells [119, 120], uterus [62, 63], placenta [121], prostate [62, 63], osteoclasts [122], retinal pericytes [123], as well as in several cell lines, such as the colon tumor cell lines CaCo-2 [124, 125], DLD-1 [125], and HT-29 [125], and the pulmonary epithelial cell line A549 [126]. Expression of NOX1 in the gastric mucosa is species dependent. It was not found in human [127] or mouse stomach, but is functionally expressed in guinea pig stomach pit cells and mucosal cells [128-130]. Within the colon, there is a gradient of NOX1 expression with levels being low in the proximal and high in the distal colon [117, 131]. However, at

this point, it is not clear whether this gradient is constitutive or secondary to bacterial colonization.

NOX1, similarly to NOX2, depends on cytosolic subunits for superoxide generation [72-75]. NOXO1 (NOX organizer 1) and NOXA1 (NOX activator 1) are homologues of the NOX2 subunits $p47^{phox}$ and $p67^{phox}$, respectively. In expression systems using the mouse proteins suggest a constitutive activity of the NOX1/NOXO1/NOXA1 system, studies using human proteins show only a weak constitutive activity, and full activation depends on activation through the Protein Kinase C (PKC) activator phorbol 12-myristate 13-acetate (PMA) [73, 74].

In addition to its dependence on cytosolic subunits, NOX1 requires the membrane subunit $p22^{phox}$ [132, 133]. The $p22^{phox}$ dependence of NOX1 might be less stringent than the one observed for NOX2 and NOX3 [84]. Also, there is evidence for an involvement of the small GTPase Rac in the regulation of NOX1 activity [74, 84, 133-137]. Rac binds to the TPR (tetratricopeptide repeat) domain of the activator subunit NOXA1 [74, 134, 137].

The physiological function of NOX1 is currently unknown. It is likely that depending on the cell type where Nox1 is expressed the enzyme can serve diverse functions. It might regulate blood pressure and play host defense role in the colon [9, 114].

2.2.2.3 NOX3 was described in 2000 based on its sequence similarity to other NOX isoforms [64], although the first studies on the function of the protein did not appear until 2004 [138, 139]. NOX3 shares ~58% amino acid identity with NOX2. The gene for human NOX3 is located on chromosome 6. Sequence alignment and hydropathy plot analysis predict the overall structure of NOX3 to be highly similar to that of NOX1 and NOX2, in terms of transmembrane domains, the length of the extracellular loops, NADPH- and FAD-binding sites, and the localization of the heme-coordinating histidines [64, 66]. To date, no splice variant of NOX3 has been reported.

Two groups independently showed that NOX3 is highly expressed in the inner ear. Characterization of the “head tilt” mutant mouse, which has vestibular

defects, revealed underlying mutations in the NOX3 gene [139]. Thus, a functional role of NOX3 in the inner ear was established. Based on an EST clone derived from the inner ear, another study performed detailed analysis of NOX3 distribution by real time PCR and in situ hybridization. These analysis showed very high NOX3 expression in the inner ear, including the cochlear and vestibular sensory epithelia and the spiral ganglion [138]. Low levels of NOX3 can also be detected in other tissues, including fetal spleen [64], fetal kidney [66, 138], skull bone, and brain [138].

In vitro, Nox3 activity is also enhanced in the presence of $p47^{phox}$ and $p67^{phox}$, Noxo1 and Noxa1, or Noxo1 alone [140], consistent with its close homology to both $gp91^{phox}$ and Nox1. However, the physiologically relevant partners of NOX3 have not been defined.

2.2.2.4 NOX4 was originally described as Renox which stands for renal oxidase, due to its abundant expression in the kidney [67, 68]. NOX4 is a 578 amino acid long protein with 39% homology to Nox2. In murine kidney, in situ hybridization experiments localized Nox4 mRNA expression to the renal cortex, where epithelial cells of proximal tubules showed high-level expression. Immunohistochemical studies also showed Nox4 expression in distal tubules of the human nephron [68]. Although glomeruli express relatively low Nox4 mRNA levels in comparison to other renal structures [67], Gorin et al. detected Nox4 mRNA in rat mesangial cells [141]. Nox4 mRNA was also found in many other tissues and cells including fetal liver, vascular endothelial cells, smooth muscle cells, murine osteoclasts, hematopoietic stem cells and adipocytes [67, 142-144].

The enzymatic activity of NOX4 was first demonstrated in experiments where Geiszt et al. detected constitutive superoxide production in Nox4-transfected NIH 3T3 fibroblasts [67]. There is little known about the regulatory factors affecting NOX4 activity. NOX4 forms a molecular complex with $p22^{phox}$ [132, 145] and the ROS production of Nox4- transfected cells is dependent on the expression of $p22^{phox}$. Known cytosolic proteins did not affect the enzymatic activity of NOX4 [145]; furthermore, co-expression of mutant $p22^{phox}$ that does not bind the known NOX organizers did not diminish NOX4 activity [133].

These observations suggest that the NOX4-p22^{phox} complex functions alone, but we cannot exclude the possibility of cooperation with some unknown endogenous proteins. Alterations in the expression level of the *Nox4* gene appear to provide an effective means for the regulation of NOX4-based ROS production. Hypoxia, for example, was shown to stimulate Nox4 expression in the murine kidney [146] and angiotensin II increased Nox4 mRNA level in A7r5 cells [147].

2.2.2.5 NOX5 was originally identified by Cheng et al. [66], who described a cDNA encoding a 565 amino acid protein. Other products of the *Nox5* gene have been identified (*Nox5α, β, γ,* and *δ*) which are larger proteins containing more than 700 amino acids [69]. Human NOX5 is abundantly expressed in T- and B-lymphocytes of spleen and lymph nodes, and in the sperm precursors of testis [69]; however, its biological role is presently unknown. Intriguingly, no orthologue for *Nox5* is found in the mouse and rat genomes. NOX5 resembles the basic structure of gp91^{phox} with the addition of an N-terminal extension that contains four Ca^{2+}-binding EF hands (Figure 3). Thus, NOX5 is activated by Ca^{2+} to produce superoxide. Cells which express NOX5 ectopically produce superoxide in response to the Ca^{2+}-ionophore ionomycin [69]; cell-free superoxide production by NOX5-containing membrane fractions is dependent on the presence of Ca^{2+} [148]. It has been suggested that the Ca^{2+}-binding domain of NOX5 N-terminus may function as a calmodulin-like activator module. The binding of Ca^{2+} causes conformational change, which leads to intramolecular interaction of the N-terminal calmodulin-like module with the C-terminal gp91^{phox}-like domain, resulting in activation of the NADPH oxidase [148]. NOX5 does not seem to form a functional complex with p22^{phox}, since knock down of p22^{phox} via RNAi does not affect the NOX5-dependent superoxide production under conditions where it abrogates the activity of Nox1–4 [133].

The fact that Nox5 is the first NADPH oxidase, which is primarily found in lymphoid tissues, would suggest a role for Nox5 in lymphocyte signaling. Interestingly, the *Nox5* gene is not present in the mouse genome, arguing against a general role in lymphocyte signaling [9, 114].

2.2.2.6 DUOX proteins were originally designated thyroid oxidases (thOX or tox), and cloned from human and porcine thyroid glands. They were proposed to serve in iodide organification during thyroxine synthesis [71, 149]. The DUOX (dual oxidase) nomenclature was suggested [150] as these proteins contain an N-terminal extracellular peroxidase-like domain and a $gp91^{phox}$-like oxidase portion [71].

The dual oxidases appear to have ancient origins, because closely related homologues have been identified in several invertebrate species, including nematodes, fruit flies, and sea urchins [150-152].

Human DUOX1 and DUOX2 proteins contain 1551 and 1548 amino acids, respectively, and show 83% sequence similarity. Additionally to the peroxidase-like domain and the NADPH oxidase portion, DUOXs have an additional transmembrane segment and two EF-hand motifs (Figure 4). The peroxidase-like domains of DUOX proteins are unusual in that they lack conserved histidine residues found in all other peroxidases, considered essential for heme binding [153]. The presence of EF-hands suggests that calcium directly regulates these enzymes, consistent with early observations showing that calcium ionophores stimulate H_2O_2 production in thyroid cells [154-157]. Among NOX/DUOX family members, elements of electron transport are largely preserved, therefore is unexpected that the mature DUOX enzymes release H_2O_2 without forming a detectable amount of $O_2^{\bullet -}$ [156].

Heterologous DUOX expression in several mammalian cell lines fails to reconstitute ROS release, suggesting other tissue-specific oxidase components are needed for DUOX activity [158]. When heterologously expressed, DUOX enzymes tend to be retained in the endoplasmic reticulum (ER) [159]. This observation led to the discovery of DUOX maturation factors, which are ER resident proteins termed DUOXA1 and DUOXA2 [76]. DUOX maturation factors seem to be crucial in overcoming ER retention of DUOX enzymes. DUOX enzymes do not require activator or organizer subunits; although, the $p22^{phox}$ requirement is still a matter of debate. DUOX enzymes coimmunoprecipitate with $p22^{phox}$ [160], but there is no evidence for enhanced DUOX function upon coexpression of $p22^{phox}$ [158-160]. Studies on the

activation of heterologously expressed DUOX2 in membrane fractions indicated that the enzyme 1.) does not require cytosolic activator or organizer subunits and 2.) can be directly activated by Ca^{2+}, suggesting that its EF-hand Ca^{2+}-binding domains are functional [159]. Studies using Clostridium difficile toxin B conclude that DUOX activation in thyrocytes does not require the small G-protein Rac [161]. A recent study found interaction of EF-hand binding protein 1 (EFP1) with DUOX1 and DUOX2, and it was suggested that this protein might be involved in the assembly of a multiprotein complex allowing ROS generation by DUOX enzymes [160].

Both DUOX1 and DUOX2 are highly expressed in the thyroid [71, 149]. In addition, DUOX1 has been described in airway epithelia [154, 162, 163] and in the prostate [160]). DUOX2 is found in the ducts of the salivary gland [154]; in rectal mucosa [154]; all along the gastrointestinal tract, including duodenum, colon, and cecum [164, 165]; in airway epithelia [162, 163]; and in prostate [160].

In the thyroid gland, Dual oxidases produce hydrogen peroxide, which is then utilized in the thyroperoxidasemediated oxidation of iodide into reactive compounds. Duox proteins are present in the apical poles of thyroid cells exposed to the colloid of hyroid follicles, where they colocalize with thyroperoxidase [71]. This localization is consistent with their suggested role in hormone biosynthesis. Both Duox isoforms are present in the thyroid [71, 149] but the reason of this apparent redundancy is currently unknown. The physiological role for DUOX2 in thyroid hormone biosynthesis was demonstrated by the identification of patients who have hypothyroidism due to mutations in the *Duox2* gene [166]. Dual oxidases might have a role in cellular signaling in host defense [9, 114].

3.2.3 Subunits and Regulatory Proteins

While NOX2 requires the assembly of at least five additional components for its activation, other NOX proteins vary in their requirements for these proteins. Table 3 summarizes all known NOX-family enzymes and their subunits[9].

Table 3. NOX enzymes and their subunits in human

	Other Names	Chromosome Location	Gene Length	Amino Acids
NOX1	NOH-1, MOX1, GP91-2	Xq22	30374	564
NOX2	CYBB, gp91^{phox}	Xp21.1	33451	570
NOX3	GP91-3	6q25.1-26	60534	568
NOX4	RENOX, KOX-1, KOX	11q14.2-q21	165139	578
NOX5		15q22.31	42392	747
DUOX1	Thox1, LNOX1, NOXEF1	15q21	35583	1,551
DUOX2	Thox2, LNOX2, NOXEF2, p138lox	15q15.3	20757	1,548
P22^{phox}	CYBA	16q24	9486	195
P47^{phox}	NOXO2, NCF1, NCF47K	7q11.23	15349	390
NOXO1	p41NOX	16p13.3	2522	370
P67^{phox}	NOXA2, NCF2	1q25	34845	526
NOXA1	p51NOX	9q34.3	11011	483
P40^{phox}	NCF4	22q1,3.1	17028	339
DUOXA1		15q21.1	12372	298
DUOXA2		15q15.1	3632	320

2.2.3.1 p22phox

Early attempts to purify the NADPH-dependent cytochrome *b* oxidase from neutrophils led to size estimates that ranged from 11 to 127 kDa [167, 168]. This discrepancy in size was partially explained by heterogeneous glycosylation; however, it soon became clear that the flavocytochrome *b*558 was actually a heterodimer consisting of NOX2 and p22^{phox} [169]. The gene for human p22^{phox} is located on chromosome 16. p22^{phox} is a membrane protein, which closely associates with NOX2 in a 1:1 ratio [105]. The membrane topology of p22^{phox} is difficult to predict based on hydropathy plots, and models have been proposed with two [170, 171], three [82, 91], and four transmembrane domains [172]. In the absence of crystallization data, there is

no consensus on this matter. However, the weight of evidence favors a two transmembrane structure with both the NH2 terminus and the COOH terminus facing the cytoplasm [171, 173, 174]. The mRNA for $p22^{phox}$ is widely expressed in both fetal and adult tissues [66] and in cell lines [175]. The expression of $p22^{phox}$ increases in response to angiotensin II [176], streptozotocin-induced diabetes [177], and hypertension [178]. $p22^{phox}$ has two major functions: *1*) binding to NOX proteins, leading to protein stabilization, and *2*) binding to organizer subunits. $p22^{phox}$ is thought to interact with NOX1 [74, 179], NOX2 [80, 175], NOX3 [133, 180], and NOX4 [132, 145]. The underlying concept is that NOX proteins and the $p22^{phox}$ protein are stable only as a heterodimer, while monomers are degraded by the proteosome [80]. The second function of $p22^{phox}$, namely, interaction with organizer subunits, is relevant only for NOX1, NOX2, and NOX3, but not for NOX4. The region of $p22^{phox}$ responsible for this interaction is the COOH terminus, which contains proline-rich regions (PRR) [170, 181], capable of interacting with Src homology 3 (SH3) domains of the organizer subunits $p47^{phox}$ or NOXO1. Truncation of $p22^{phox}$ or mutations within the COOH-terminal domain lead to a loss of activation of NOX1, NOX2, and NOX3 [133, 182]. In agreement with the concept that NOX4 activation does not involve cytosolic organizer subunits, truncations or mutations of the $p22^{phox}$ COOH terminus do not decrease NOX4 activity.

The importance of the $p22^{phox}$ subunit for the phagocyte NADPH oxidase was revealed with the identification of CGD patients with mutations in $p22^{phox}$ [43, 44]. However, given the good *in vitro* data on the role of $p22^{phox}$ for NOX1, NOX3, and NOX4, it is puzzling that the phenotype of these $p22^{phox}$ -deficient CGD patients did not show obvious differences from CGD patients with other underlying mutations. This may in part be due to the small number of cases, the young age of the patients, and the limited scope of the clinical examination performed in them. Thus, at this point, it is unclear whether $p22^{phox}$ is indispensable in vivo for the other NOX enzymes.

3.2.3.2 Organizer subunits: NOXO1, p47phox

Two NOX organizer subunits are $p47^{phox}$ [48, 49] and NOXO1[72, 73, 140] [74]. The genes for human $p47^{phox}$ and NOXO1 are located on chromosomes 7 and 16, respectively. The proteins NOXO1 and $p47^{phox}$ share ~25% sequence identity to one another and share a high degree of similarity in their functional domains (Figure 6A). The organizer role of $p47^{phox}$ and NOXO1 is also visible from the motifs found within the two proteins. NOXO1 and $p47^{phox}$ each have phox (PX) domains that interact with membrane phospholipids. Both also have two SH3 domains that interact with the proline-rich regions in the COOH terminal of $p22^{phox}$ [74, 170], and a COOH-terminally located proline- rich region allows interaction with $p67^{phox}$ or NOXA1. $p47^{phox}$ possesses an autoinhibitory region (AIR) that prevents this interaction until the protein is phosphorylated and undergoes a conformational change. A major difference between $p47^{phox}$ and NOXO1 is that AIR is absent in NOXO1, suggesting that NOXO1 is constitutively active. Finally, both NOXO1 and $p47^{phox}$ also contain a COOH-terminal proline-rich region that can interact with SH3 domains in NOXA1 and $p67^{phox}$, respectively [74, 183]. Patients lacking $p47^{phox}$ fail to translocate the activator subunit $p67^{phox}$, the small $p40^{phox}$ subunit, and the GTPase Rac2 to the membrane in neutrophils [184, 185] thus, resulting in CGD.

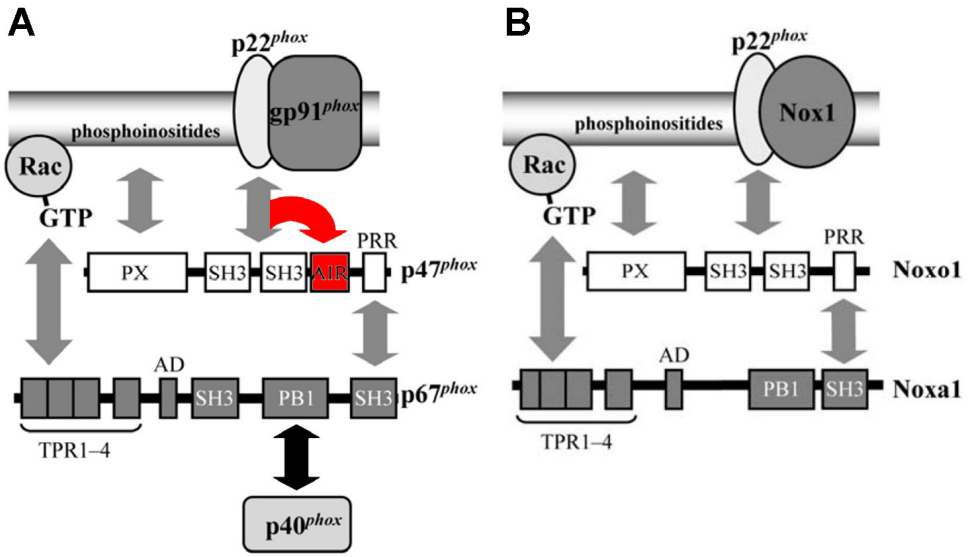

Figure 6. (A) Structure of the classical organizer p47phox and the classical activator p67phox, and interactions involved in activation of the phagocyte oxidase gp91phox. AD, activation domain; PRR, proline-rich region; AIR, autoinhibitory region; TPR, tetratricopeptide repeat.**(B)** Structure of the novel organizer Noxo1 and the novel activator Noxa1, and interactions involved in Nox1 activation. AD, activation domain; PRR, proline-rich region; TPR, tetratricopeptide repeat.

3.2.3.3 Activator subunits: NOXA1 and p67phox

The two activator subunits p67phox and NOXA1 were discovered in parallel with the respective organizer subunits. The human p67phox and NOXA1 genes are found on chromosomes 1 and 9, respectively. Although p67phox and NOXA1 share only ~28% amino acid identity, their overall domain structure is similar (Figure 6B). They are both cytoplasmic proteins and contain an NH2-terminal tetratricopeptide repeat (TPR) which interacts with Rac, a highly conserved activation domain (AD), a less conserved "Phox and Bem1" (PB1) domain, and a COOH-terminal SH3 domain.

The p67phox PB1 domain binds p40phox while NOXA1 fails to interact with p40phox [74]. The general view of NOX2 activation events is that p47phox phosphorylation leads to translocation of the p47phox/p67phox complex to the plasma membrane where p47phox interacts with p22phox, and p67phox subsequently acts as the NOX activator through a direct protein-protein interaction [83, 186]. In p47phox-deficient neutrophils p67phox does not

translocate to the membrane upon stimulation suggesting that the translocation of p67phox requires the presence of p47phox [185, 187, 188]. As NOXO1 constitutively associates with the membrane (see above and Ref. [75]), it is likely that NOXA1 is constitutively associated with membranes as well, although this has not been experimentally proven. Similarly, it is presently unknown whether NOXA1 can be phosphorylated. p67phox and NOXA1 interact through their COOH-terminal SH3 domain with the proline-rich region of p47phox and NOXO1 [74, 82, 189]. p67phox and, presumably, NOXA1 also interact directly with NOX proteins (NOX1 to NOX3) through their activation domain [72, 74, 87, 93, 113]. Thus, the overall structure and protein-protein interactions of the two homologous subunits are highly similar

3.2.3.4 p40phox

$p40^{phox}$ was detected by coimmunoprecipitation with $p47^{phox}$ and $p67^{phox}$ [59]. The human $p40^{phox}$ gene is located on chromosome 22. The structural domains of $p40^{phox}$ include an SH3 domain, a PX domain, and a PB1 domain. $p40^{phox}$ has been shown to interact with $p47^{phox}$ and $p67^{phox}$ with a 1:1:1 stoichiometry [190]. $p40^{phox}$ protein is expressed in phagocytes [191], B lymphocytes [192], spermatozoa [193], hippocampus [194], and vascular smooth muscle [195]. $p40^{phox}$ expression is induced by angiotensin II treatment in rostral ventrolateral medulla [196] and in vascular smooth muscle [195]. $p40^{phox}$ is absent from CGD patients who lack $p67^{phox}$ [197], suggesting that the protein is stable only upon binding to $p67^{phox}$. $p40^{phox}$ is involved in the regulation of NOX2. One study suggests that $p40^{phox}$ might inhibit NOX2 function [198]; however, most evidence indicates that it enhances oxidase function [61, 199, 200]. Unlike $p47^{phox}$ and $p67^{phox}$, $p40^{phox}$ is dispensable for NOX2 activity and no CGD patients with $p40^{phox}$ deficiency have been described [201]. Presently available data also suggest that $p40^{phox}$ is specific for NOX2. However, as NOX1 and NOX3 could potentially be activated by the $p47^{phox}$/$p67^{phox}$ complex, a role of $p40^{phox}$ in this scenario cannot be excluded.

3.2.3.5 Rac GTPases

There are three highly homologous Rac proteins in mammals: Rac1, ubiquitously distributed; Rac2, mostly expressed in myeloid cells; and Rac3, predominantly found in the central nervous system. Rac proteins are clearly involved in the regulation of the phagocyte NADPH oxidase NOX2. However, Rac proteins are not NOX subunits in the strict sense because they regulate other cellular functions, in particular the cytoskeleton [58, 202-204].

3.3 Anatomy of the inner ear

Anatomists typically divide the ear into three compartments: the outer (external) ear, middle ear, and inner ear (labyrinth). The outside part of the ear and the ear canal make up the outer ear. They function to collect sound (acoustic energy), and funnel it to the eardrum (tympanic membrane). Usually considered part of the middle ear, the eardrum is a thin, flexible membrane that separates the outer ear from the middle ear. The middle ear is an air filled space that houses the three middle ear bones that transmit sound. The first bone is the hammer (malleus), which is connected to the anvil (incus), which is joined to the stirrup (stapes). These tiny bones are named to reflect their particular shapes. Similarly to the outer ear, the middle ear is involved in hearing.

The mammalian inner ear is made up of both hearing (auditory) and balance (vestibular) components, these two sensory organs are the cochlea and the vestibule, respectively. The space within the bony labyrinth and around the membranous labyrinth is the perilymphatic space and filled with a fluid called perilymph. The fluid of the endolymphatic space within the membranous labyrinth is called endolymph (Figure 7). A delicate membranous labyrinth is enclosed and protected by a bony chamber that is referred to as the bony labyrinth.

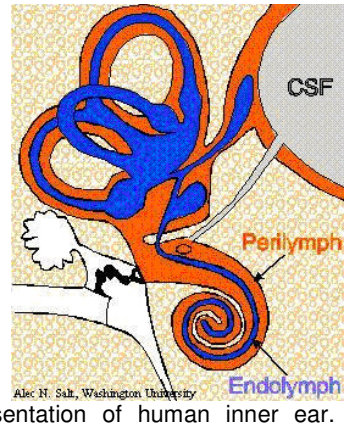

Figure 7. Schematic representation of human inner ear. Perilymph is shown orange, endolymph is blue and cerebrospinal fluid (CSF) is gray.

The ionic composition of perilymph is comparable to that of plasma and cerebrospinal fluid (CSF) and it is not secreted and resorbed in volume. Studies have shown that neither endolymph nor perilymph "flow" along their

respective compartments in the normal cochlea. Maintenance of the chemical composition of both fluids is dominated by ion transport processes, which are localized in each region. If the bony capsule of the inner ear is perforated, a condition known as a perilymphatic fistula, the perilymph escapes, driven by the hydrostatic pressure of CSF. CSF entering into the cochlea through the cochlear aqueduct replaces the escaping fluid. In this condition, a longitudinal flow will exist between the cochlear aqueduct and the site of the perforation. The chemical composition of perilymph will be disturbed because the perilymph will continually be "washed out" and replaced by CSF.

Megjegyzés [o1]: ,

3.3.1 Vestibule

The vestibule, part of the vestibular system (Figure 8), is the sensory organ that provides the dominant input about our movement and orientation in space. As our movements consist of rotations and translations, the vestibule comprises two components: the three semicircular canals, which are sensitive to angular acceleration, and the vestibular sacs, which detect linear acceleration.

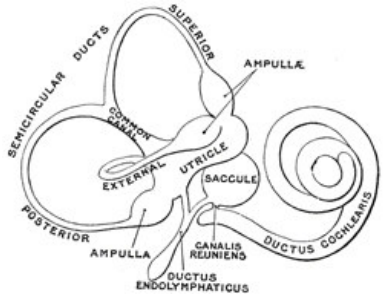

Figure 8. Schematic representation of the membranous labyrinth of the human inner ear.

Sensitivity to gravity is essential for spatial orientation. Consequently, the gravity receptor system is one of the phylogenetically oldest sensory systems, and the special adaptations that enhance sensitivity to gravity are highly conserved. The gravity receptor cells of the macular epithelia do not differ in any significant way from other vertebrate mechanoreceptor cells, which are conserved from the lateral-line organ of the fish to the mammalian vestibular and auditory organs.

3.3.1.1 Vestibular Sacs

The portion of the vestibular apparatus which is responsible for the detection of directional (positional) movement (i.e., tilting of head) consists of two flattened, spot–like areas (maculae) located in the saccular and utricular cavities of the membranous labyrinth. The plane of orientation of the macula sacculi is vertical, while that of the macula utriculi is horizontal. In transverse section, the macula utriculi and macula sacculi are both organized into a single layer of cells in association with an overlying otoconial membrane. The single cell layer consists of supportive cells residing on a basement membrane and two types of sensory hair cells, type I and type II (Figure 9) [205]. Each type I and type II cell has approximately 50-100 stereocilia, and one long kinocilium eccentric to each bundle of stereocilia.

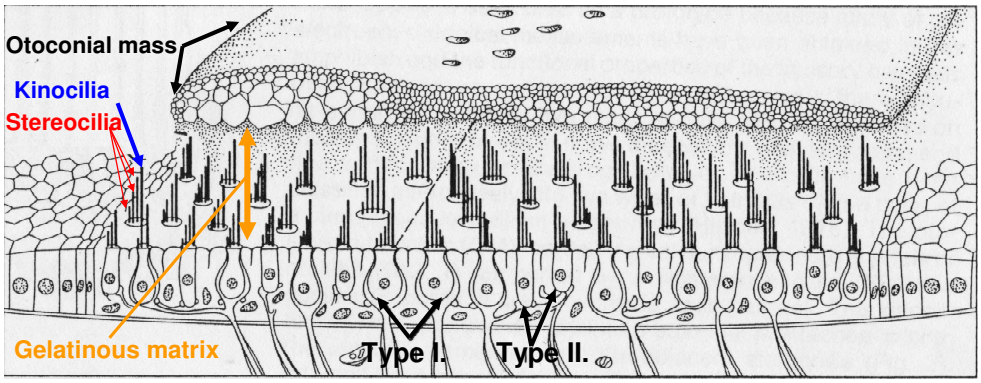

Figure 9. Schematic representation of the Macula Utriculi

The sensory cells of the macula utriculi are morphologically polarized, so that the kinocilium of each cell faces toward an arbitrary line termed the striola, which roughly divides the population of hair cells into two oppositely polarized groups. The hair cell polarization differs in the macula sacculi in that the kinocilium of each cell faces away from the striola.

The vestibular system of the inner ear continuously informs the brain about the accelerations and the position of the head [206]. Even during freefall, when there is no stimulus, the sensory cells exhibit a resting activity, thus the flow of information never stops. Perhaps, because of that, the continuous presence of the vestibular sensation is not readily recognizable and

localizable; it is a “silent sense” [207]. Detection of gravity requires special structures with large inert mass and some mobility. Biominerals, called otoconia, fulfill these requirements. They are also called ear dust in mammals because they are numerous and small. In medical practice, they are often erroneously referred to as otolith, which in fact, means the single, large ear stone of the fish.

Otoconia are strategically positioned at the tip of the kinocilia and the stereocilia bundles of the hair cells embedded in an extracellular matrix called gelatinous membrane (Figure 9). During acceleration of the head, the entire layer of otoconia shifts, thereby deflecting the cilia and modifying the membrane potential of the sensory cells. When mechanical shearing forces displace the acellular membrane relative to the sensory epithelia leads to the deflection of the kinocilium-stereocilia complex of sensory hair cells, which in turn opens the mechanotransduction channels. Kinocilium moving toward the stereocilia leads to cell depolarization, and kinocilium moving away from the stereocilia leads to sensory cell hyperpolarisation.

In the absence of otoconia, the otolith organs “mislead” the brain by continuously conveying the signal of freefall independently from the movements of the head. Thus, the information, “which way is up” is lost.

In mammals, otoconia range in size from 0.1 to 25 µm and consist of a glycoprotein matrix in a mosaic of $CaCO_3$ microcrystals organized in a calcite lattice [208-210]. The inorganic phase is characterized by an evolutionary trend toward deposition of crystal polymorphs of $CaCO_3$ of increasing stability. The least stable polymorph (vaterite) is present in the primitive otoconia of the hagfish; aragonite predominates in amphibians and reptiles, while birds and mammals are characterized by calcite, the most stable polymorph [210]. The organic phase of otoconia consists of a single major glycoprotein species (which accounts for >90% of the total protein) and several less abundant proteins [211].

The major protein component of otoconia is protein called otoconin-90/95 (OC-90/95) a 90-95 kDa secretory phospholipase A2 (sPLA2) homolog protein with two sPLA2 domains [212, 213]. The biological mechanisms responsible for development, biosynthesis, and maintenance of otoconia are not completely understood [214].

4. Aims of the present study

The goal of the present study is the *in vivo* characterization of the vestibular NADPH oxidase 3 (NOX3) complex. We sought to determine the biological importance of NOXO1, the only $p47^{phox}$ homolog found in the vestibular system. *In vitro*, the absence of NOXO1 leads to the inactivation of NOX3 [138, 215]. Thus, we hypothesized that inactivation of NOXO1 in mice reproduce the vestibular developmental defect observed in NOX3 mutants.[139].

Other *in vitro* studies implicated the importance of NOXA1 [140] and $p22^{phox}$ [180] as the activator and regulatory subunits, respectively, in the regulation of NOX3. We hypothesized that gene-targeted deletion of NOXA1 and mutation in the $p22^{phox}$ gene will result in a phenotype similar to that of NOX3 mutations.

The results of the present study are organized into three main parts:

I. NOXO1 is the physiologic organizer subunit of the NOX3 complex in the inner ear

II. Generation and characterization of NOXA1 deficient mouse strain

III. Identification and characterization of a $p22^{phox}$ deficient mouse strain.

5. Materials and methods

5.1 Mouse lines and genotyping

Hslt and wild type mice (SJL.Thy1^{a}) were obtained from Jackson Laboratory (Stock Number: 003961). Genomic DNA of a heterozygous hslt mouse was prepared from tail snips using proteinase K digestion followed by phenol-chloroform extraction. The *Noxo1* gene is relatively short (coding region is 2.5 kb) and placed between two closely adjacent genes (*transducin beta-like 3* and *growth factor erv1*). Thus, the Noxo1 gene and its promoter are localized to a 4.5 kb region of the genome. That region was amplified with Pfu proofreading DNA polymerase (Stratagene, see primers in (Table 4), after A-tailing procedure it was cloned into pGEM-T easy cloning vector (Promega) and transformed into JM109 high competent Escherichia coli according to manufacturer's recommendations. Ten bacterial colonies were selected and their plasmids were sequenced on both strands using internal primers.

For genotyping, the one nucleotide difference between the *Noxo1*^{wt} and *Noxo1*^{hslt} alleles was detected by PCR using HotStart Taq DNA polymerase (Qiagen) capitalizing on the importance of a perfect match for the 3' end of the PCR primers (Table 4). The following PCR cycle was used for genotyping: for *Noxo1*^{wt}: Initial Denaturation Step 95°C for 15 min, Denaturation Step 94°C for 30 sec, Primer Annealing Step 73°C for 30 sec, Extending Step 73°C for 30 sec, Number of Cycles 36, Final Extending Step 73°C for 10 min, product size 248bp, for *Noxo1*^{hslt}: Initial Denaturation Step 95°C for 15 min, Denaturation Step 94°C for 30 sec, Primer Annealing Step 71°C for 30 sec, Extending Step 72°C for 30 sec, Number of Cycles 36, Final Extending Step 72°C for 10 min, product size 368bp and for *Noxo1*^{transgenic}: Initial Denaturation Step 95°C for 15 min, Denaturation Step 94°C for 30 sec, Primer Annealing Step 65°C for 30 sec, Extending Step 72°C for 1min and 20 sec, Number of Cycles 38, Final Extending Step 72°C for 10 min, product size 1331bp. For swim test, wild type (n=21) and homozygous hslt (n=21) mice were placed into room temperature tap water for 30 and 7 s, respectively. All mice used in the experiments were rescued. All procedures were performed in accordance with the regulations of the University of Iowa Animal Care and Use Committee.

5.2 Conventional and real-time RT-PCR

Total RNA was isolated with Trizol reagent (Life Technologies, Inc.) or with RNeasy Mini Kit (Qiagen). The integrity of the total RNA was checked by denaturating formaldehyde agarose gel electrophoresis and the quantity was assessed by UV spectrophotometry. The total RNA samples were DNase I treated, reverse transcribed by SuperScript II (Invitrogen), and used in PCR experiments. PCR primers are shown in Table 4.

Table 4 List of primer sequences used for PCR analysis for Noxo1 study.

Primer application	Forward primer (5'→3')	Reverse primer (5'→3')
Noxo1 gene full length GeneID: 71893	agatgcttctcgcatcacccccatc	ggctgaccgaggcgtcatctctagg
Noxo1^{wt} genotyping	gcaagcccaagacacccagtatcag	gactctggactggagccaatacccact
Noxo1^{hslt} genotyping	tgaagttgaggcggcaggtgctt	gcaccaaggctacagcatgggctt
Noxo1 transgene genotyping	tccacaggtgtccactcccagttca	acctcccacatctccccctgaacct
Internal primers for generation of human *Noxo1*^{hslt} cDNA	tacccagtttcaagtgcaaggggcag ccctggtg	tgcccttgcacttgaaactgggtatcg ggggcc
Internal primers for generation of mouse *Noxo1*^{hslt} cDNA	cacccagtatcaagcccatgctgtag cc	tacagcatgggcttgatactgggtgtctt gggcttg
Mouse *Noxa1* cDNA GeneID: 241275	ccatgagctctctaggggatcagata	tgctagttctggtctcctggctg
Mouse and rat LPO GeneID: 76113	tcttgctggccacatcccacac	gaaccagaggatcaattccaccat
Mouse and rat TPO GeneID: 22018	tggagagagttctgtggcttgtca	gtggcaaggtgggtgtgtcagat
Mouse and rat MPO GeneID: 17523	accattcgcaaccagatcaacgc	catctcgctggagcgcatgtcc
Mouse and rat EPO GeneID: 13861	tggcatcgaccctatcctccga	ccatttctgccaccagaatctgtc
Mouse *Noxo1* real-time RT-PCR	tcccaagcttcctgatgctc	tgccagcaatgcctgtacat
Mouse *18S* real-time RT-PCR GeneID: 19791	acatccaaggaaggcagcag	ttttcgtcactacctccccg

For Quantitative Real-time PCR, total RNA was extracted from homogenized tissues using Trizol reagent, then DNase I. treated, further purified using RNeasy kit (Qiagen), and reverse-transcribed by Thermoscript reverse transcriptase. Real-time PCR was performed with primers specific for the gene of interests and the control 18S transcripts (primers are listed in Table 4). The amounts of PCR products were measured using SYBR Green and ABI PRISM 7700 Sequence Detection System.

5.3 Generation of Noxo1 transgenic mice

Three expression cassettes were constructed following the same cloning strategy (Figure 10, 34). Noxo1 transgenic mice with putative *Noxo1* promoter were created: a 2 kb region of genomic DNA localized 5' from the start codon of *Noxo1* gene was amplified from wild type C57Bl/6 mice using Pfu polymerase (Stratagene), cloned, and sequenced. The sequencing results were compared with The Entrez Nucleotide database DNA sequences (NCBI, GenBank, RefSeq, and PDB, and perfect clones were identified. The promoter region (CMV, CBA, or putative endogenous NOXO1 promoter) was subcloned into pSTEC-1 vector, which contains an artificial intron between the promoter and the cDNA sequence, and routinely used to generate DNA constructs [216]. Then, Noxo1 cDNA was subcloned 3' from the promoter and the artificial intron and 5' from an SV40 polyA signal. The expression plasmid was digested by KpnI restriction enzyme, the cassette was isolated by agarose gel purificationgel and microinjected into pronuclei of fertilized oocytes (C57BL/6 X SJL.F2) that were transferred into pseudopregnant foster mothers [216]. The presence of the transgene was determined by PCR (see primers in Table 4) using Taq DNA polymerase (Qiagen). Transgene positive mice were bred with *Noxo1*^{hslt}/*Noxo1*^{hslt} mice for two consecutive generations to obtain *Noxo1*^{hslt}/*Noxo1*^{hslt} and transgene positive genotype.

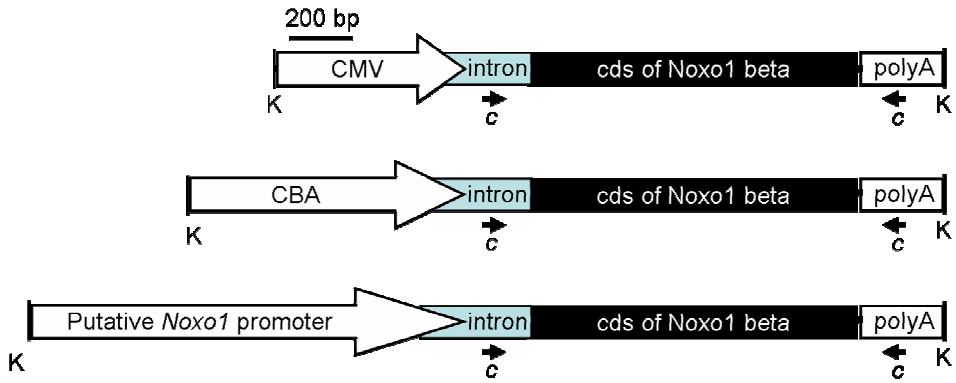

Figure 10. Map of Noxo1 transgenic constructs generated in pSTEC-1 vector. *CMV, CBA, putative Noxo1 promoter* : promoter. *Intron:* chimeric intron composed of the 5' splice site of the b-globin gene and the 3' splice site of an IgG intron. *CDS*: Noxo1 coding sequence. *polyA*: simian virus 40 polyadenylation site. *K*: KpnI restriction sites. For restriction digestion KpnI enzyme was used to isolate Noxo1 containing DNA cassettes. Arrows labeled with 'c' show the positions of primers used for detection of the transgene.

5.4 Functional testing of the auditory system

Animals were anesthetized by intraperitoneal injection of ketamine (100 mg/kg) and xylazine (9 mg/kg). Body temperature was maintained at 37 ℃ using a heating pad. Stimulus signals were generated by custom designed software (Labview version 5). Biphasic click sounds (100 μs/phase) with 31 ms interstimulus intervals were unilaterally presented to the right ear via a Beyer-DT-48 microphone inserted into the external auditory canal. Auditory brainstem responses (ABR) were recorded in a double-walled sound isolated chamber using subdermal stainless steel needle electrodes that were placed at vertex as a reference, ventrolateral to right ear as active and ventrolateral to left ear as ground. Responses recorded from the needle electrodes were amplified with a gain of 1000 with a DL instruments model 1201 differential amplifier, and stimulus levels were gradually reduced by 10 dB and finally by 5 dB steps. For each mouse, ABR growth function was determined by plotting the amplitudes of ABR 'peak I' (detected between 1.75-2.7 ms depending on the stimulus level; (Y axis) against dB attenuation levels (X axis). 0.5 μV amplitude of 'peak I' was defined as the smallest amplitude that could be distinguished reliably from noise, and the corresponding dB attenuation levels (thresholds) were determined from the ABR growth functions [217].

5.5 Histology, immunohistochemistry, and scanning electron microscopy

Inner ears of hslt, wild type, and Noxo1 transgene rescued hslt mice embryonic day 17 and postnatal day 0-2(ED17 and P0-2) were fixed in 4% PBS-buffered paraformaldehyde, paraffin embedded, sectioned (10 μm), and deparaffinized. For von Kossa staining, slides were incubated for 10 min in 5% silver nitrate, exposed to UV light for 3 min. After rinsing, slides were incubated for 2 min in 5% sodium thiosulfate and counter stained with Nuclear Fast Red Stain. To investigate acellular membranes of the organ of Corti and crista ampullaris, hslt and wild type temporal bones (P21) were removed, fixed with 1% OsO_4 in perfluorocarbon, decalcified with 5% EDTA in 0.1 M cacodylate buffer, dehydrated in graded alcohol and acetone, and embedded into Spurr's resin. Finally, Richardson's staining was used to visualize acellular membranes in 1μm thick sections. To detect OC-90/95 we used two

different rabbit polyclonal anti-OC-90/95 antibodies [212, 213] which produced identical results following the described procedure [214]. For scanning electron microscopy, mouse heads (P1) were fixed in 4% PBS-buffered paraformaldehyde and embedded into paraffin. After preparing coronal sections, tissue blocks were deparaffinized and fixed in 4% osmium tetroxide in distilled water. Samples were dehydrated, critical-point-dried in CO_2, coated with gold-palladium, and examined using a Hitachi S4000 scanning electron microscope at 5 kV.

5.6 Transmission electron microscopy

The temporal bones of ED16.5 wild type and hslt mutant mice were removed and fixed in Karnowsky's fixative [218], postfixed for 2h in 1% OsO_4, dehydrated in graded alcohol and acetone, and embedded into Spurr's resin. Thin sections (150 nm) were cut and stained with uranyl acetate and lead citrate, and then examined with JEOL JEM-1230 Transmission Electron Microscope.

5.7 X-ray photoelectron spectroscopy

Wild type and hslt newborn mouse heads (P0) were placed into specimen molds containing Tissue-Tek O.C.T. Compound, and rapidly frozen by plunging into liquid nitrogen cooled propane. Thus, tissue samples were frozen within 1 min after euthanasia. Heads were cryosectioned until the plane of saccule was reached. In wild type mice, saccule section planes containing otoconia were avoided. The block surface area was trimmed to 4-9 mm^2. Samples were further sectioned following a described protocol [219] and mounted onto aluminum stubs (Ted Pella, INC). All XPS measurements were performed using Kratos Axis Ultra XPS spectrometer with the base pressure of ~$5x10^{-9}$ Torr. All spectra were calibrated with respect to C1s line at 285.0 eV binding energy. Survey scans were collected for the samples under the following acquisition parameters: Al Kα monochromated excitation source, energy range 1200 to -5 eV, pass energy 160 eV, step size 1eV, dwelling time 200 ms. High resolution scans were collected using the following acquisition parameters: Al Kα monochromated excitation source, pass energy 40 eV,

step size 0.1 eV, dwelling time 1s. Varying X-ray spot sizes were used depending on the size of endo- and perilymphatic spaces: 110 x 100 µm and 55 x 55 µm Number of sweeps varied from 3 to 10. All spectra were analyzed using the CasaXPS software (CasaXPS Version 2.3.10, 1999-2005). XPS data fitting was performed using Shirley background subtraction.

5.8 In situ hybridization

For *in situ* hybridization, mouse heads (ED17 and P0) were fixed in 4% PBS-buffered paraformaldehyde, and 10 µm thick coronal cryosections were mounted onto poly-L-lysine slides. P^{33}-labeled antisense and sense cRNA probes (nucleotide 431-630 base pair of mNoxo1 cDNA) were generated with MAXIscript *in vitro* transcription kit (Ambion) and hybridized with the tissue sections using mRNA locator kit (Ambion) following the manufacturer's instructions. Slides were stained with hematoxylin & eosin and exposed to photosensitive emulsion. To visualize silver grains only and exclude outlines of the tissue, dark field microscopy images were taken using Kodak Wratten 31 medium magenta filters.

5.9 Cell culture, DNA constructs, transfection, and superoxide detection

HEK293T cells were maintained in Dulbecco's modified Eagle's medium, culture media were supplemented with 10% fetal calf serum, penicillin (100 units/ml), streptomycin (100 µg/ml), and 4 mmol/liter L-glutamine.

Human and mouse Noxo1^{hslt} mutant cDNAs were generated with PCR using internal, overlapping primers (Table 4). cDNAs with inserted Kozak sequences were subcloned into pcDNA3.1 (Invitrogen). To obtain stable clones, HEK293 cells were selected with 400µg/ml Genetricin an aminoglycoside antibiotic G418 starting on the 2nd day after transfection, and 13 surviving colonies were isolated 10 days after the transfection.

ROS generation was measured, by the peroxidase-dependent luminol-amplified chemiluminescence technique on a Luminometer Wallac 1420 Multilabel Counter (PerkinElmer Life Sciences). Superoxide production was measured as described previously [72]. Briefly, cells were plated into 96/48-

well microplates and superoxide production was measured following SOD-dependent reduction of 100µM ferricytochrome c at 550 nm in Hanks' balanced salt solution, or Hanks' balanced salt solution supplemented with 6 units/ml horseradish peroxidase and 250µM luminol.

5.10 Generation of NOXA1 knockout mouse model

RPCI - 21 Female (129S6/SvEvTac) Mouse PAC Library was screened for NOXA1 gene by hybridization of NOXA1 probe on high density filter (BACPAC RESOURCES Children's Hospital Oakland) [220]. P1 artificial clone (PAC) vector RP21-96I18 was identified as containing mouse NOXA1 gene and was used for the amplification of the left (2331bp) and right arm (3551bp) of the targeting vector (PfuTurbo DNA Polymerase, Stratagene). The arms were cloned into pRAY-2 cloning vector (Genbank accession no.U63120).

A targeting vector designed to replace exons II–VI of the NOXA1 gene was constructed (Figure 11). Probes for Southern blotting were chosen outside the flanking sequence of the targeting vector. Genomic DNA was used for Southern blots, left arm and right arm were digested with BglII (3707bp) and BamHI (5632bp), respectively (data not shown). For the generation of NOXA1-deficient mice, 129SvJ embryonic stem cells were electroporated with NotI linearized targeting vector construct (9954bp). G418 resistant clones were analysed by PCR screen and verified by Southern blot. Clone #1F3 was selected for blastocyst injection. Primers used for generation of NoxA1 target vector are the following: Forward primer of left arm (LaNF) 5'-agcggccgctccatgagctctctagggga-3', Reverse primer of left arm (LaCBgR) 5'-aatcgatagatcttagtcactgcttggtcaaatgcct-3', Forward primer of right arm (RaXBaF) 5'-actcgaggatccaggcctaactttgtctggtt-3', Reverse primer of right-arm (RaSfiR) 5'-aggccatactggcctgtggttggttctctttatcatc-3'.

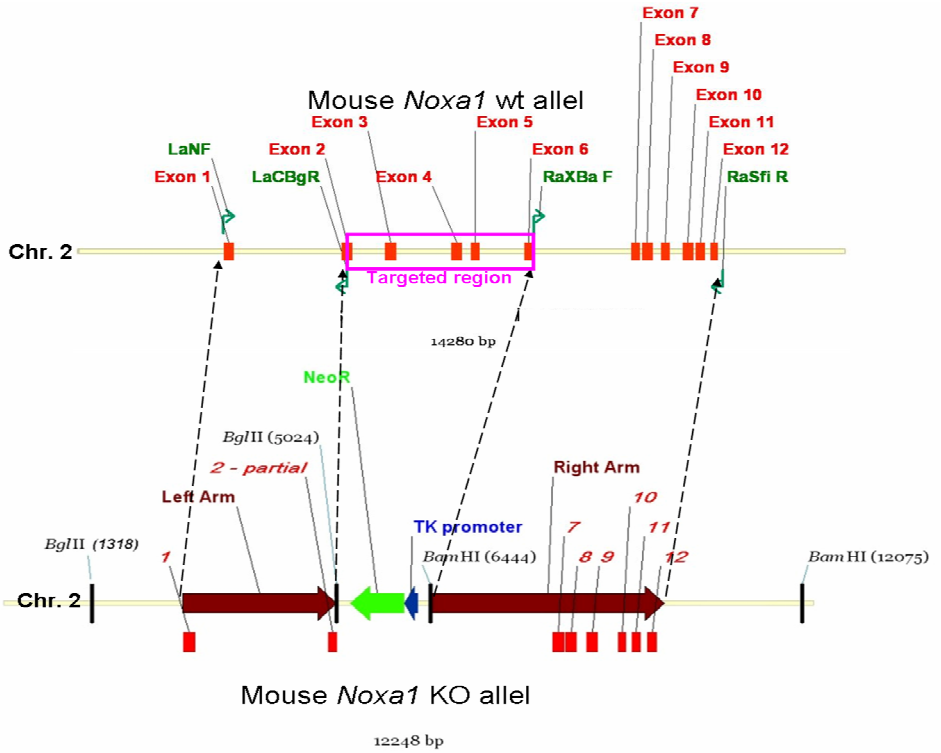

Figure 11. Targeting vector for the generation of NOXA1-deficient mice. A targeting vector designed to replace exons II–VI of the NOXA1 gene was constructed. Overview over the NOXA1 gene locus (upper part) and the knocked-out allele (lower part).

5.11 p22phox deficient mouse strain

Nmf333 (neuroscience mutagenesis facility 333) and wild type mice (A.B6-Tyr+/J) were obtained from Jackson Laboratory (Stock Number: 005445). Genomic DNA of a heterozygous nmf333 mouse was prepared from tail snips using proteinase K digestion followed by phenol-chloroform extraction. Mouse *p22*^{phox} gene (CYBA, GeneID: 13057) region was amplified by mCYBA-F 5'-accatggagcgatggtaagt -3' and mCYBA-R 5'-agcttcatcagggaagtgcccagga-3' using Pfu proofreading DNA polymerase (Stratagene), after A-tailing procedure it was cloned into pGEM-T easy cloning vector and transformed into JM109 bacteria. Bacterial colonies were isolated, and their plasmids with the insert were sequenced using internal primers. Sequencing primer mCYBA-R 5'-agcttcatcagggaagtgcccagga-3' was used to identify the mutation in exon 5.

5.12 p22phox transgenic mouse strain

The CBA promoter region was subcloned into pSTEC-1 vector. *p22^{phox}* cDNA was subcloned 3' from the promoter and 5' from an SV40 polyA signal. The expression cassette (1907bp) was isolated by KpnI restriction enzyme and microinjected into pronuclei of fertilized oocytes (C57BL/6 X SJL.F2) that were transferred into pseudopregnant foster mothers. The presence of the transgene was determined by PCR using Taq DNA polymerase (Qiagen). Transgene positive mice were bred with homozygous nmf333 mice for two consecutive generations to obtain *nmf333/nmf333* and transgene positive genotype.

5.13 Nitroblue Tetrazolium test (NBT)

Blood was taken from the tail vain of either wt or nmf333 mutant mice. Blood cells were seeded onto microscopic slide in the presence or absence of 10µg/ml PMA (phorbol 12-myristate 13-acetate) and incubated for 45 minutes at 37°C. After gently washed with PBS, cells were incubated at 37°C for 15 min in Hanks' balanced salt solution containing 0.5 mg/ml nitroblue tetrazolium (NBT). After incubation, the cells were washed with PBS and fixed in 100% methanol. The percent of NBT-positive (i.e. blue-gray staining of cytoplasm) granulocytes were determined [221].

6. Results

6.1 I. NOXO1 is the physiological organizer subunit of the vestibular NADPH oxidase complex

6.1.1 Identification of a Noxo1 mutant mouse strain

Very recently, mutations in the *Nox3* gene have been identified in mouse lines with impaired balance [139]. NOX3 requires a NOX organizer and a NOX activator protein in transfected cells. Although very little *Noxo1* mRNA expression had been previously detected in the adult inner ear [138], the possibility emerged that NOXO1 might be a critical regulator of a vestibular NADPH oxidase complex.

We hypothesized that NOXO1 is the organizer subunit of the NOX3 complex. Thus, NOXO1 mutant mice should reproduce the NOX3-deficient phenotype. Mouse strains with spontaneous or induced mutations accompanied with visible phenotypes are now selected, collected, sorted, and stored at a few centers in the U.S. Many of the stored strains are characterized at a basic level, and the results of those characterizations are available in public databases (Mouse Genome Informatics, Ensembl ect.). We scrutinized the available mutant mouse databases for a NOX3-like phenotype.

The position of the *Noxo1* gene has not been determined on the linkage map of mouse chromosome 17, but one of its neighboring genes, *growth factor erv1-like* (*Gfer*), was mapped at ~10 cM from the centromere. Therefore, we searched mutant mouse databases for phenotypic alleles localized to the 10±1 cM region with impaired balance. Only two phenotypic alleles without known corresponding genes were found: 'neuroscience mutagenesis facility, 329' (nmf329) and 'head slant' (*hslt*) [222].

Nmf329 is a chemically induced, recessively inherited phenotypic allele that causes deafness, whereas hslt is a spontaneously arisen, recessively inherited allele that causes non-syndromic vestibular disorder. The 'head

slant' (hslt) spontaneous mutant strain carries a mutation on chromosome 17 at ~10 cM from the centromere.
(http://www.informatics.jax.org/searches/allele.cgi?24943).
Since the approximate location of the mutation agreed with the location of the *Noxo1* gene (chr. 17, 10 cM) and differed sufficiently from the location of the *Nox3* gene (chr. 17, 4.1 cM), we hypothesized that the mutation have occurred in the *Noxo1* gene.

Noxo1 is comprised in a 4.5 kb stretch of DNA between *Gfer* and *transducin (beta)-like 3 (Tbl3)* (Figure 12).

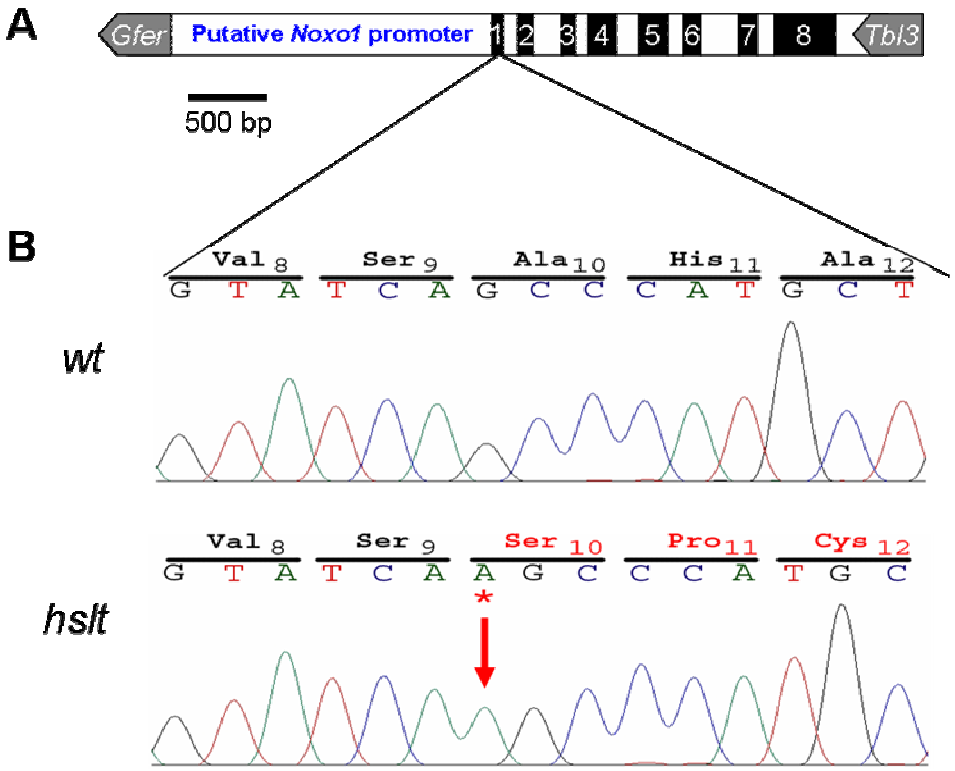

Figure 12. (A) Map of *Noxo1* showing exons (numbered black boxes) and untranslated regions (white boxes) between the two neighboring genes, *Gfer* and *Tbl3* (gray arrows). (B) Sequence chromatographs of the mutated region of *Noxo1hslt (hslt)* as compared to *Noxo1wt (wt)*. Insertion of a deoxyadenosine (red asterisk) into Noxo1hslt is marked with a red arrow, and changes caused in the amino acid sequence are highlighted with red characters. The resultant frame-shift was predicted to truncate the 349-amino acid long NOXO1 and yield a peptide of 34 amino acids with the 9 first original amino acid.

We compared the DNA sequence of the entire 4.5 kb region of balance deficient hslt and wild type mice of identical strain of origin, and identified a single insertion of a deoxyadenosine into exon 1 of *Noxo1*, 28 nucleotides downstream from the start codon (Figure 13). This insertion resulted in a premature STOP.

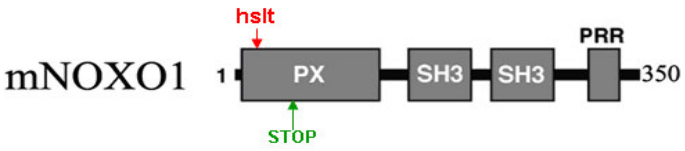

Figure 13. Schematic representation of the domain arrangement of mouse NOXO1. Location of hslt mutation indicated by red arrow. The rise of early stop codon in hslt mutant is shown by green arrow.

In order to easily and quickly genotype mice of the *hslt* colony, we developed a PCR based assay. Capitalizing on the importance of a perfect match at the 3' end of PCR oligos, we detected the one nucleotide insertion between the wild type and *hslt Noxo1* alleles (*Noxo1*^{wt} *vs. Noxo1*^{hslt}) using HPLC purified primers, HotStart Taq DNA polymerase, and high quality tail DNA as template (Figure 14).

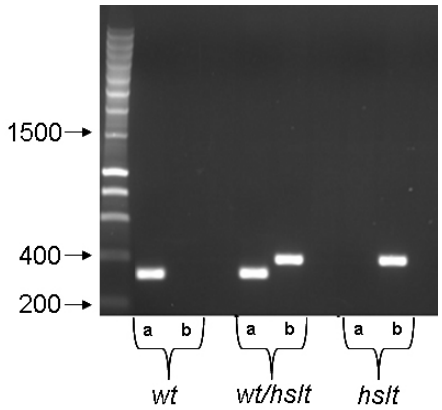

Figure 14. Genotyping of hslt mice. PCR identification of wild type (wt), heterozygous (wt/hslt), and hslt homozygous (hslt) mice. 'a','b' indicate PCR reactions to detect Noxo1wt and Noxo1hslt alleles, respectively. The first lane shows DNA molecular size markers in base pairs.

6.1.2 NOXO1-deficient mice unable to balance

Our working hypothesis was that NOXO1 is a subunit required for NOX3 function *in vivo*. Since NOX3 was demonstrated to be involved in otoconia formation, its regulatory subunit was expected to have similar importance. Therefore, the absence of NOXO1 was predicted to cause impaired balance. The balance deficit of homozygous mice of hslt line was manifested as early as day 4 after birth. Pups that were placed on their back did not attempt to right themselves to the ventral position. From day 18, they exhibited distinct head and body tilt (Figure 15A) and an abnormal reaching response during falling (Figure 15C) compared to heterozygous littermates or in wild type mice (Figure 15B, D). In areas where the cage top was close to the bedding, they frequently rolled supine, grabbed the metal grid above them, and crawled on their back (Figure 15E).

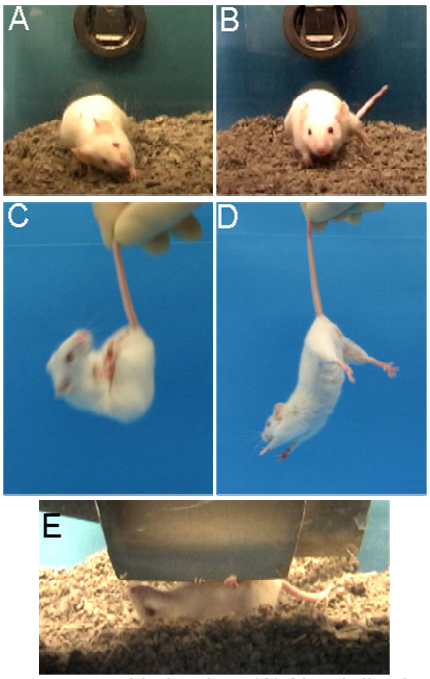

Figure 15. Phenotype and genotype of hslt mice. (A) Head tilt of an hslt mouse. (B) Straight head position of a wild type littermate. (C, D) Lack of reaching response in hslt mice. (C) Hslt mouse keeps its head and trunk curled up and its legs clasped when suddenly moved downward, (D) whereas wild type mouse stretches out its forepaws to contact with the surface below. (E) Hslt mice often roll to supine position and crawl on the bedding.

Unlike control mice, affected mutants could not orient themselves in water and thus became submerged and introduced a so-called “non-swimming” phenotype (Figure 16). These movement anomalies clearly demonstrated that homozygous hslt mice could not orient themselves with respect to the gravitational force. The balance deficit was completely penetrative.

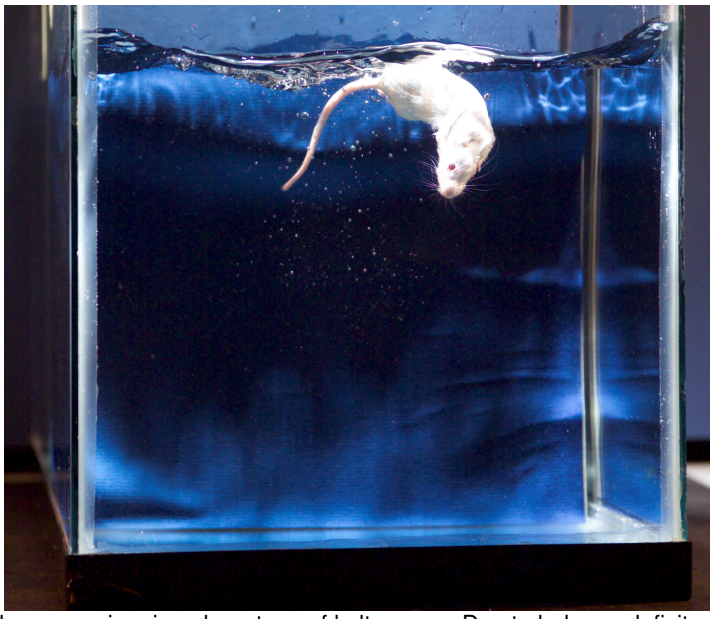

Figure 16. The non-swimming phenotype of hslt mouse. Due to balance deficit, mutants cannot orient themselves in water and thus become submerged.

In contrast, hearing tests measuring auditory-evoked brainstem responses did not show differences between hslt and wild type mice (Figure 17).

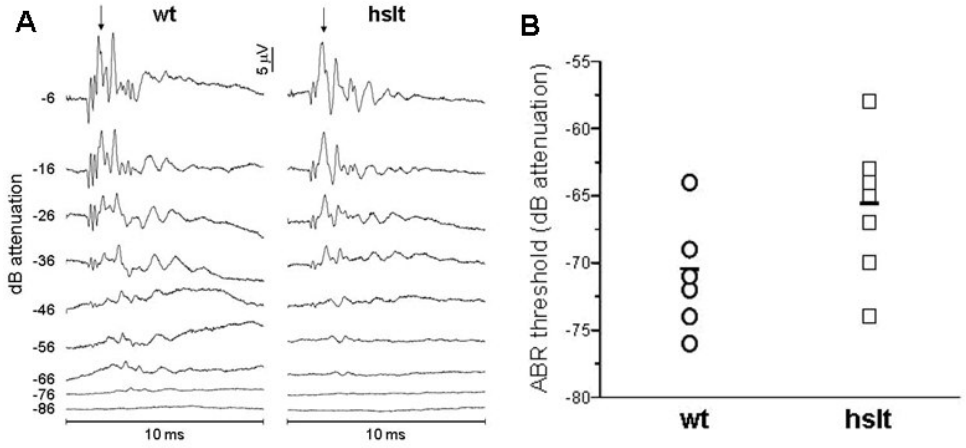

Figure 17. Comparison of auditory brain stem responses (ABR) of wild type *(wt)* and 'head slant' *(hslt)* mice. (A) Representative ABR waveforms of a wild type (left) and a 'head slant' (right) mouse. Arrows indicate 'peak I' that was chosen to determine ABR respond thresholds. The delay of response peaks increases, as dB attenuation (negative numbers) is gradually changed from -6 to -86. (B) Scatter plot showing the ABR thresholds of individual wild type (circles) and 'head slant' (squares) mice. The mean thresholds are represented by short, horizontal lines. The ABR threshold difference between *wt* and hslt mice was not statistically significant (p=0.077) using unpaired Students' t-test.

6.1.3 Absence of otoconia mineralization and accumulation of OC-90/95 containing conglomerates in the inner ear of 'head slant' mice

Homozygous *Noxo1* mutant mice do not sense gravity or other linear acceleration because otoconia formation is likely to be absent. To verify the lack of otoconia formation in homozygous *Noxo1* mutant mice, we established histological procedures to visualize otoconia in wt mice.

In order to identify the anatomical cause of the balance deficit, we performed histological analysis of inner ears of embryonic day (ED) 17 and newborn (postnatal day 0-2, P0-2) wild type, and $Noxo1^{hslt}/Noxo1^{hslt}$ mice. In both age-groups, von Kossa staining demonstrated the complete absence of calcium carbonate crystallization in $Noxo1^{hslt}/Noxo1^{hslt}$ inner ears (compare Figure 18A and B).

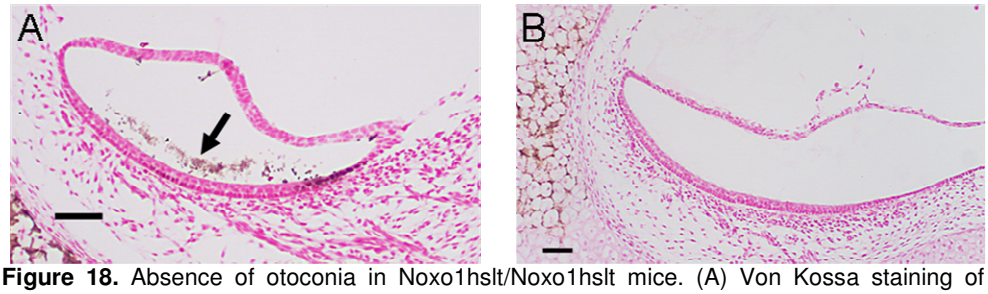

Figure 18. Absence of otoconia in Noxo1hslt/Noxo1hslt mice. (A) Von Kossa staining of calcium salts in the saccular otoconia (arrow) and in the adjacent bone (lower left corner) of a wild type mouse (P1). (B) Von Kossa staining does not detect otoconia in the saccule of a Noxo1hslt/Noxo1hslt mouse (P1) but stains calcium salts in the adjacent bone (upper left corner). Bars indicate 50 µm.

Scanning electron microscopy not only verified the lack of otoconia in *Noxo1*^{hslt}/*Noxo1*^{hslt} animals (compare Figure 19A with Figure 19C) but also showed coral-like conglomerates above the hair cells (Figure 19D). The developmental defect of the hslt mice seemed specific to otoconia genesis, since all other structures of the inner ear appeared intact including the sensory epithelia and acellular membranes of the organ of Corti and the ampullae of semicircular canals (Figure 20).

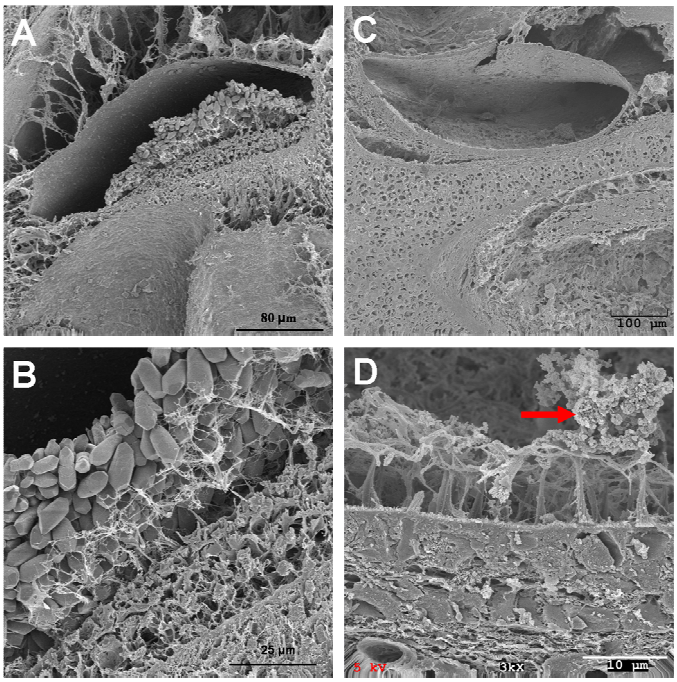

Figure 19. Scanning electron microscopy pictures of macula sacculi of wild type (A, B) and *Noxo1hslt/Noxo1hslt* mice. (C, D) Otoconia are associated with each other and the sensory epithelium by a cobweb-like matrix. (B) In *Noxo1hslt/Noxo1hslt* mice, coral-like conglomerates of various sizes were detected (red arrow D).

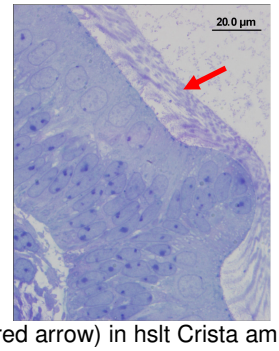

Figure 20. Acellular membrane (red arrow) in hslt Crista ampullaris stained by Richardson's stain at ED17.5.

At the onset of otoconia genesis (~ED14.5), OC-90/95 conglomerates have been described in the utricle and saccule of wild type embryos [214, 223]. Therefore, conglomerates observed in newborn hslt mice may be largely composed of OC-90/95 and may preserve a brief developmental stage prior to calcium carbonate mineralization. Indeed, OC-90/95 was incorporated into the otoconia of P0 *wild type* mice (Figure 21A), whereas anti-OC-90/95 antibody staining showed patchy precipitates in the saccule (Figure 21B) and utricle (data not shown) of newborn *Noxo1*^{hslt}/*Noxo1*^{hslt} mice.

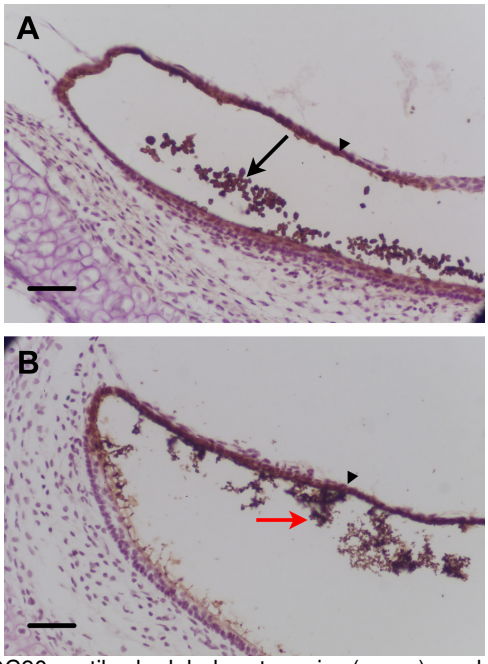

Figure 21. (A) Anti-OC90 antibody labels otoconia (arrow) and the OC-90 producing epithelium (arrowhead) in wild type mice. (B) In hslt mice, anti-OC90 antibody labels protein conglomerates (arrow) in the saccule and the vestibular epithelial cells (arrowhead). Bars indicate 25 µm.

Interestingly, lipid vesicles similar to the previously described globular substance were found in the both hslt and wild type ED16.5 utricle and saccule (Figure 22). Although, OC-90/95 and globular substance-like vesicles were present in the endolymph of Noxo1 mutants, the calcium carbonate component of otoconia was absent indicating an arrest in the process of otoconia genesis.

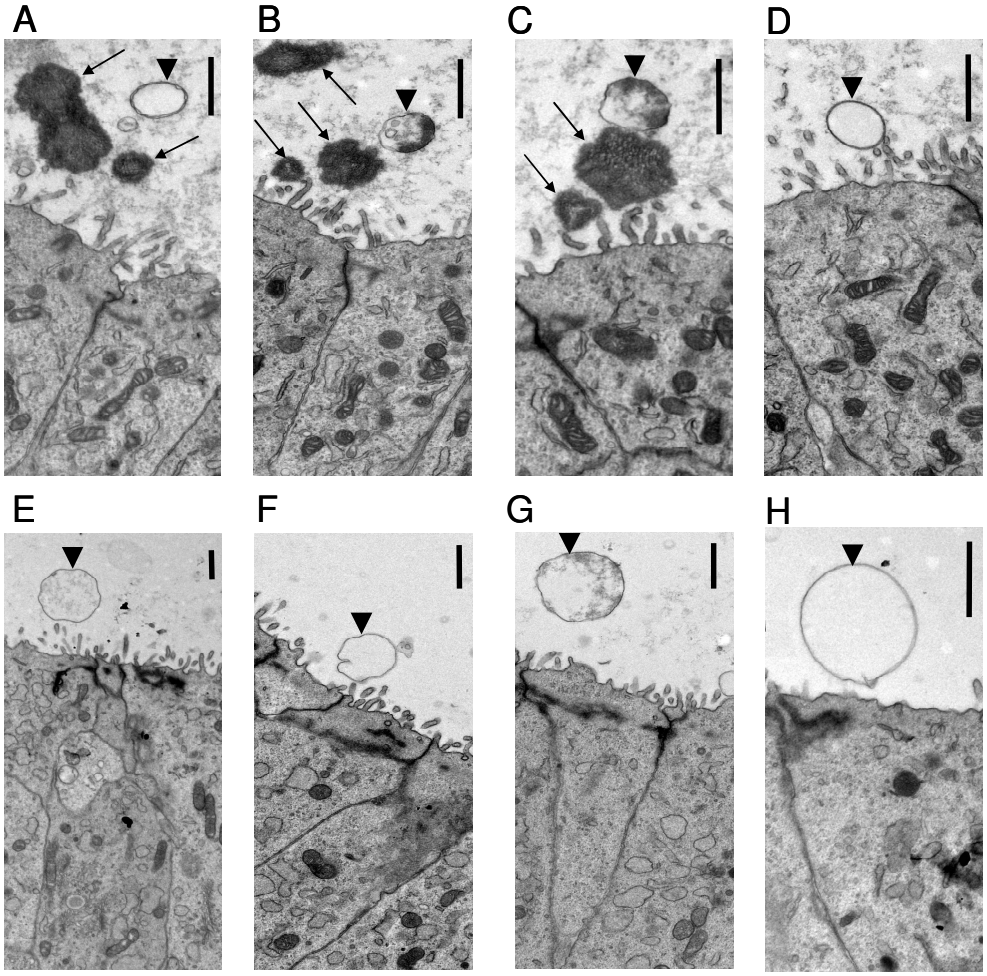

Figure 22. Globular substance-like vesicles in the developing inner ears of *wild type* and *hslt* mice. Transmission electron micrographs of *wild type* (A-D) and *hslt* (E-H) mouse (ED16.5) sacculi. Arrowheads indicate lipid vesicles similar to previously described globular substance (A-H), and arrows indicate developing otoconia (A-C). Electrodense material was observed in several vesicles (B, C, G). Bars represent 1 µm.

6.1.4 Noxo1 mRNA is widely expressed in the embryonic inner ear

Only low levels of Noxo1 mRNA had been detected in the inner ear of adult mice and rats [138], but the phenotype of hslt mice suggested a function for Noxo1 during embryonic development and during the first few neonatal days, especially when otoconia genesis is intense. Therefore, we quantified Noxo1 mRNA expression in inner ears at different time points in mouse inner ears using quantitative real time RT-PCR (Figure 23). Indeed, Noxo1 expression declined by 93% in the inner ear during the first two postnatal weeks.

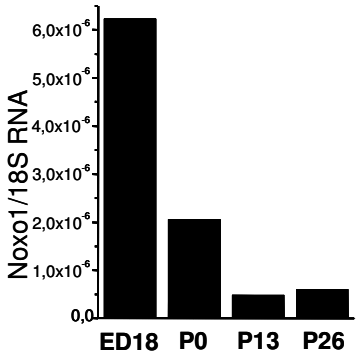

Figure 23. Representative data of the quantification of NOXO1 mRNA in the inner ear of ED18, P0, P13, and P26 mice relative to 18S rRNA expression. The amounts of NOXO1 and 18S PCR products were measured by quantitative real time PCR using SYBR Green.

Noxo1 was expected to be localized in the utricle and saccule where otoconia are formed. To test this prediction, we performed in situ hybridization experiments. Surprisingly, in situ hybridization experiments demonstrated a much broader expression of Noxo1 mRNA in the inner ear of ED17 and P0 mice. The antisense probe labeled both the sensory and non-sensory cell layers of the saccule, an underlying region rich in neurons (Figure 24A), the ampullae of semicircular canals (Figure 24C), the epithelium lining the scala media of the cochlea, especially at the stria vascularis, as well as the spiral ganglion neurons (Figure 24D), whereas the surrounding connective tissue retained only low amounts of the antisense probe (Figure 24B). The specificity of the hybridization was confirmed by a sense probe that produced a weak, uniform signal (Figure 24B). The hslt mutation of *Noxo1* did not abolish Noxo1

mRNA expression as the transcript containing the frame-shift mutation was detected in the inner ears of *Noxo1*^{hslt}/*Noxo1*^{hslt} mice (data not shown).

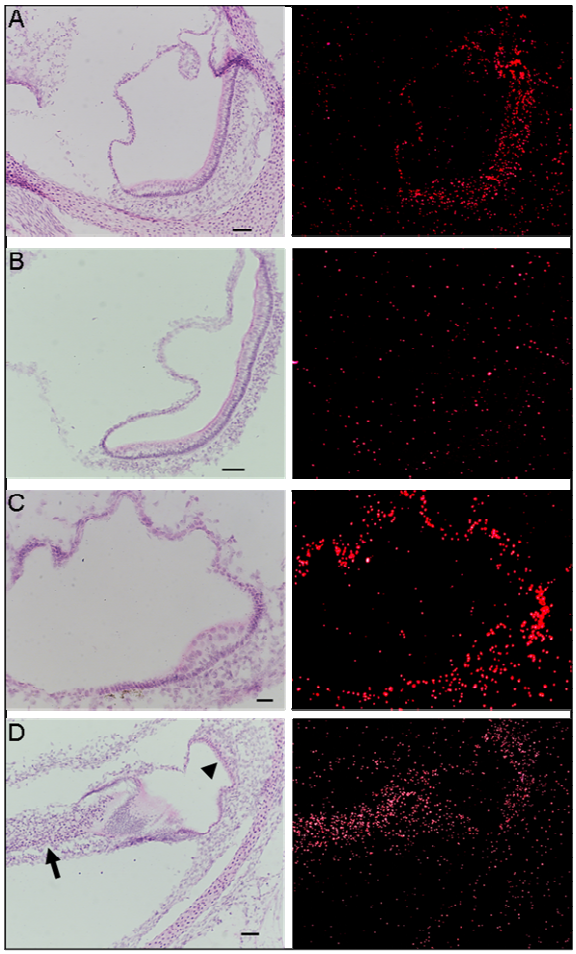

Figure 24. Localization of Noxo1 mRNA in the inner ear by in situ hybridization at ED17. Various regions of wild type mouse inner ear were hybridized with P^{33}-labeled antisense (A, C, D right panels) and sense (B, right panel) Noxo1 probes and developed for autoradiography. The same sections were contrast stained with hematoxylin & eosin, and bright field images were photographed (A-D, left panels). The antisense Noxo1 probe labeled both sensory and non-sensory epithelial cells of the saccule and an underlying region rich in neurons (A). Whereas the sense probe produced only a weak, uniform signal in the saccule (B). The antisense Noxo1 probe also labeled the non-sensory epithelium of the ampulla (C), the stria vascularis (arrowhead) and the spiral ganglion neurons (arrow) of the cochlea (D). Bars indicate 50 µm (A, B, D) and 25 µm (C).

6.1.5 The hslt mutation of Noxo1 prevents its biochemical function

Previously, we localized Nox3 mRNA to the epithelial cells of the saccule and utricle of adult mice, whereas in the cochlea, Nox3 was found mainly in the spiral ganglion neurons. As the expression patterns of Noxo1 and Nox3 mRNA [138] largely overlap, and the phenotype of Noxo1 and Nox3 deficient [139] mice are similar, we hypothesized that Noxo1 may regulate Nox3 function. We investigated whether the hslt mutation of Noxo1 may prevent ROS production by a NOX3-NOXO1 containing enzyme complex. As a basal, regulatory subunit-independent activity of human Nox3 had been reported in transfected cells we tested mouse and human oxidase subunits [180]. HEK293T cells were transfected with human or mouse sets of Nox3, Noxo1^{wt} (beta splice variant [133]) or Noxo1^{hslt} with or without Nox activator 1 (Noxa1). Superoxide production was measured by the superoxide dismutase-dependent reduction of ferricytochrome *c*. We chose NOXA1 as the potential activator subunit of Nox3, since it was expressed in embryonic inner ear (Figure 25) and the lack of the only other known Nox activator, p67^{phox}, does not cause balance problems in patients with p67^{phox}-deficient chronic granulomatous disease.

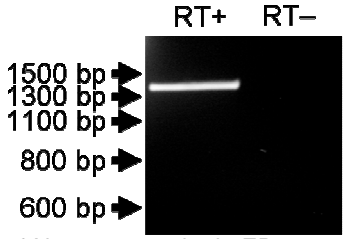

Figure 25. RT-PCR detection of Noxa1 transcript in ED16.5 mouse inner ear. Noxa1 mRNA expression was detected by RT-PCR in developing mouse inner ear (ED16.5). "RT+" and "RT–" indicate reverse transcribed and not reverse transcribed RNA samples, respectively. Arrows show the positions of DNA size markers.

Superoxide generation by human and mouse Nox3 was low in the absence of regulatory subunits and was only slightly increased by co-transfection of Noxa1 (Figure 26A,B and [75, 119, 138]). Human Noxo1^{wt} alone, but not Noxo1^{hslt}, induced Nox3 activation that was not enhanced by Noxa1 (Figure 26B). In contrast, mouse Nox3 required the co-transfection of both mouse

Noxo1^{wt} and Noxa1 to achieve maximal superoxide generation (Figure 26A). Nevertheless, replacement of Noxo1^{wt} by Noxo1^{hslt} drastically reduced Nox3 enzyme activity independent of species origin and combination of the subunits (Figure 26A, B).

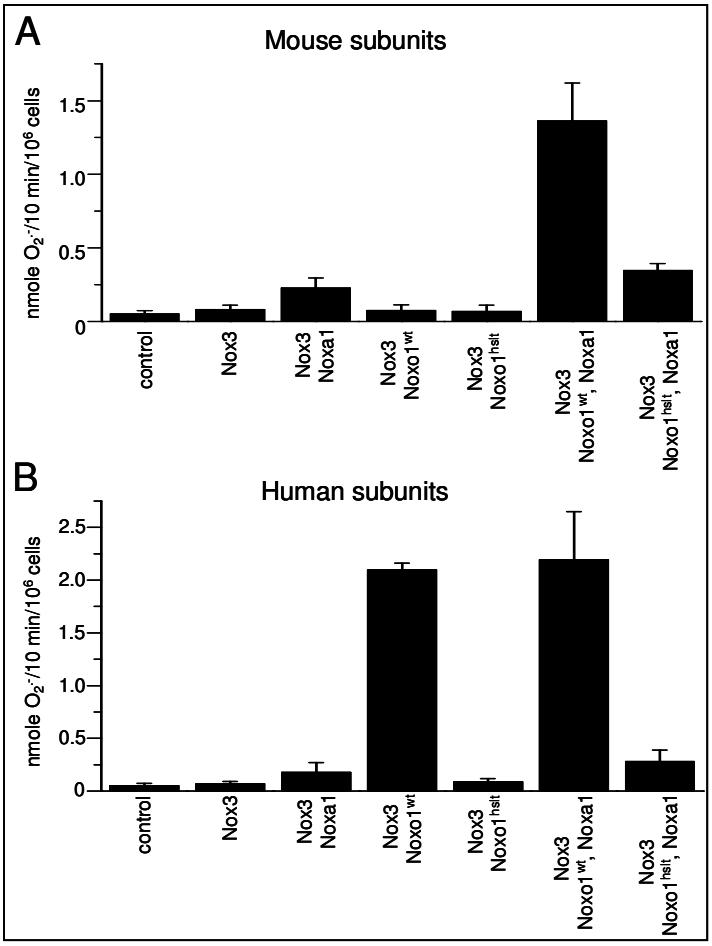

Figure 26. Hslt mutations of human and mouse Noxo1 are biochemically inactive. (A, B) Superoxide production of HEK293T cells transfected with the indicated combinations of (A) mouse and (B) human NADPH oxidase subunits or with empty vector (control). Each transfection was performed with equal amounts of DNA constructs encoding the subunits (0.125 mg/ml DNA construct for each subunit). When only one or two subunits were transfected, proportional amounts of empty vector was included into the transfection solution to obtain total DNA concentration of 0.375 mg/ml. Values are mean ± SD (n=3).

The very different need for Noxa1 in the human and mouse oxidase complexes may be explained by the great dissimilarities in the C-termini of the two NOXO1 proteins. Indeed, in our model human NOXO1 could activate mouse NOXO3 in the absence of NOXA1 (data not shown).

6.1.6 Analysis of the Ca2+, Na+, K+, and Cl- content of the endo- and perilymph by X-Ray Photoelectron Spectrometer

Our preliminary results indicated that OC-90 and globular substance were present in the endolymph of balance organs of *hslt* mice (Figure 22). Therefore, we investigated the presence and concentration of one other critical component, the Ca^{2+}. This approach was further justified by the fact that $[Ca^{2+}]_{endolymph}$ has not been determined during otoconia genesis even in wild type animals and is only assumed to be as low as in the developed inner ear (~30 µM) [224]. The conventional method of applying double-barreled electrodes to measure ion concentrations is not suitable because of the very small volume of the endolymph in the embryonic inner ear. Therefore, we determined Ca^{2+} concentration using new technology, a state-of-the-art ultra high performance x-ray photoelectron spectrometry system developed for surface sciences.

Solid specimens exhibit complex interactions with primary beam electrons, which result in a variety of signals that carry information about the atomic composition of the specimens. The energy characteristic of the X-ray emitted from the specimen can be detected and analyzed by X-ray spectrometry.

The Microscopy Facility of the University of Iowa operates a Kratos Axis Ultra X-Ray Photoelectron Spectrometer (XPS), which allows *quantitative* analysis of elements bigger than He with an excellent peak to background ratio. In previous studies, we investigated ionic composition of the endolymph using Energy Dispersive Spectroscopy (EDS, Figure 27) which operates on a similar bases than XPS but provides *qualitative* data and, due to a much poorer peak to background ratio, elements with low concentrations (e.g. Ca^{2+} not incorporated into otoconia) could not be investigated [223, 225].

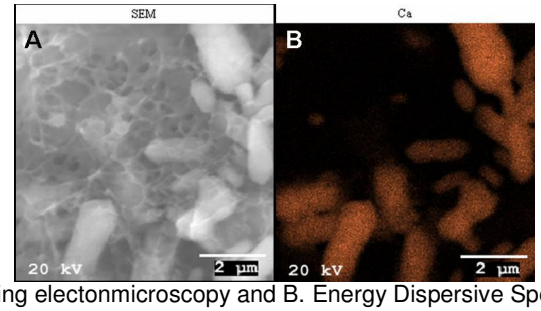

Figure 27. A. Scanning electonmicroscopy and B. Energy Dispersive Spectroscopy for Ca2+ on macula sacculi with otoconia at ED 17.5.

Therefore, we used XPS to determine the Ca^{2+}, Na^{+}, K^{+}, and Cl^{-} content of the endo- and perilymph of the inner ear and to calculate the ratio of these elements in newborn (P0) hslt and wild type mice (Figure 28). Wild type P8 inner ear samples with developed K^{+} and Na^{+} gradients between the endo- and perilymph provided positive controls to validate our method.

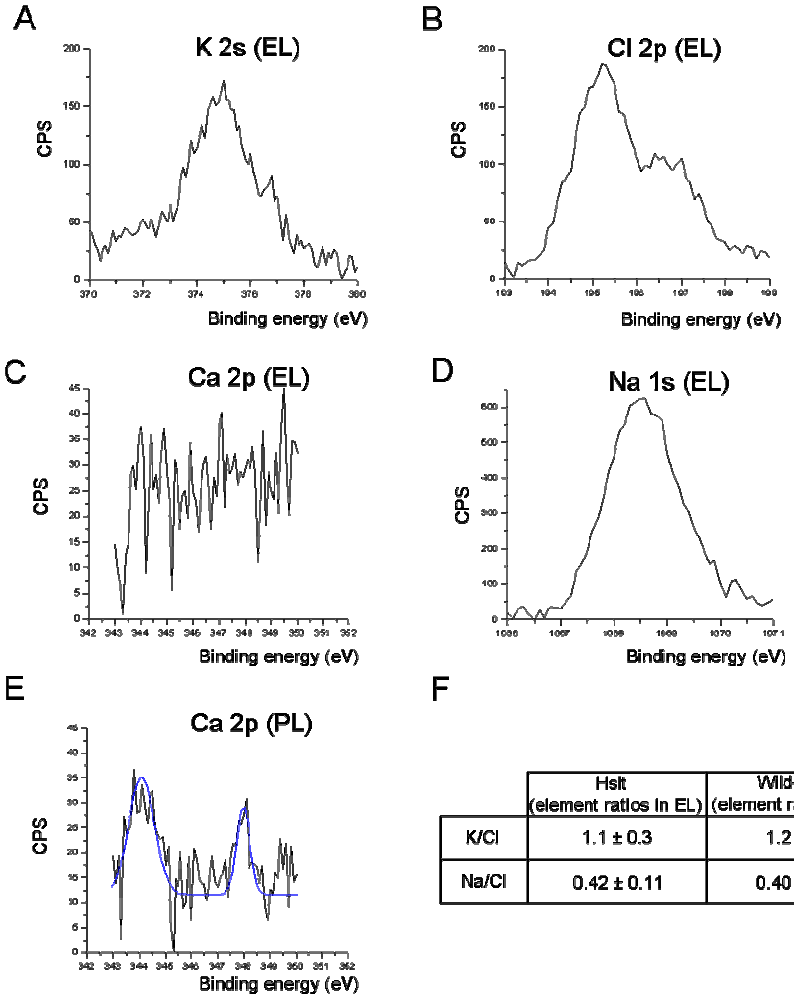

	Hslt (element ratios in EL)	Wild-type (element ratios in EL)
K/Cl	1.1 ± 0.3	1.2 ± 0.2
Na/Cl	0.42 ± 0.11	0.40 ± 0.08

Figure 28. Elemental composition of the endolymph of hslt and wild type mice using X-ray photoelectron spectroscopy. Representative K 2s (A), Cl 2p (B), Ca 2p (C,E), and Na 1s (D) high-resolution X-ray photoelectron spectra were obtained from endolymphatic space (EL, A-D) or perilymphatic space (PL, E) of a newborn (P0) hslt mouse. Whereas Ca 2p is below detection limit in the endolymph, a small Ca 2p doublet was detected in the perilymphatic space (C vs. E). The blue line indicates two-peak Gauss-curve fit (E). (F) The molar ratios between elements in the endolymphatic space (EL) of P0 mice were calculated with CasaXPS software based on high resolution photoelectron spectra using relative sensitivity factors. Ca 2p was below detection limit in both hslt and wild type P0 EL. In the perilymph, Ca/Cl molar ratio was 0.02 ± 0.01. Data shown in F are the mean ± S.E. of three independent experiments.

Ca 2p was below detection limit in both hslt and wild type P0 endolymph, and X-ray photoelectron spectroscopy indicated unaltered ratios of Na^+, K^+, and Cl^- in the endolymph of Noxo1 deficient mice (Figure 28) compared to wild type [143].

6.1.7 Lactoperoxidase expression in the utricle

Otoconia formation is thought to require an interaction between OC-90 and Ca^{2+}-rich vesicles ("globular substance") secreted by the sensory epithelium [223, 226], which takes place in a gelatinous membrane consisting of tectorins [227] and otogelin [228, 229]. However, the nature of the protein-lipid interaction remains obscure. Otoconins have been found to be unable to disrupt lipid vesicles *in vitro* despite their classification as members of the sPLA2 enzyme family [210]. In Noxo1 mutant mice, otoconia genesis is arrested at an early stage prior to calcium carbonate mineralization, suggesting that Ca^{2+} is not released from the globular substance.

ROS are well known to cause lipid peroxidation [230], and the resulting lipoperoxides have a distinct physicochemical state compared to unoxidized phospholipids that makes them more accessible to sPLA2 [231, 232]. Lipid peroxidation requires not only superoxide but also transition metals (*viz.* Fe^{3+}, Cu^{2+}) or a peroxidase [233]. Transition metals have not been described in the endolymph. However, when we isolated utricles to extract RNA specifically from otolith organs (Figure 29), lactoperoxidase (LPO) gene expression was readily detectable by PCR (Figure 30).

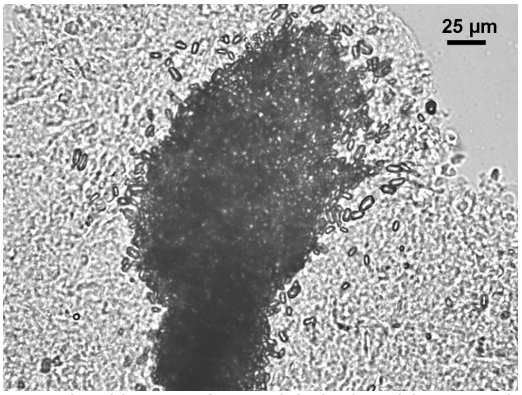

Figure 29. Bright field, unstained image of an utricle isolated from newborn wild type mouse. The dark islet in the middle is composed of otoconia.

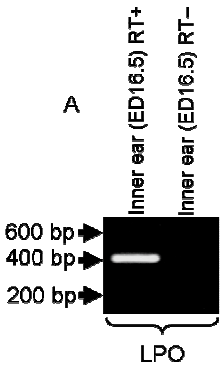

Figure 30. LPO mRNA expression was detected by RT-PCR in developing mouse inner ear (ED16.5). "RT+" and "RT–" indicate reverse transcribed and not reverse transcribed RNA samples, respectively.

Other peroxidases were absent including myeloperoxidase (MPO), which suggested that phagocyte "contamination" was minimal during dissection (Figure 31). We planned to verify the PCR results by detecting LPO protein in the inner ear using Western blot. However, the available antibodies were raised against bovine LPO and do not cross-react with the mouse protein (not shown). In addition, no LPO deficient mouse line has been described.

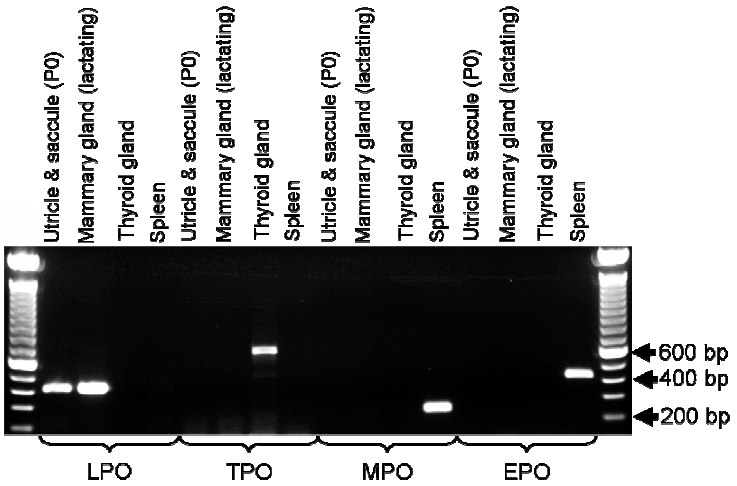

Figure 31. Lactoperoxidase expression in P0 utricle and saccule and in embryonic inner ear. (A) RT-PCR detection of lactoperoxidase (LPO), thyroid peroxidase (TPO), myeloperoxidase (MPO), and eosinophil peroxidase (EPO) transcripts in the indicated tissues. Mouse mammary gland, as opposed to rat, is likely to be devoid of LPO. Therefore, lactating mammary gland RNA was isolated from rat but all other RNA samples were extracted from mouse tissues. All PCR primers were designed to anneal with both mouse and rat peroxidase cDNA.

6.1.8 Secretion of recombinant mouse OC-90 by transfected HEK293T cells

The hypothesis that lipid peroxidation facilitates OC-90-lipid vesicle interaction by using an *in vitro* system consisting of recombinant OC-90 and H_2O_2/LPO peroxidized or untreated large unilamellar vesicles. First, an expression system suitable for the generation of recombinant mouse OC-90 was identified. We performed a pilot experiment with the easily transfectable human HEK293T cell line. OC-90 cDNA (NCBI accession # NM010953) was PCR amplified from mouse utricle cDNA, a Kozak sequence was inserted before the start codon to enhance translation efficiency, and the cDNA was subcloned into pcDNA3.1. Then, OC-90 or empty vector was transfected into HEK293 cells seeded on matrigel (BD Biosciences) coated 10-cm dishes. Two days after transfection, the medium was replaced by 4 ml serum-free medium and harvested 18 hours later. The collected supernatant was centrifuged, concentrated with Amicon Ultrafilter Devices (30,000 MW cut-off), and Western blotted. The anti-OC-90 antibody detected a ~75 kDa band in the supernatant of transfected cells, whereas the medium of empty vector transfected (negative control) cells was devoid of any signal (Figure 32).

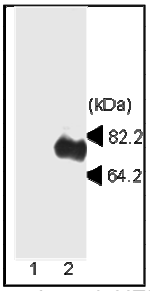

Figure 32. Secretion of OC-90 by transfected HEK293 cells. Western blot detection of recombinant OC-90 in the serum-free, concentrated medium of mouse OC-90 transfected HEK293T cells (lane 2), whereas no signal was found in the concentrated medium of HEK293T cells transfected with the empty vector (negative control, lane 1). Arrowheads indicate molecular size markers.

Importantly, although otoconin is thought to have a molecular mass of ~90 kDa (the molecular mass of the non-glycosylated protein is 50.8 kDa), mouse "OC-90" was detected at 75-80 kDa by Ignatova and colleagues who extracted OC-90 from otoconia and used the same primary antibody [214].

Thus, the HEK293 cells appear to be a suitable expression system for the production of recombinant OC-90.

6.1.9 Noxo1 transgene rescues 'head slant' phenotype

In the hslt mouse colony, all mice (*n*=102) with the balance deficit were homozygous for the mutant *Noxo1* allele (*Noxo1*^{hslt}), and all mice (*n*=144) without balance deficit were heterozygous or wild type. In order to demonstrate that the severe imbalance of hslt mice was caused by the mutation in *Noxo1*, and not in a linked gene, we used transgenic rescue.

The promoter of *Noxo1* has not been characterized, and no vestibular system-specific promoter has been tested in transgenic animals. Therefore, we chose to generate three groups of Noxo1 transgenic mice using three different promoters to drive *Noxo1* beta isoform in collaboration with the Transgenic Facility of the University of Iowa (Figure 10).

In the first transgenic constructs, the putative Noxo1 promoter was used to drive. There is only a 2kb region between the start codon of NOXO1 and the start codon of the neighboring growth factor erv1 gene (they have opposite orientations in the genome). Therefore, the 2 kb stretch between the two genes was used as putative Noxo1 promoter.

In the second transgenic construct, Noxo1 was downstream of the promoter-enhancer of human cytomegalovirus (CMV) which is highly functional in the inner ear during embryonic development but the expressor cell types has not been specified [234]. Importantly, the CMV promoter has minimal or no activity in phagocytes [132, 234]. Therefore, spontaneous ROS production by the phagocyte NADPH oxidase is not probable in transgenic animals generated with the CMV-Noxo1 expression cassette.

In the third transgenic construct, Noxo1 was under the control of the almost ubiquitously functional CMV enhancer/chicken β-actin (CBA) promoter. By investigating the expression of the green fluorescence protein (GFP) in the inner ears of CBA-enhanced GFP (EGFP) transgenic mice (purchased from the Jackson Laboratory) and of wild type animals (negative control, not shown) we verified that the CBA promoter was active in both non-sensory and sensory vestibular epithelial cells (Figure 33). However, the CBA promoter is

likely to function in leukocytes [235], which may result in an overproduction of ROS by non-activated phagocytes.

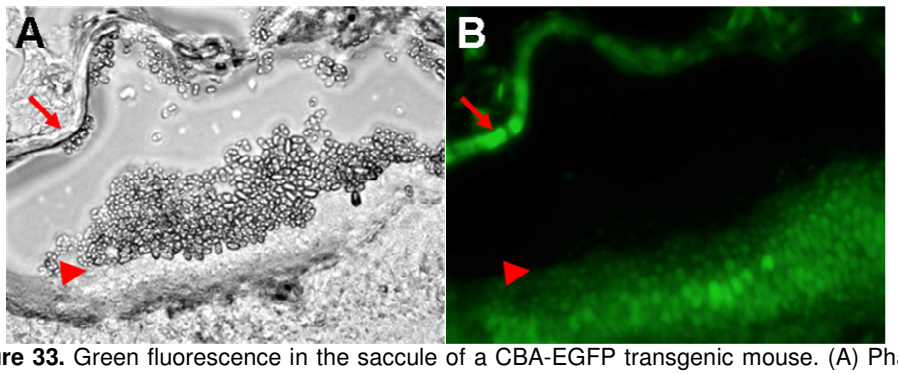

Figure 33. Green fluorescence in the saccule of a CBA-EGFP transgenic mouse. (A) Phase contrast and (B) fluorescence images of cryosectioned newborn CBA-EGFP transgenic mouse saccule. Non-sensory and sensory epithelia are labeled with arrow and arrowhead, respectively. Otoconia are readily visible in panel A.

As there is no known mouse NOXO1 expressing cell line, we could only test the CMV and the CBA driven transgenic constructs. NOX3 and NOXA1 expressing stable HEK293 cells were co-transfected with the transgenic constructs and superoxide production was measured (Figure 34).

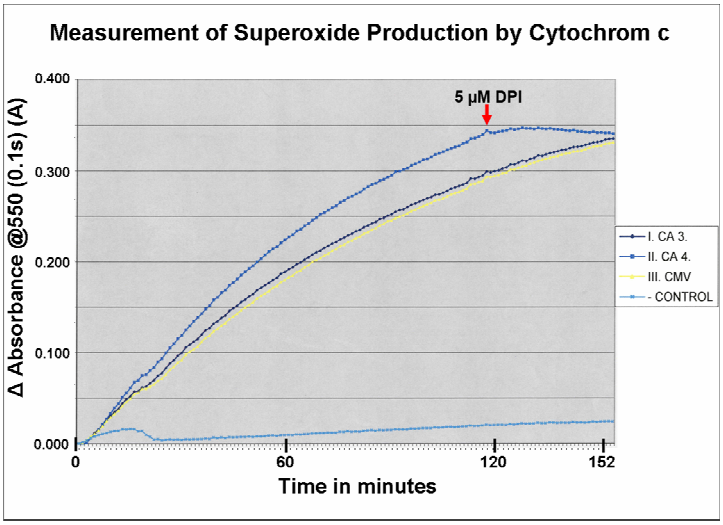

Figure 34. Superoxide production in HEK293 cells measured by Cytochrome c. *Control*: nontransfected cells; *CA 3*, *CA 4*: CMV enhancer/chicken β-actin promoter driven mNOXO1 constructs; *CMV*: CMV- promoter-enhancer of human cytomegalovirus driven mNOXO1. After 2 hours, CA 4 was inhibited by 5 µM BPI (red arrow).

First, we generated mice containing CMV promoter-driven Noxo1 transgene. Figure 35 shows the map of Noxo1 transgenic construct generated in pStec-1 vector. The expression cassette was isolated by KpnI restriction enzyme and microinjected into pronuclei of fertilized oocytes (C57BL/6 X SJL.F2) that were transferred into pseudopregnant foster mother. Mice were bred with Noxo1hslt/Noxo1hslt mice for two consecutive backcross generations to obtain transgene positive Noxo1hslt/Noxo1hslt mice (Figure 35).

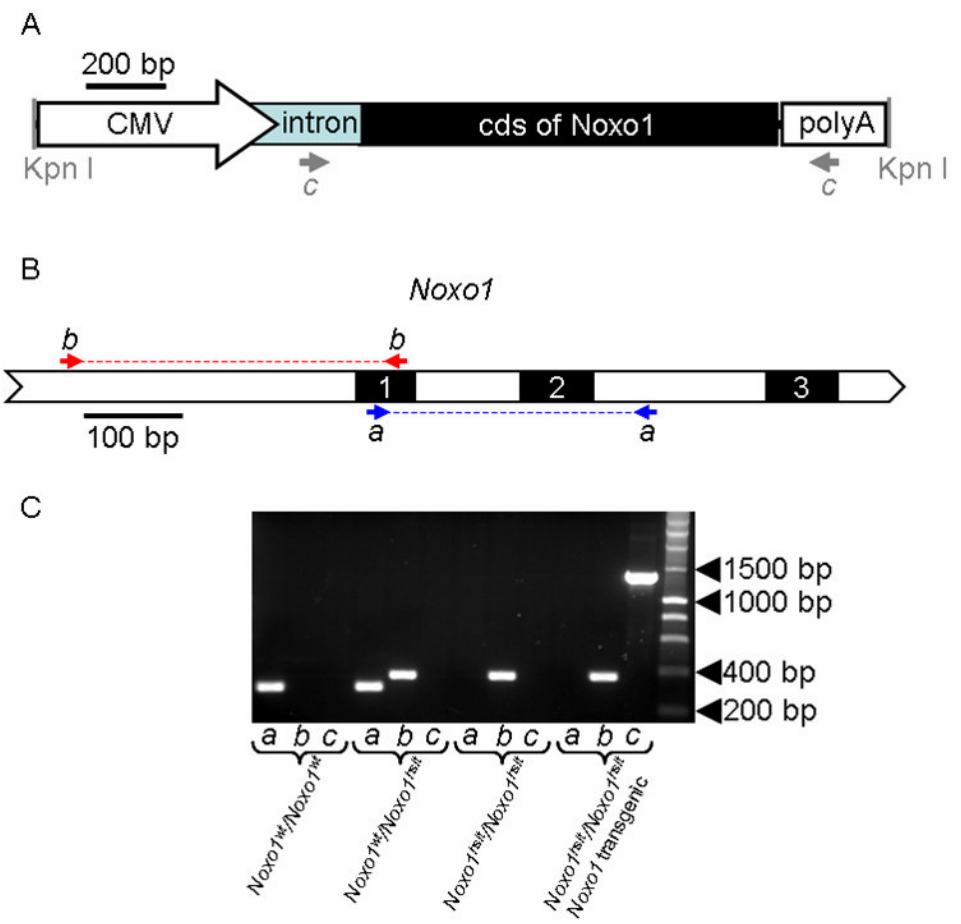

Figure 35. Generation of Noxo1 transgenic mice. (A) Map of Noxo1 transgenic construct using CMV promoter. Arrows labeled with *c* show the positions of primers used for detection of the transgene. (B) Schematic map of a 920 base pair (bp) long region of the Noxo1 gene. Numbered black boxes indicate exons, white boxes symbolize introns. Red arrows labeled 'b' show the annealing sites of genotyping primers used to detect Noxo1hslt allele; blue arrows labeled 'a' show the annealing sites of genotyping primers used to detect Noxo1wt allele. (C) Identification of Noxo1wt/Noxo1wt, Noxo1wt/Noxo1hslt, Noxo1hslt/Noxo1hslt, and Noxo1 transgene positive Noxo1hslt/Noxo1hslt genotypes using PCR primers 'a', 'b', and 'c' indicated in panel A and B. The last lane shows DNA molecular size markers.

Fourteen transgene positive *Noxo1*^{hslt}/*Noxo1*^{hslt} animals have been identified with wild type phenotype including their ability to swim (data not shown) and by von Kossa staining showing restored otoconia (Figure 36), suggesting that expression of the transgene rescued defects in the *Noxo1*^{hslt}/*Noxo1*^{hslt} mice and formally proving that the mutation in *Noxo1* was indeed responsible for the balance deficit of the hslt line.

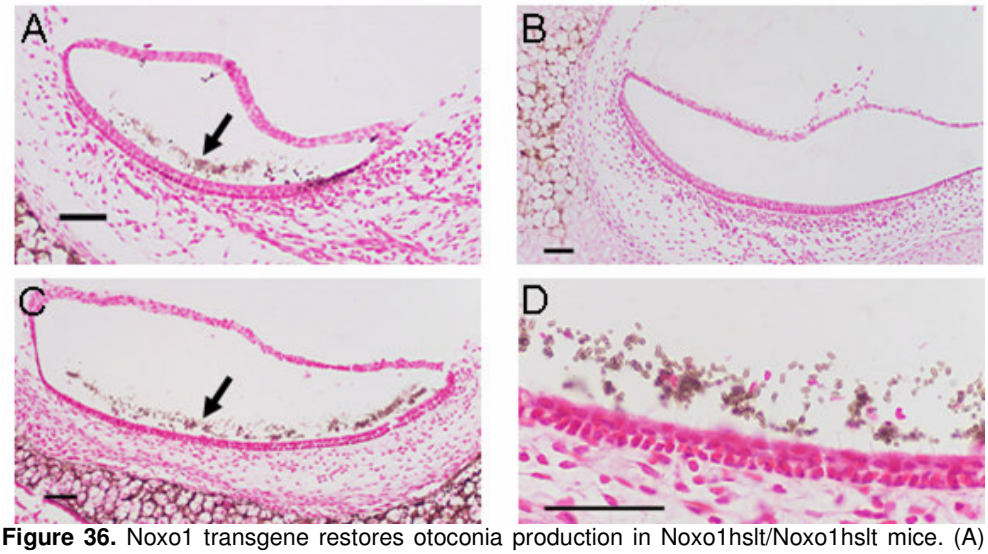

Figure 36. Noxo1 transgene restores otoconia production in Noxo1hslt/Noxo1hslt mice. (A) Von Kossa staining of calcium salts in the saccular otoconia (arrow) and in the adjacent bone (lower left corner) of a wild type mouse (P1). (B) Von Kossa staining does not detect otoconia in the saccule of a Noxo1hslt/Noxo1hslt mouse (P1) but stains calcium salts in the adjacent bone (upper left corner). (C, D) Otoconia (arrow) genesis is restored in the saccule of a Noxo1 transgene positive Noxo1hslt/Noxo1hslt mouse (P2), (C) low, and (D) high magnifications. Bars indicate 50 µm.

6.2 II. Functional deletion of NOXA1 gene in mice results in non-functional NOX3 complex

We and others have previously demonstrated that NOX3, similarly to NOX2, requires NOX regulator proteins: an “activator” subunit (NOXA1 or p67^{phox}) and an “organizer” subunit (NOXO1 or p47^{phox}) to function in transfected cells [72, 74, 138, 236]. However, Cheng *et al.* found that NOX3 was perfectly functional in the absence of NOXA1 or p67^{phox} in HEK293 cells, if NOXO1 was present [215]. The cause of the conflicting results is not known. However, it may be that NOXA1 is expressed at low levels in certain batches of HEK293

cells. As we found a complete dependence of NOX3 on a NOX activator protein in each of our transfection experiments with mouse proteins. we hypothesized that NOX3 requires such a protein at least *in vitro*. We chose NOXA1 as the potential activator subunit of NOX3, since it was expressed in embryonic inner ear (Figure 25) and the lack of the only other known NOX activator, p67^{phox}, does not cause balance problems in patients with p67^{phox}-deficient chronic granulomatous disease.

NOX activators have a characteristic domain structure. They contain 4 TPR (tetratricopeptide repeat) domains at their N-terminus that is likely to serve as a Rac binding site [90]. TPR domains are followed by an activation domain (AD), which is required for inducing superoxide production of NOX proteins. The C-terminal half of the NOX activators contains one (NOXA1) or two (p67^{phox}) SH3 domains and a PB1 domain. Both SH3 and PB1 domains are involved in protein-protein interactions with other NOX regulator subunits in p67^{phox} [74] and most likely in NOXA1 as well (Figure 37).

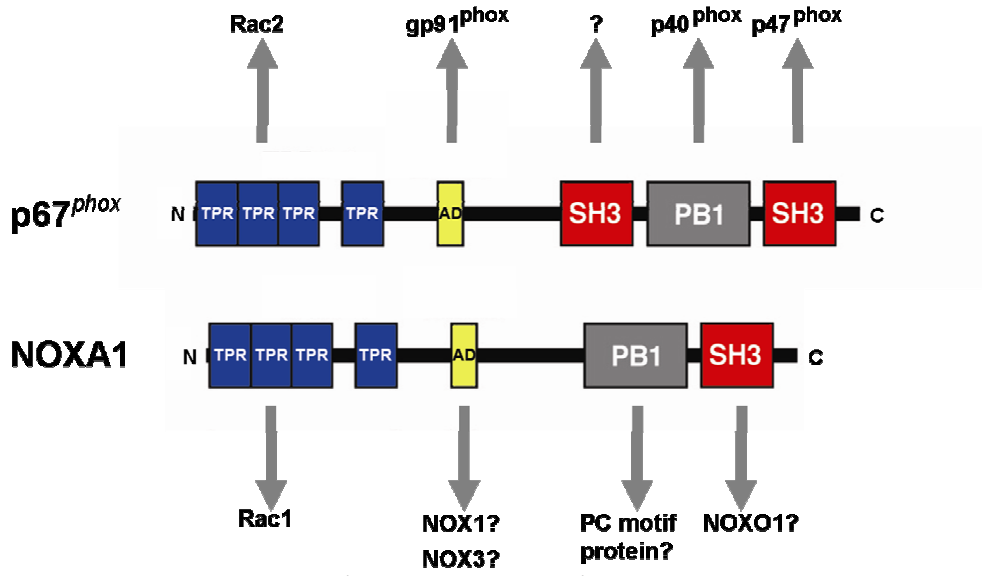

Figure 37. Comparison of p67^{phox} and NOXA1. p67^{phox} comprises TPR (tetratricopeptide) repeats, an activation domain (AD), two SH3 domains, and a PB1 domain. TPR repeats, activation domain, and C-terminal SH3 domain are conserved in NOXA1, probably allowing interaction with Rac1, NOX1/NOX3, and NOXO1. The NOXA1 PB1 domain does not interact with p40^{phox}, but possibly with another PC motif protein.

Until now, only two NOX activator genes have been identified: p67^{phox} and more recently NOXA1. We have screened the available complete, or almost

complete, mammalian genomic databases (e.g. human, mouse, and rat) but found no novel NOX activator gene. Therefore, based on *in vitro* data, either p67^{phox} or NOXA1 are likely important for NOX3 enzyme activity. NOXA1 mRNA was detected in the inner ear [72, 138], whereas p67^{phox} mRNA expression is restricted mainly to phagocytes. Furthermore, p67^{phox}-deficient CGD patients do not have vestibular dysfunction. Thus, we hypothesized that NOX3 requires NOXA1, and not p67^{phox} *in vivo.*

We tested our hypothesis in mouse models and studied NOXA1 expression in poorly characterized mutant mouse strains that show severe and non-syndromic balance deficit. The search criteria was the following: 1) recessive inheritance, 2) impaired balance including head tilt and bi-directional circling, 3) no other major defect, such as deafness, infertility, or early lethality, 4) chromosomal localization on chromosome 2 (location of mouse *NOXA1*) or unknown. Using these criterias, we identified two possible strains: “baln” and “nur39”, but neither were NOXA1 mutant mouse strain, which would serve as a functional NOXA1 KO (knockout) model.

Because of the absence of available Noxa1 mutant mice, we generated a Noxa1 deficient mouse strain. It was previously shown that the N-terminal half of the protein is crucial for its function, while the C-terminus can be deleted and the function would be still preserved *in vitro* [89]. Interestingly, the domain structure of p67^{phox} N-terminus is conserved in NOXA1, and there are very few differences in the activator domain sequence of the two proteins confirming the special importance of that region. In addition, the so-called activator domain seems to be essential to trigger superoxide production of gp91^{phox}. Since exon 6 of the *Noxa1* gene encodes the activator domain, we decided to target this region (Figure 11 and Figure 38).

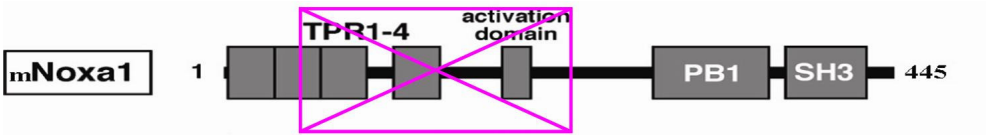

Figure 38. Targeting vector for the generation of NOXA1-deficient mice. A targeting vector designed to replace exons II–VI of the NOXA1 gene was constructed. Overview over the mouse NOXA1 protein targeting the tetratricopeptide repeat (TPR) domains and the activator domain (AD).

We hypothesize that NOXA1 deficiency causes the same phenotype which is observed in NOXO1-deficient hslt mice, i.e. impaired balance due to the absence of otoconia. The mice are currently in the process of breading.

6.3 III. Identification of a p22phox deficient mouse strain

Noxo1 and Nox3 are not sufficient to form a ROS-producing complex in transfected cells (Figure 26). We found that an activator subunit, either Noxa1 or p67^{phox}, was required for enzymatic activity in HEK293 cells, whereas other groups reported that p22^{phox}, a subunit of the phagocyte NADPH oxidase expressed endogenously in HEK293 cells [180], was also indispensable [180, 237]. Importantly, no p22^{phox} homolog has been identified in human, mouse, or rat genomic databases. Thus, either p22^{phox} or another protein with functional but not structural similarities is likely a critical subunit of the vestibular NADPH oxidase. Interestingly, the phenotypic allele of a balance deficient mutant mouse line, nmf333, has been localized to the region where the p22^{phox} gene (*CYBA*) is found (chr. 8, ~67 cM). This phenotype is described as head- and body tilt that can be observed at approximately 4 weeks of age with average onset of 4.6 +/- 0.6 weeks. (http://www.informatics.jax.org/searches/reference.cgi?83212)

We hypothesized that the nmf333 mutant mouse possesses a mutation in the mouse p22^{phox} gene, thus we ordered the nmf333 strain from Jackson Laboratories for further characterization. We got two homo- and two heterozygote mice and used the tails to isolate DNA for genotypization. The sequencing results revealed that the mutation is indeed located in the p22^{phox} gene. The thymidine at position 361 was substituted with a cytosine, which resulted in tyrosine to histidine amino acid change at position 121 (Figure 39).

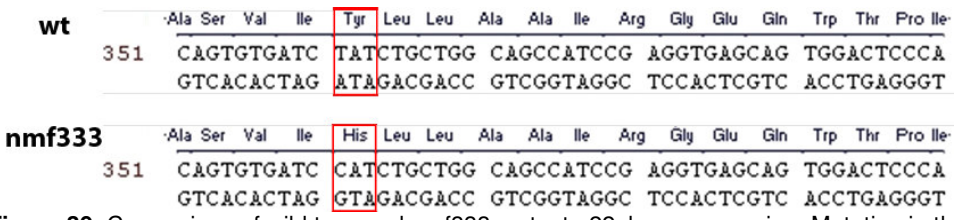

Figure 39. Comparison of wild type and nmf333 mutant p22phox gene region. Mutation in the nmf333 gene results in tyrosine to histidine amino acid change at amino acid position 121.

To determine whether the mutation also results in functional loss of the protein, we performed the well-known diagnostic nitroblue tetrazolium NBT test, which determines the functional loss of the phagocytic NADPH oxidase complex in neutrophils. As the stability of each subunit of the flavocytochrome b558 depends on heterodimer formation [80], mutations in either $gp91^{phox}$ or $p22^{phox}$ result in the absence of both subunits from the cell surface.

If the phagocytic NADPH oxidase complex is intact the NBT test turns the cytoplasm and phagosome into blue. The NBT test performed on blood from heterozygote nmf333 mice resulted in positive stain (Figure 40) while neutrophils from homozogote mice showed negative NBT test result (data not shown).

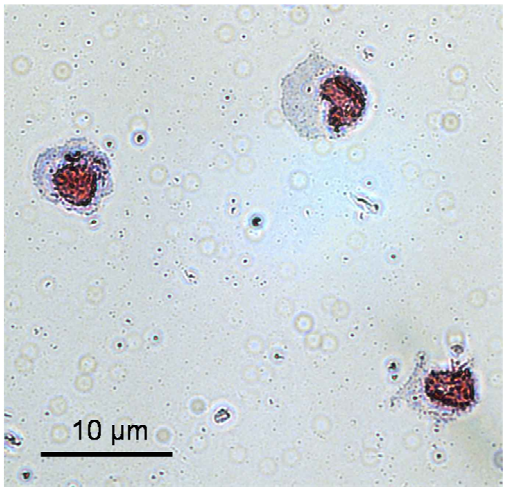

Figure 40. NBT test on activated, wild type mouse neutrophils. The blue staining of the cytoplasm and the phagosomes represents superoxide production by functional NOX2 complex.

We generated a construct expressing the mutant protein and overexpressed it in Epstein-Barr virus (EBV) transformed B cells derived from $p22^{phox}$ deficient patient. While the wt p22phox protein expressing construct restored the phenotype of the p22phox deficient B cells (data not shown), the mutant protein failed to restore superoxide production. This further supports our hypothesis that the tyrosine to histidine mutation results in fuctional loss of the p22phox protein.

To confirm the balance deficit reported by Jackson Laboratories in these mice, we performed the swimming test that showed results similar to Noxo1 deficient mice. These results suggest that $p22^{phox}$ might be a component of the vestibular NADPH complex. To prove this, we designed a transgenic construct to overexpress $p22^{phox}$ in nmf333 mice. The map of the construct is shown in Figure 41. We tested the construct by transfecting it into EBV transformed B cells derived from $p22^{phox}$ deficient patient. Overexpression of p22phox by our transgenic construct resulted in superoxide production in this deficient cell line (data not shown).

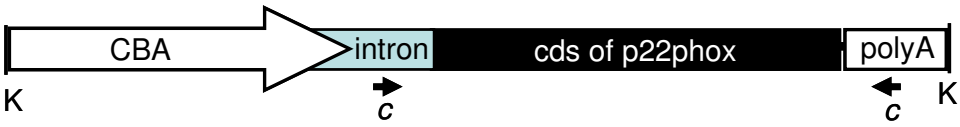

Figure 41. Map of $p22^{phox}$ transgenic constructs generated in pSTEC-1 vector. *CBA*: promoter. *Intron:* chimeric intron composed of the 5' splice site of the b-globin gene and the 3' splice site of an IgG intron. *CDS*: *p22phox* coding sequence. *polyA*: simian virus 40 polyadenylation site. *K*: KpnI restriction sites. For restriction digestion KpnI enzyme was used to isolate $p22^{phox}$ containing DNA cassettes. Arrows labeled with *c* show the positions of primers used for detection of the transgene.

If the overexpression of the transgene restores the phenotype it will prove our hypothesis that it is indeed the p22phox gene which when mutated resulted in balance problem in nmf333 mice. That will not only prove that p22phox is a indispensable partner of NOX3 but will also provide a useful tool to study the function of NOX1 in the colon that also likely require p22phox as a subunit for its full function.

7. Discussion

Reactive oxygen species (ROS) have been mainly recognized for their toxic effects in anti-microbial host defense as well as in aging and carcinogenesis. Several enzymes evolved for ROS production belong to the recently discovered NADPH oxidase (NOX) enzyme family, which consists of seven members in human: NOX1- 5, and the dual oxidases (DUOX1, 2). These enzymes share the capacity to transport electrons across a biological membrane and to generate superoxide and/or hydrogen peroxide.

The phagocytic NADPH oxidase (NOX2) is a well-known enzyme complex that plays a critical role in antimicrobial host defenses, which requires several regulatory subunits for its function. NOX3, based on its close homology to NOX2, may also require regulatory subunits for its function.

The goal of this study was to characterize the components and to understand the function of the vestibular NADPH oxidase system. NOX3 was shown to be highly expressed in the inner ear and its inactivation is resulted in balance deficit in mice. To further understand the function of the vestibular NADPH oxidase we looked for mutants in the mouse database with non-syndromic vestibular deficit in genes of potential subunits of the vestibular NADPH complex, such as NOXO1, NOXA1, and p22phox.

First, we identified and characterized a mutant hslt mouse strain with severe balance deficit. We demonstrated that this phenotype is resulted from an insertion of a deoxyadenosine into exon 1 of the *Noxo1* gene, causing a premature STOP signal during protein synthesis, thus functioning as a null allele. Noxo1 is highly expressed in the inner ear during otoconia genesis and its inactivation leads to severe imbalance caused by an arrest in the process of otoconia formation prior to calcium carbonate mineralization. Our data shows that NOXO1-dependent ROS production has an important and beneficial role in development.

Why ROS are required for otoconia genesis is an intriguing question. The main organic component of otoconia is OC-90/95, a 90-95 kDa glycoprotein that belongs to the family of secretory phospholipase A2 (sPLA2) [212, 213]

but appears to be catalytically inactive [210]. In the low [Ca^{2+}] environment of the endolymph, Ca^{2+} is thought to be supplied for crystal formation by lipid vesicles called “globular substance” [223, 238]. Both OC-90/95 and globular substance-like vesicles were present in the balance organs of hslt mice, and X-ray photoelectron spectroscopy indicated unaltered ratios of Na^+, K^+, and Cl^- in the endolymph of Noxo1 deficient mice (Figure 28) compared to wild type [143]. Therefore, we speculate that the lack of ROS may cause qualitative changes in OC-90/95 or in the lipid vesicles, or it may prevent the interaction of the two. Paffenholz *et al.* proposed that H_2O_2 induces disulfide bridge formation and conformation change in secreted OC-90/95 [139]. NADPH oxidase activity may determine the Ca^{2+} content of the nascent globular substance as well, since it can drive ion fluxes into intracellular vesicles [239] due to its depolarizing effect [240]. However, there is no report of extracellular formation of disulfide bridges in a sPLA2 family member, and the type of Ca^{2+} conductance that may be found in the globular substance is unknown.

Otoconia genesis is thought to require an interaction between OC-90/95 and the globular substance [214] that takes place in a gelatinous membrane consisting of tectorins [227] and otogelin [228, 229]. The nature of the protein-lipid interaction remains obscure, because otoconins did not disrupt lipid vesicles *in vitro* despite their classification as members of the sPLA2 enzyme family.

It is well known that ROS can cause lipid peroxidation [230] and the resulting lipoperoxides have a distinct physicochemical state that makes them readily accessible to sPLA2 [231, 232]. Lipid peroxidation requires not only ROS but also a peroxidase [233]. We detected lactoperoxidase (LPO) mRNA in the utricle and saccule but other peroxidases were absent (Figure 31). These data raise the possibility that a Noxo1-dependent NADPH oxidase and LPO form an oxidative system that peroxidizes the lipid envelope of the globular substance, which may render it accessible and susceptible to OC-90/95. Vesicle disruption by OC-90/95 may not require catalytic activity, as has been observed with sPLA2-like myotoxins [241]. When Ca^{2+} is released from the vesicles, its high local concentration will promote mineralization upon an OC-90/95 containing protein scaffold.

In vitro studies have demonstrated that NOX3, similar to NOX1 and NOX2, is also depended on a NOX activator (e.g. NOXA1 or p67phox) in transfected HEK293 cells [72, 74, 138, 236]. We hypothesized that NOX3 requires NOXA1, since it was expressed in embryonic inner ear (Figure 25) and the lack of the only other known NOX activator, p67phox, does not cause balance problems in patients with p67phox-deficient chronic granulomatous disease.
To test this hypothesis we generated NOXA1 deficient mice. Analysis of these mice will not only reveal whether NOXA1 is indeed the activator subunit of the vestibular NADPH complex but it will provide a useful tool for the understanding of the function of the NOX1 complex that very likely utilizes NOXA1 as its activator subunit [72, 74, 87, 93, 113].
The other possible candidate that might play an important role in the regulation of NOX3 is $p22^{phox}$ [180, 237]. We identified a mutant nmf333 mouse strain, which has a missense mutation in the $p22^{phox}$ gene which results in the loss of $p22^{phox}$ protein function. These mice have balance deficit and their phagocytes have a defect in superoxide generation. We used transgenic rescue to confirm that the balance deficit in nmf333 mice is due to the loss of p22phox function. If p22phox were a component of the vestibular NADPH complex, it would raise the question why CGD patients with p22phox deficiency have not been reported who have balance deficit as well. It is possible that patients with p22phox deficiency are very rare and they are in bad condition due to serious immunodeficiency. This contradiction can be solved, however, by specifically testing patients with p22phox deficiency about their balance.

In conclusion, this work has identified NOXO1 as the organizer subunit of the vestibular NADPH oxidase system and provided evidence that $p22^{phox}$ and possibly NOXA1 are also part of the vestibular ROS generating enzyme complex. These data help our understanding about the development of the inner ear and give further insights into the biological function of reactive oxygen species.

8. Summary

In this work, I have summarized those studies that I performed at the University of Geneva, Switzerland and the Department of Internal Medicine at the University of Iowa, USA between 2001 and 2008. We had been studying the role of NADPH oxidases in host defense and were interested in the role and function of the vestibular NADPH oxidase.

Based on the literature and our results we hypothesized that the vestibular NADPH oxidase NOX3 requires NADPH oxidase organizer 1 (NOXO1), activator 1 (NOXA1), as well as the $p22^{phox}$ regulatory subunits for its function.

We identified a 'head slant' (hslt) mouse strain with a spontaneous mutation in the *Noxo1* gene. The balance deficit of homozygous mice of hslt line was manifested as early as day 4 after birth. Pups that were placed on their back did not attempt to right themselves to the ventral position. From day 18, they exhibited distinct head and body tilt and an abnormal reaching response during falling compared to heterozygous littermates or in wild type mice. Unlike control mice, affected mutants could not orient themselves in water and thus became submerged and introduced a so-called "non-swimming" phenotype. Histological analysis by von Kossa staining of inner ears of embryonic day (ED) 17 and newborn (postnatal day 0-2, P0-2) $Noxo1^{hslt}/Noxo1^{hslt}$ mice demonstrated the complete absence of calcium carbonate crystallization in $Noxo1^{hslt}/Noxo1^{hslt}$ inner ears. Scanning electron microscopy not only verified the lack of otoconia in $Noxo1^{hslt}/Noxo1^{hslt}$ animals but also showed coral-like conglomerates above the hair cells. Immunohistological analysis has shown that the conglomerates are composed of OC-90/95 protein and may preserve a brief developmental stage prior to calcium carbonate mineralization.

In order to demonstrate that the severe imbalance of hslt mice was caused by the mutation in *Noxo1*, and not in a linked gene, we used transgenic rescue. We generated mice containing CMV promoter-driven *Noxo1* transgene. Transgenic mice were bred with *Noxo1hslt/Noxo1hslt* mice for two consecutive backcross generations to obtain transgene positive *Noxo1hslt/Noxo1hslt* mice. Fourteen transgene positive $Noxo1^{hslt}/Noxo1^{hslt}$

animals have been identified with wild type phenotype including their ability to swim and by von Kossa staining showing restored otoconia suggesting that expression of the transgene rescued defects in the *Noxo1*^{hslt}/*Noxo1*^{hslt} mice and formally proving that the mutation in *Noxo1* was indeed responsible for the balance deficit of the hslt line.

We investigated whether the hslt mutation of Noxo1 may prevent ROS production by a NOX3-NOXO1 containing enzyme complex. HEK293T cells were transfected with mouse Nox3, Noxo1^{wt} or Noxo1^{hslt} with or without Nox activator 1 (Noxa1). Superoxide production was measured by the superoxide dismutase-dependent reduction of ferricytochrome *c*. We chose NOXA1 as the potential activator subunit of Nox3, since it was expressed in embryonic inner ear and the lack of the only other known Nox activator, p67^{phox}, does not cause balance problems in patients with p67^{phox}-deficient chronic granulomatous disease. Mouse Nox3 required the co-transfection of both mouse Noxo1^{wt} and Noxa1 to achieve maximal superoxide generation. Furthermore, replacement of Noxo1^{wt} by Noxo1^{hslt} drastically reduced Nox3 enzyme activity independent of combination of the subunits.

In order to demonstrate that NOX3 requires NOXA1 we generated NOXA1 deficient mice. It was previously shown that the N-terminal half of the protein is crucial for its function, we decided to target this region. Analysis of these mice will provide a useful tool for the understanding of the function of the NOX3 and NOX1 complex which very likely utilizes NOXA1 as its activator subunit.

NOXO1 and NOX3 are not sufficient to form a ROS-producing complex in transfected cells. Thus, either p22^{phox} or another protein with functional similarities is likely a critical subunit of the vestibular NADPH oxidase. We identified a mutant mouse strain, nmf333, which possesses a mutation in the mouse p22^{phox} gene. Further characterization of these mice revealed that the thymidine at position 361 was substituted with a cytosine, which resulted in tyrosine to histidine amino acid change at position 121. To determine whether the mutation also results in functional loss of the protein, we performed the well-known diagnostic nitroblue tetrazolium (NBT) test, which determines the functional loss of the phagocytic NADPH oxidase complex in neutrophils. The

NBT test performed on blood from homozygous mice showed negative results. We generated a construct expressing the mutant protein and overexpressed it in EBV transformed B cells derived from $p22^{phox}$ deficient patient. While the wt $p22^{phox}$ protein expressing construct restored the phenotype of the $p22^{phox}$ deficient B cells, the mutant protein failed to restore superoxide production. To confirm the balance deficit reported by Jackson Laboratories in these mice, we performed the swimming test that showed results similar to Noxo1 deficient mice. These results suggest that $p22^{phox}$ might be a component of the vestibular NADPH complex. To prove this, we designed a transgenic construct to overexpress $p22^{phox}$ in nmf333 mice. If the overexpression of the transgene restores the phenotype will not only prove that p22phox is an indispensable partner of NOX3 but it will also provide a useful tool to study the function of NOX1 in the colon that also likely require p22phox as a subunit for its full function.

9. References

1. **Commoner, B., J. Townsend, and G. Pake, *Free radicals in biological materials*, in *Nature*. 1954. p. 689-691.**
2. **Harman, D., *Aging: a theory based on free radical and radiation chemistry.* J Gerontol, 1956. 11(11): p. 298-300.**
3. **Herman, D., *The aging process.* Proc Natl Acad Sci USA, 1981. 78: p. 7124-7128.**
4. **Droge, W., *Free radicals in the physiological control of cell function.* Physiol Rev, 2002. 82(1): p. 47-95.**
5. **Ricciarelli, R., J.M. Zingg, and A. Azzi, *Vitamin E 80th anniversary: a double life, not only fighting radicals.* IUBMB Life, 2001. 52(1-2): p. 71-6.**
6. **Reiter, R.J., et al., *Melatonin: detoxification of oxygen and nitrogen-based toxic reactants.* Adv Exp Med Biol, 2003. 527: p. 539-48.**
7. **Kojo, S., *Vitamin C: basic metabolism and its function as an index of oxidative stress.* Curr Med Chem, 2004. 11(8): p. 1041-64.**
8. **Lambeth, J.D., *NOX enzymes and the biology of reactive oxygen.* Nat Rev Immunol, 2004. 4(3): p. 181-9.**
9. **Bedard, K. and K.H. Krause, *The NOX family of ROS-generating NADPH oxidases: physiology and pathophysiology.* Physiol Rev, 2007. 87(1): p. 245-313.**
10. **Cross, A.R. and A.W. Segal, *The NADPH oxidase of professional phagocytes--prototype of the NOX electron transport chain systems.* Biochim Biophys Acta, 2004. 1657(1): p. 1-22.**
11. **Machlin, L.J. and A. Bendich, *Free radical tissue damage: protective role of antioxidant nutrients.* Faseb J, 1987. 1(6): p. 441-5.**
12. **Ames, B.N., M.K. Shigenaga, and T.M. Hagen, *Oxidants, antioxidants, and the degenerative diseases of aging.* Proc Natl Acad Sci U S A, 1993. 90(17): p. 7915-22.**
13. **Pacifici, R.E. and K.J. Davies, *Protein, lipid and DNA repair systems in oxidative stress: the free-radical theory of aging revisited.* Gerontology, 1991. 37(1-3): p. 166-80.**
14. **Traber, M.G., *Vitamin E, oxidative stress and 'healthy ageing'.* Eur J Clin Invest, 1997. 27(10): p. 822-4.**
15. **Brand, M.D., et al., *Mitochondrial superoxide: production, biological effects, and activation of uncoupling proteins.* Free Radic Biol Med, 2004. 37(6): p. 755-67.**
16. **Cadenas, E. and K.J. Davies, *Mitochondrial free radical generation, oxidative stress, and aging.* Free Radic Biol Med, 2000. 29(3-4): p. 222-30.**
17. **Inoue, M., et al., *Mitochondrial generation of reactive oxygen species and its role in aerobic life.* Curr Med Chem, 2003. 10(23): p. 2495-505.**
18. **Turrens, J.F., *Mitochondrial formation of reactive oxygen species.* J Physiol, 2003. 552(Pt 2): p. 335-44.**
19. **Lesnefsky, E.J. and C.L. Hoppel, *Ischemia-reperfusion injury in the aged heart: role of mitochondria.* Arch Biochem Biophys, 2003. 420(2): p. 287-97.**
20. **Haynes, V., et al., *Mitochondrial nitric-oxide synthase: enzyme expression, characterization, and regulation.* J Bioenerg Biomembr, 2004. 36(4): p. 341-6.**

21. **Nelson, D.R., et al.,** ***Comparison of cytochrome P450 (CYP) genes from the mouse and human genomes, including nomenclature recommendations for genes, pseudogenes and alternative-splice variants.*** **Pharmacogenetics, 2004. 14(1): p. 1-18.**
22. **Schrader, M. and H.D. Fahimi,** ***Mammalian peroxisomes and reactive oxygen species.*** **Histochem Cell Biol, 2004. 122(4): p. 383-93.**
23. **Babior, B.M., J.D. Lambeth, and W. Nauseef,** ***The neutrophil NADPH oxidase.*** **Arch Biochem Biophys, 2002. 397(2): p. 342-4.**
24. **Babior, B.M.,** ***The NADPH oxidase of endothelial cells.*** **IUBMB Life, 2000. 50(4-5): p. 267-9.**
25. **Baldridge, C. and R. Gerard,** ***The extra respiration of phagocytosis.*** **Am J Physiol., 1932. 103(1): p. 235-6.**
26. **Sbarra, A.J. and M.L. Karnovsky,** ***The biochemical basis of phagocytosis. I. Metabolic changes during the ingestion of particles by polymorphonuclear leukocytes.*** **J Biol Chem, 1959. 234(6): p. 1355-62.**
27. **Selvaraj, R.J. and A.J. Sbarra,** ***The role of the phagocyte in host-parasite interactions. VII. Di- and triphosphopyridine nucleotide kinetics during phagocytosis.*** **Biochim Biophys Acta, 1967. 141(2): p. 243-9.**
28. **Berendes, H., R.A. Bridges, and R.A. Good,** ***A fatal granulomatosus of childhood: the clinical study of a new syndrome.*** **Minn Med, 1957. 40(5): p. 309-12.**
29. **Curnutte, J.T.,** ***Conventional versus interferon-gamma therapy in chronic granulomatous disease.*** **J Infect Dis, 1993. 167 Suppl 1: p. S8-12.**
30. **Baehner, R.L. and D.G. Nathan,** ***Leukocyte oxidase: defective activity in chronic granulomatous disease.*** **Science, 1967. 155(764): p. 835-6.**
31. **Babior, B.M., R.S. Kipnes, and J.T. Curnutte,** ***Biological defense mechanisms. The production by leukocytes of superoxide, a potential bactericidal agent.*** **J Clin Invest, 1973. 52(3): p. 741-4.**
32. **Mills, E.L. and P.G. Quie,** ***Congenital disorders of the function of polymorphonuclear neutrophils.*** **Rev Infect Dis, 1980. 2(3): p. 505-17.**
33. **Bellavite, P.,** ***The superoxide-forming enzymatic system of phagocytes.*** **Free Radic Biol Med, 1988. 4(4): p. 225-61.**
34. **Segal, A.W., Jones, O.T., Webster, D., Allison, A.C.,** ***Absence of a newly described cytochrome b from neutrophils of patients with chronic granulomatous disease.*** **Lancet, 1978. 2(8087): p. 446-449.**
35. **Segal, A.W., Jones, O.T.,** ***Novel cytochrome b system in phagocytic vacuoles of human granulocytes.*** **Nature, 1978. 276(5687): p. 515-517.**
36. **Royer-Pokora, B., et al.,** ***Cloning the gene for an inherited human disorder--chronic granulomatous disease--on the basis of its chromosomal location.*** **Nature, 1986. 322(6074): p. 32-8.**
37. **Teahan, C., et al.,** ***The X-linked chronic granulomatous disease gene codes for the beta-chain of cytochrome b-245.*** **Nature, 1987. 327(6124): p. 720-1.**
38. **Parkos, C.A., et al.,** ***The quaternary structure of the plasma membrane b-type cytochrome of human granulocytes.*** **Biochim Biophys Acta, 1988. 932(1): p. 71-83.**
39. **Segal, A.W.,** ***Absence of both cytochrome b-245 subunits from neutrophils in X-linked chronic granulomatous disease.*** **Nature, 1987. 326(6108): p. 88-91.**

40. **Dinauer, M.C., et al.,** ***The glycoprotein encoded by the X-linked chronic granulomatous disease locus is a component of the neutrophil cytochrome b complex.*** **Nature, 1987. 327(6124): p. 717-20.**
41. **Segal, A.W.,** ***Absence of both cytochrome b-245 subunits from neutrophils in X-linked chronic granulomatous disease.*** **Nature, 1987. 326(6108): p. 88-91.**
42. **Parkos, C.A., Dinauer, M.C., Walker, L.E., Allen, R.A., Jesaitis, A.J., Orkin, S.H.,** ***Primary structure and unique expression of the 22-kilodalton light chain of human neutrophil cytochrome b.*** **Proc. Natl. Acad. Sci. U.S.A., 1988. 85(10): p. 3319-3323.**
43. **Parkos, C.A., et al.,** ***Absence of both the 91kD and 22kD subunits of human neutrophil cytochrome b in two genetic forms of chronic granulomatous disease.*** **Blood, 1989. 73(6): p. 1416-20.**
44. **Dinauer, M.C., et al.,** ***Human neutrophil cytochrome b light chain (p22-phox). Gene structure, chromosomal location, and mutations in cytochrome-negative autosomal recessive chronic granulomatous disease.*** **J Clin Invest, 1990. 86(5): p. 1729-37.**
45. **Borregaard, N., et al.,** ***Cytochrome b is present in neutrophils from patients with chronic granulomatous disease.*** **Lancet, 1979. 1(8123): p. 949-51.**
46. **Heyneman, R.A. and R.E. Vercauteren,** ***Activation of a NADPH oxidase from horse polymorphonuclear leukocytes in a cell-free system.*** **J Leukoc Biol, 1984. 36(6): p. 751-9.**
47. **Bromberg, Y. and E. Pick,** ***Activation of NADPH-dependent superoxide production in a cell-free system by sodium dodecyl sulfate.*** **J Biol Chem, 1985. 260(25): p. 13539-45.**
48. **Volpp, B.D., W.M. Nauseef, and R.A. Clark,** ***Two cytosolic neutrophil oxidase components absent in autosomal chronic granulomatous disease.*** **Science, 1988. 242(4883): p. 1295-7.**
49. **Nunoi, H., et al.,** ***Two forms of autosomal chronic granulomatous disease lack distinct neutrophil cytosol factors.*** **Science, 1988. 242(4883): p. 1298-301.**
50. **Segal, A.W., et al.,** ***Stimulated neutrophils from patients with autosomal recessive chronic granulomatous disease fail to phosphorylate a Mr-44,000 protein.*** **Nature, 1985. 316(6028): p. 547-9.**
51. **Leto, T.L., et al.,** ***Cloning of a 67-kD neutrophil oxidase factor with similarity to a noncatalytic region of p60c-src.*** **Science, 1990. 248(4956): p. 727-30.**
52. **Volpp, B.D., et al.,** ***Cloning of the cDNA and functional expression of the 47-kilodalton cytosolic component of human neutrophil respiratory burst oxidase.*** **Proc Natl Acad Sci U S A, 1989. 86(18): p. 7195-9.**
53. **Abo, A., et al.,** ***Activation of the NADPH oxidase involves the small GTP-binding protein p21rac1.*** **Nature, 1991. 353(6345): p. 668-70.**
54. **Seifert, R., W. Rosenthal, and G. Schultz,** ***Guanine nucleotides stimulate NADPH oxidase in membranes of human neutrophils.*** **FEBS Lett, 1986. 205(1): p. 161-5.**
55. **Ligeti, E., J. Doussiere, and P.V. Vignais,** ***Activation of the O2(.-)-generating oxidase in plasma membrane from bovine polymorphonuclear neutrophils by arachidonic acid, a cytosolic factor of protein nature, and nonhydrolyzable analogues of GTP.*** **Biochemistry, 1988. 27(1): p. 193-200.**

56. **Gabig, T.G., et al.,** ***Regulation of neutrophil NADPH oxidase activation in a cell-free system by guanine nucleotides and fluoride. Evidence for participation of a pertussis and cholera toxin-insensitive G protein.*** **J Biol Chem, 1987. 262(4): p. 1685-90.**

57. **Knaus, U.G., et al.,** ***Regulation of phagocyte oxygen radical production by the GTP-binding protein Rac 2.*** **Science, 1991. 254(5037): p. 1512-5.**

58. **Bokoch, G.M. and B.A. Diebold,** ***Current molecular models for NADPH oxidase regulation by Rac GTPase.*** **Blood, 2002. 100(8): p. 2692-6.**

59. **Wientjes, F.B., et al.,** ***p40phox, a third cytosolic component of the activation complex of the NADPH oxidase to contain src homology 3 domains.*** **Biochem J, 1993. 296 (Pt 3): p. 557-61.**

60. **Someya, A., I. Nagaoka, and T. Yamashita,** ***Purification of the 260 kDa cytosolic complex involved in the superoxide production of guinea pig neutrophils.*** **FEBS Lett, 1993. 330(2): p. 215-8.**

61. **Cross, A.R.,** ***p40(phox) Participates in the activation of NADPH oxidase by increasing the affinity of p47(phox) for flavocytochrome b(558).*** **Biochem J, 2000. 349(Pt 1): p. 113-7.**

62. **Suh, Y.A., et al.,** ***Cell transformation by the superoxide-generating oxidase Mox1.*** **Nature, 1999. 401(6748): p. 79-82.**

63. **Banfi, B., et al.,** ***A mammalian H+ channel generated through alternative splicing of the NADPH oxidase homolog NOH-1.*** **Science, 2000. 287(5450): p. 138-42.**

64. **Kikuchi, H., et al.,** ***NADPH oxidase subunit, gp91(phox) homologue, preferentially expressed in human colon epithelial cells.*** **Gene, 2000. 254(1-2): p. 237-43.**

65. **Lambeth, J.D., et al.,** ***Novel homologs of gp91phox.*** **Trends Biochem Sci, 2000. 25(10): p. 459-61.**

66. **Cheng, G., et al.,** ***Homologs of gp91phox: cloning and tissue expression of Nox3, Nox4, and Nox5.*** **Gene, 2001. 269(1-2): p. 131-40.**

67. **Geiszt, M., et al.,** ***Identification of renox, an NAD(P)H oxidase in kidney.*** **Proc Natl Acad Sci U S A, 2000. 97(14): p. 8010-4.**

68. **Shiose, A., et al.,** ***A novel superoxide-producing NAD(P)H oxidase in kidney.*** **J Biol Chem, 2001. 276(2): p. 1417-23.**

69. **Banfi, B., et al.,** ***A Ca(2+)-activated NADPH oxidase in testis, spleen, and lymph nodes.*** **J Biol Chem, 2001. 276(40): p. 37594-601.**

70. **Dupuy, C., et al.,** ***Purification of a novel flavoprotein involved in the thyroid NADPH oxidase. Cloning of the porcine and human cdnas.*** **Journal of Biological Chemistry, 1999. 274(52): p. 37265-37269.**

71. **De Deken, X., et al.,** ***Cloning of two human thyroid cDNAs encoding new members of the NADPH oxidase family.*** **J Biol Chem, 2000. 275(30): p. 23227-33.**

72. **Banfi, B., et al.,** ***Two novel proteins activate superoxide generation by the NADPH oxidase NOX1.*** **J Biol Chem, 2003. 278(6): p. 3510-3.**

73. **Geiszt, M., et al.,** ***Proteins homologous to p47phox and p67phox support superoxide production by NAD(P)H oxidase 1 in colon epithelial cells.*** **J Biol Chem, 2003. 278(22): p. 20006-12.**

74. **Takeya, R., et al.,** ***Novel human homologues of p47phox and p67phox participate in activation of superoxide-producing NADPH oxidases.*** **J Biol Chem, 2003. 278(27): p. 25234-46.**

75. **Cheng, G. and J.D. Lambeth,** ***NOXO1, regulation of lipid binding, localization, and activation of Nox1 by the Phox homology (PX) domain.*** **J Biol Chem, 2004. 279(6): p. 4737-42.**

76. **Grasberger, H. and S. Refetoff,** ***Identification of the maturation factor for dual oxidase. Evolution of an eukaryotic operon equivalent.*** **J Biol Chem, 2006. 281(27): p. 18269-72.**

77. **Kawahara, B.T., M.T. Quinn, and J.D. Lambeth,** ***Molecular evolution of the reactive oxygen-generating NADPH oxidase (Nox/Duox) family of enzymes.*** **BMC Evol Biol, 2007. 7: p. 109.**

78. **Harper, A.M., M.F. Chaplin, and A.W. Segal,** ***Cytochrome b-245 from human neutrophils is a glycoprotein.*** **Biochem J, 1985. 227(3): p. 783-8.**

79. **Yu, L., et al.,** ***Biosynthesis of flavocytochrome b558 . gp91(phox) is synthesized as a 65-kDa precursor (p65) in the endoplasmic reticulum.*** **J Biol Chem, 1999. 274(7): p. 4364-9.**

80. **DeLeo, F.R., et al.,** ***Processing and maturation of flavocytochrome b558 include incorporation of heme as a prerequisite for heterodimer assembly.*** **J Biol Chem, 2000. 275(18): p. 13986-93.**

81. **Paclet, M.H., et al.,** ***P67-phox-mediated NADPH oxidase assembly: imaging of cytochrome b558 liposomes by atomic force microscopy.*** **Biochemistry, 2000. 39(31): p. 9302-10.**

82. **Groemping, Y. and K. Rittinger,** ***Activation and assembly of the NADPH oxidase: a structural perspective.*** **Biochem J, 2005. 386(Pt 3): p. 401-16.**

83. **Nauseef, W.M.,** ***Assembly of the phagocyte NADPH oxidase.*** **Histochem Cell Biol, 2004. 122(4): p. 277-91.**

84. **Sumimoto, H., K. Miyano, and R. Takeya,** ***Molecular composition and regulation of the Nox family NAD(P)H oxidases.*** **Biochem Biophys Res Commun, 2005. 338(1): p. 677-86.**

85. **Stasia, M.J., et al.,** ***A novel and unusual case of chronic granulomatous disease in a child with a homozygous 36-bp deletion in the CYBA gene (A22(0)) leading to the activation of a cryptic splice site in intron 4.*** **Hum Genet, 2002. 110(5): p. 444-50.**

86. **Sumimoto, H., et al.,** ***Assembly and activation of the phagocyte NADPH oxidase. Specific interaction of the N-terminal Src homology 3 domain of p47phox with p22phox is required for activation of the NADPH oxidase.*** **J Biol Chem, 1996. 271(36): p. 22152-8.**

87. **Han, C.H., et al.,** ***Regulation of the neutrophil respiratory burst oxidase. Identification of an activation domain in p67(phox).*** **J Biol Chem, 1998. 273(27): p. 16663-8.**

88. **Diebold, B.A. and G.M. Bokoch,** ***Molecular basis for Rac2 regulation of phagocyte NADPH oxidase.*** **Nat Immunol, 2001. 2(3): p. 211-5.**

89. **Koga, H., et al.,** ***Tetratricopeptide repeat (TPR) motifs of p67(phox) participate in interaction with the small GTPase Rac and activation of the phagocyte NADPH oxidase.*** **J Biol Chem, 1999. 274(35): p. 25051-60.**

90. **Lapouge, K., et al.,** ***Structure of the TPR domain of p67phox in complex with Rac.GTP.*** **Mol Cell, 2000. 6(4): p. 899-907.**

91. **Vignais, P.V.,** ***The superoxide-generating NADPH oxidase: structural aspects and activation mechanism.*** **Cell Mol Life Sci, 2002. 59(9): p. 1428-59.**

92. **Finegold, A.A., et al.,** ***Intramembrane bis-heme motif for transmembrane electron transport conserved in a yeast iron reductase and the human NADPH oxidase.*** **J Biol Chem, 1996. 271(49): p. 31021-4.**
93. **Nisimoto, Y., et al.,** ***The p67(phox) activation domain regulates electron flow from NADPH to flavin in flavocytochrome b(558).*** **J Biol Chem, 1999. 274(33): p. 22999-3005.**
94. **Clark, R.A., et al.,** ***NADPH oxidase of human neutrophils. Subcellular localization and characterization of an arachidonate-activatable superoxide-generating system.*** **J Biol Chem, 1987. 262(9): p. 4065-74.**
95. **Doussiere, J., J. Gaillard, and P.V. Vignais,** ***Electron transfer across the O2- generating flavocytochrome b of neutrophils. Evidence for a transition from a low-spin state to a high-spin state of the heme iron component.*** **Biochemistry, 1996. 35(41): p. 13400-10.**
96. **Serrano, F., et al.,** ***NADPH oxidase immunoreactivity in the mouse brain.*** **Brain Res, 2003. 988(1-2): p. 193-8.**
97. **Heymes, C., et al.,** ***Increased myocardial NADPH oxidase activity in human heart failure.*** **J Am Coll Cardiol, 2003. 41(12): p. 2164-71.**
98. **Javesghani, D., et al.,** ***Molecular characterization of a superoxide-generating NAD(P)H oxidase in the ventilatory muscles.*** **Am J Respir Crit Care Med, 2002. 165(3): p. 412-8.**
99. **Reinehr, R., et al.,** ***Involvement of NADPH oxidase isoforms and Src family kinases in CD95-dependent hepatocyte apoptosis.*** **J Biol Chem, 2005. 280(29): p. 27179-94.**
100. **Gorlach, A., et al.,** ***A gp91phox containing NADPH oxidase selectively expressed in endothelial cells is a major source of oxygen radical generation in the arterial wall.*** **Circ Res, 2000. 87(1): p. 26-32.**
101. **Jones, S.A., et al.,** ***Expression of phagocyte NADPH oxidase components in human endothelial cells.*** **Am J Physiol, 1996. 271(4 Pt 2): p. H1626-34.**
102. **Li, J.M. and A.M. Shah,** ***Intracellular localization and preassembly of the NADPH oxidase complex in cultured endothelial cells.*** **J Biol Chem, 2002. 277(22): p. 19952-60.**
103. **Piccoli, C., et al.,** ***Characterization of mitochondrial and extra-mitochondrial oxygen consuming reactions in human hematopoietic stem cells. Novel evidence of the occurrence of NAD(P)H oxidase activity.*** **J Biol Chem, 2005. 280(28): p. 26467-76.**
104. **Borregaard, N., et al.,** ***Subcellular localization of the b-cytochrome component of the human neutrophil microbicidal oxidase: translocation during activation.*** **J Cell Biol, 1983. 97(1): p. 52-61.**
105. **Huang, J., N.D. Hitt, and M.E. Kleinberg,** ***Stoichiometry of p22-phox and gp91-phox in phagocyte cytochrome b558.*** **Biochemistry, 1995. 34(51): p. 16753-7.**
106. **Ambruso, D.R., N. Cusack, and G. Thurman,** ***NADPH oxidase activity of neutrophil specific granules: requirements for cytosolic components and evidence of assembly during cell activation.*** **Mol Genet Metab, 2004. 81(4): p. 313-21.**
107. **Karlsson, A. and C. Dahlgren,** ***Assembly and activation of the neutrophil NADPH oxidase in granule membranes.*** **Antioxid Redox Signal, 2002. 4(1): p. 49-60.**
108. **Kjeldsen, L., et al.,** ***Isolation and characterization of gelatinase granules from human neutrophils.*** **Blood, 1994. 83(6): p. 1640-9.**

109. **Garcia, R.C. and A.W. Segal,** ***Changes in the subcellular distribution of the cytochrome b-245 on stimulation of human neutrophils.*** **Biochem J, 1984. 219(1): p. 233-42.**
110. **Goldblatt, D. and A.J. Thrasher,** ***Chronic granulomatous disease.*** **Clin Exp Immunol, 2000. 122(1): p. 1-9.**
111. **Lundqvist, H., et al.,** ***Phorbol myristate acetate-induced NADPH oxidase activity in human neutrophils: only half the story has been told.*** **J Leukoc Biol, 1996. 59(2): p. 270-9.**
112. **Vaissiere, C., V. Le Cabec, and I. Maridonneau-Parini,** ***NADPH oxidase is functionally assembled in specific granules during activation of human neutrophils.*** **J Leukoc Biol, 1999. 65(5): p. 629-34.**
113. **Geiszt, M. and T.L. Leto,** ***The Nox family of NAD(P)H oxidases: host defense and beyond.*** **J Biol Chem, 2004. 279(50): p. 51715-8.**
114. **Geiszt, M.,** ***NADPH oxidases: new kids on the block.*** **Cardiovasc Res, 2006. 71(2): p. 289-99.**
115. **Geiszt, M., K. Lekstrom, and T.L. Leto,** ***Analysis of mRNA transcripts from the NAD(P)H oxidase 1 (Nox1) gene. Evidence against production of the NADPH oxidase homolog-1 short (NOH-1S) transcript variant.*** **J Biol Chem, 2004. 279(49): p. 51661-8.**
116. **Harper, R.W., et al.,** ***A reappraisal of the genomic organization of human Nox1 and its splice variants.*** **Arch Biochem Biophys, 2005. 435(2): p. 323-30.**
117. **Szanto, I., et al.,** ***Expression of NOX1, a superoxide-generating NADPH oxidase, in colon cancer and inflammatory bowel disease.*** **J Pathol, 2005. 207(2): p. 164-76.**
118. **Lassegue, B., et al.,** ***Novel gp91(phox) homologues in vascular smooth muscle cells : nox1 mediates angiotensin II-induced superoxide formation and redox-sensitive signaling pathways.*** **Circ Res, 2001. 88(9): p. 888-94.**
119. **Ago, T., et al.,** ***NAD(P)H oxidases in rat basilar arterial endothelial cells.*** **Stroke, 2005. 36(5): p. 1040-6.**
120. **Kobayashi, S., et al.,** ***Nox1 regulates apoptosis and potentially stimulates branching morphogenesis in sinusoidal endothelial cells.*** **Exp Cell Res, 2004. 300(2): p. 455-62.**
121. **Cui, X.L., et al.,** ***Expression of NADPH oxidase isoform 1 (Nox1) in human placenta: involvement in preeclampsia.*** **Placenta, 2006. 27(4-5): p. 422-31.**
122. **Lee, N.K., et al.,** ***A crucial role for reactive oxygen species in RANKL-induced osteoclast differentiation.*** **Blood, 2005. 106(3): p. 852-9.**
123. **Manea, A., M. Raicu, and M. Simionescu,** ***Expression of functionally phagocyte-type NAD(P)H oxidase in pericytes: effect of angiotensin II and high glucose.*** **Biol Cell, 2005. 97(9): p. 723-34.**
124. **Clark, R.A., T.K. Epperson, and A.J. Valente,** ***Mechanisms of activation of NADPH oxidases.*** **Jpn J Infect Dis, 2004. 57(5): p. S22-3.**
125. **Perner, A., et al.,** ***Superoxide production and expression of NAD(P)H oxidases by transformed and primary human colonic epithelial cells.*** **Gut, 2003. 52(2): p. 231-6.**
126. **Griendling, K.K.,** ***Novel NAD(P)H oxidases in the cardiovascular system.*** **Heart, 2004. 90(5): p. 491-3.**
127. **Salles, N., et al.,** ***Expression of mRNA for ROS-generating NADPH oxidases in the aging stomach.*** **Exp Gerontol, 2005. 40(4): p. 353-7.**

128. **Kawahara, T., et al., *Toll-like receptor 4 regulates gastric pit cell responses to Helicobacter pylori infection.* J Med Invest, 2001. 48(3-4): p. 190-7.**
129. **Kawahara, T., et al., *Type I Helicobacter pylori lipopolysaccharide stimulates toll-like receptor 4 and activates mitogen oxidase 1 in gastric pit cells.* Infect Immun, 2001. 69(7): p. 4382-9.**
130. **Teshima, S., et al., *Regulation of growth and apoptosis of cultured guinea pig gastric mucosal cells by mitogenic oxidase 1.* Am J Physiol Gastrointest Liver Physiol, 2000. 279(6): p. G1169-76.**
131. **Glebov, O.K., et al., *Distinguishing right from left colon by the pattern of gene expression.* Cancer Epidemiol Biomarkers Prev, 2003. 12(8): p. 755-62.**
132. **Ambasta, R.K., et al., *Direct interaction of the novel Nox proteins with p22phox is required for the formation of a functionally active NADPH oxidase.* J Biol Chem, 2004. 279(44): p. 45935-41.**
133. **Kawahara, T., et al., *Point mutations in the proline-rich region of p22phox are dominant inhibitors of Nox1- and Nox2-dependent reactive oxygen generation.* J Biol Chem, 2005. 280(36): p. 31859-69.**
134. **Cheng, G., et al., *Nox1-dependent reactive oxygen generation is regulated by Rac1.* J Biol Chem, 2006. 281(26): p. 17718-26.**
135. **Miyano, K., et al., *Direct involvement of the small GTPase Rac in activation of the superoxide-producing NADPH oxidase Nox1.* J Biol Chem, 2006. 281(31): p. 21857-68.**
136. **Park, H.S., et al., *Sequential activation of phosphatidylinositol 3-kinase, beta Pix, Rac1, and Nox1 in growth factor-induced production of H2O2.* Mol Cell Biol, 2004. 24(10): p. 4384-94.**
137. **Ueyama, T., M. Geiszt, and T.L. Leto, *Involvement of Rac1 in activation of multicomponent Nox1- and Nox3-based NADPH oxidases.* Mol Cell Biol, 2006. 26(6): p. 2160-74.**
138. **Banfi, B., et al., *NOX3, a superoxide-generating NADPH oxidase of the inner ear.* J Biol Chem, 2004. 279(44): p. 46065-72.**
139. **Paffenholz, R., et al., *Vestibular defects in head-tilt mice result from mutations in Nox3, encoding an NADPH oxidase.* Genes Dev, 2004. 18(5): p. 486-91.**
140. **Cheng, G., D. Ritsick, and J.D. Lambeth, *Nox3 regulation by NOXO1, p47phox, and p67phox.* J Biol Chem, 2004. 279(33): p. 34250-5.**
141. **Gorin, Y., et al., *Angiotensin II-induced ERK1/ERK2 activation and protein synthesis are redox-dependent in glomerular mesangial cells.* Biochem J, 2004. 381(Pt 1): p. 231-9.**
142. **Ago, T., et al., *Nox4 as the major catalytic component of an endothelial NAD(P)H oxidase.* Circulation, 2004. 109(2): p. 227-33.**
143. **Kuroda, J., et al., *The superoxide-producing NAD(P)H oxidase Nox4 in the nucleus of human vascular endothelial cells.* Genes Cells, 2005. 10(12): p. 1139-51.**
144. **Yang, S., et al., *A new superoxide-generating oxidase in murine osteoclasts.* J Biol Chem, 2001. 276(8): p. 5452-8.**
145. **Martyn, K.D., et al., *Functional analysis of Nox4 reveals unique characteristics compared to other NADPH oxidases.* Cell Signal, 2006. 18(1): p. 69-82.**

146. **Suliman, H.B., M. Ali, and C.A. Piantadosi,** ***Superoxide dismutase-3 promotes full expression of the EPO response to hypoxia.*** **Blood, 2004. 104(1): p. 43-50.**
147. **Wingler, K., et al.,** ***Upregulation of the vascular NAD(P)H-oxidase isoforms Nox1 and Nox4 by the renin-angiotensin system in vitro and in vivo.*** **Free Radic Biol Med, 2001. 31(11): p. 1456-64.**
148. **Banfi, B., et al.,** ***Mechanism of Ca2+ activation of the NADPH oxidase 5 (NOX5).*** **J Biol Chem, 2004. 279(18): p. 18583-91.**
149. **Dupuy, C., et al.,** ***Purification of a novel flavoprotein involved in the thyroid NADPH oxidase. Cloning of the porcine and human cdnas.*** **J Biol Chem, 1999. 274(52): p. 37265-9.**
150. **Edens, W.A., et al.,** ***Tyrosine cross-linking of extracellular matrix is catalyzed by Duox, a multidomain oxidase/peroxidase with homology to the phagocyte oxidase subunit gp91phox.*** **J Cell Biol, 2001. 154(4): p. 879-91.**
151. **Ha, E.M., et al.,** ***A direct role for dual oxidase in Drosophila gut immunity.*** **Science, 2005. 310(5749): p. 847-50.**
152. **Wong, J.L., R. Creton, and G.M. Wessel,** ***The oxidative burst at fertilization is dependent upon activation of the dual oxidase Udx1.*** **Dev Cell, 2004. 7(6): p. 801-14.**
153. **O'Brien, P.J.,** ***Peroxidases.*** **Chem Biol Interact, 2000. 129(1-2): p. 113-39.**
154. **Geiszt, M., et al.,** ***Dual oxidases represent novel hydrogen peroxide sources supporting mucosal surface host defense.*** **Faseb J, 2003. 17(11): p. 1502-4.**
155. **Dupuy, C., et al.,** ***Ca2+ regulation of thyroid NADPH-dependent H2O2 generation.*** **FEBS Lett, 1988. 233(1): p. 74-8.**
156. **Leseney, A.M., et al.,** ***Biochemical characterization of a Ca2+/NAD(P)H-dependent H2O2 generator in human thyroid tissue.*** **Biochimie, 1999. 81(4): p. 373-80.**
157. **Nakamura, Y., S. Ogihara, and S. Ohtaki,** ***Activation by ATP of calcium-dependent NADPH-oxidase generating hydrogen peroxide in thyroid plasma membranes.*** **J Biochem (Tokyo), 1987. 102(5): p. 1121-32.**
158. **De Deken, X., et al.,** ***Characterization of ThOX proteins as components of the thyroid H(2)O(2)-generating system.*** **Exp Cell Res, 2002. 273(2): p. 187-96.**
159. **Ameziane-El-Hassani, R., et al.,** ***Dual oxidase-2 has an intrinsic Ca2+-dependent H2O2-generating activity.*** **J Biol Chem, 2005. 280(34): p. 30046-54.**
160. **Wang, D., et al.,** ***Identification of a novel partner of duox: EFP1, a thioredoxin-related protein.*** **J Biol Chem, 2005. 280(4): p. 3096-103.**
161. **Fortemaison, N., et al.,** ***Regulation of H2O2 generation in thyroid cells does not involve Rac1 activation.*** **Eur J Endocrinol, 2005. 152(1): p. 127-33.**
162. **Forteza, R., et al.,** ***Regulated hydrogen peroxide production by Duox in human airway epithelial cells.*** **Am J Respir Cell Mol Biol, 2005. 32(5): p. 462-9.**
163. **Schwarzer, C., et al.,** ***NADPH oxidase-dependent acid production in airway epithelial cells.*** **J Biol Chem, 2004. 279(35): p. 36454-61.**
164. **Dupuy, C., et al.,** ***Thyroid oxidase (THOX2) gene expression in the rat thyroid cell line FRTL-5.*** **Biochem Biophys Res Commun, 2000. 277(2): p. 287-92.**
165. **El Hassani, R.A., et al.,** ***Dual oxidase2 is expressed all along the digestive tract.*** **Am J Physiol Gastrointest Liver Physiol, 2005. 288(5): p. G933-42.**

166. **Moreno, J.C., et al.,** ***Inactivating mutations in the gene for thyroid oxidase 2 (THOX2) and congenital hypothyroidism.*** **N Engl J Med, 2002. 347(2): p. 95-102.**
167. **Lutter, R., et al.,** ***Purification and partial characterization of the b-type cytochrome from human polymorphonuclear leukocytes.*** **J Biol Chem, 1985. 260(4): p. 2237-44.**
168. **Pember, S.O., et al.,** ***Cytochrome b558 from (bovine) granulocytes. Partial purification from Triton X-114 extracts and properties of the isolated cytochrome.*** **J Biol Chem, 1984. 259(16): p. 10590-5.**
169. **Parkos, C.A., et al.,** ***Purified cytochrome b from human granulocyte plasma membrane is comprised of two polypeptides with relative molecular weights of 91,000 and 22,000.*** **J Clin Invest, 1987. 80(3): p. 732-42.**
170. **Leto, T.L., A.G. Adams, and I. de Mendez,** ***Assembly of the phagocyte NADPH oxidase: binding of Src homology 3 domains to proline-rich targets.*** **Proc Natl Acad Sci U S A, 1994. 91(22): p. 10650-4.**
171. **Taylor, R.M., et al.,** ***Site-specific inhibitors of NADPH oxidase activity and structural probes of flavocytochrome b: characterization of six monoclonal antibodies to the p22phox subunit.*** **J Immunol, 2004. 173(12): p. 7349-57.**
172. **Dahan, I., et al.,** ***Mapping of functional domains in the p22(phox) subunit of flavocytochrome b(559) participating in the assembly of the NADPH oxidase complex by "peptide walking".*** **J Biol Chem, 2002. 277(10): p. 8421-32.**
173. **Burritt, J.B., et al.,** ***Antibody imprint of a membrane protein surface. Phagocyte flavocytochrome b.*** **J Biol Chem, 1998. 273(38): p. 24847-52.**
174. **Imajoh-Ohmi, S., et al.,** ***Topology of cytochrome b558 in neutrophil membrane analyzed by anti-peptide antibodies and proteolysis.*** **J Biol Chem, 1992. 267(1): p. 180-4.**
175. **Parkos, C.A., et al.,** ***Primary structure and unique expression of the 22-kilodalton light chain of human neutrophil cytochrome b.*** **Proc Natl Acad Sci U S A, 1988. 85(10): p. 3319-23.**
176. **Mollnau, H., et al.,** ***Effects of angiotensin II infusion on the expression and function of NAD(P)H oxidase and components of nitric oxide/cGMP signaling.*** **Circ Res, 2002. 90(4): p. E58-65.**
177. **Etoh, T., et al.,** ***Increased expression of NAD(P)H oxidase subunits, NOX4 and p22phox, in the kidney of streptozotocin-induced diabetic rats and its reversibity by interventive insulin treatment.*** **Diabetologia, 2003. 46(10): p. 1428-37.**
178. **Zalba, G., et al.,** ***Oxidative stress in arterial hypertension: role of NAD(P)H oxidase.*** **Hypertension, 2001. 38(6): p. 1395-9.**
179. **Laude, K., et al.,** ***Hemodynamic and biochemical adaptations to vascular smooth muscle overexpression of p22phox in mice.*** **Am J Physiol Heart Circ Physiol, 2005. 288(1): p. H7-12.**
180. **Ueno, N., et al.,** ***The NADPH oxidase Nox3 constitutively produces superoxide in a p22phox-dependent manner: its regulation by oxidase organizers and activators.*** **J Biol Chem, 2005. 280(24): p. 23328-39.**
181. **DeLeo, F.R., et al.,** ***Mapping sites of interaction of p47-phox and flavocytochrome b with random-sequence peptide phage display libraries.*** **Proc Natl Acad Sci U S A, 1995. 92(15): p. 7110-4.**
182. **Leusen, J.H., et al.,** ***156Pro-->Gln substitution in the light chain of cytochrome b558 of the human NADPH oxidase (p22-phox) leads to***

defective translocation of the cytosolic proteins p47-phox and p67-phox. **J Exp Med, 1994. 180(6): p. 2329-34.**

183. **Leusen, J.H., et al.,** ***Interactions between the cytosolic components p47phox and p67phox of the human neutrophil NADPH oxidase that are not required for activation in the cell-free system.*** **J Biol Chem, 1995. 270(19): p. 11216-21.**
184. **Fantone, J.C. and P.A. Ward,** ***Polymorphonuclear leukocyte-mediated cell and tissue injury: oxygen metabolites and their relations to human disease.*** **Hum Pathol, 1985. 16(10): p. 973-8.**
185. **Heyworth, P.G., et al.,** ***Neutrophil nicotinamide adenine dinucleotide phosphate oxidase assembly. Translocation of p47-phox and p67-phox requires interaction between p47-phox and cytochrome b558.*** **J Clin Invest, 1991. 87(1): p. 352-6.**
186. **Clark, R.A., et al.,** ***Two cytosolic components of the human neutrophil respiratory burst oxidase translocate to the plasma membrane during cell activation.*** **J Clin Invest, 1990. 85(3): p. 714-21.**
187. **Dusi, S., M. Donini, and F. Rossi,** ***Mechanisms of NADPH oxidase activation: translocation of p40phox, Rac1 and Rac2 from the cytosol to the membranes in human neutrophils lacking p47phox or p67phox.*** **Biochem J, 1996. 314 (Pt 2): p. 409-12.**
188. **Uhlinger, D.J., et al.,** ***The respiratory burst oxidase of human neutrophils. Guanine nucleotides and arachidonate regulate the assembly of a multicomponent complex in a semirecombinant cell-free system.*** **J Biol Chem, 1993. 268(12): p. 8624-31.**
189. **de Mendez, I., N. Homayounpour, and T.L. Leto,** ***Specificity of p47phox SH3 domain interactions in NADPH oxidase assembly and activation.*** **Mol Cell Biol, 1997. 17(4): p. 2177-85.**
190. **Lapouge, K., et al.,** ***Architecture of the p40-p47-p67phox complex in the resting state of the NADPH oxidase. A central role for p67phox.*** **J Biol Chem, 2002. 277(12): p. 10121-8.**
191. **Lu, L., M.T. Quinn, and Y. Sun,** ***Oxidative stress in the infarcted heart: role of de novo angiotensin II production.*** **Biochem Biophys Res Commun, 2004. 325(3): p. 943-51.**
192. **Grandvaux, N., et al.,** ***The Ku70 autoantigen interacts with p40phox in B lymphocytes.*** **J Cell Sci, 1999. 112 (Pt 4): p. 503-13.**
193. **Shukla, S., et al.,** ***Identification of non-mitochondrial NADPH oxidase and the spatio-temporal organization of its components in mouse spermatozoa.*** **Biochem Biophys Res Commun, 2005. 331(2): p. 476-83.**
194. **Tejada-Simon, M.V., et al.,** ***Synaptic localization of a functional NADPH oxidase in the mouse hippocampus.*** **Mol Cell Neurosci, 2005. 29(1): p. 97-106.**
195. **Touyz, R.M., et al.,** ***Expression of a functionally active gp91phox-containing neutrophil-type NAD(P)H oxidase in smooth muscle cells from human resistance arteries: regulation by angiotensin II.*** **Circ Res, 2002. 90(11): p. 1205-13.**
196. **Gao, L., et al.,** ***Superoxide mediates sympathoexcitation in heart failure: roles of angiotensin II and NAD(P)H oxidase.*** **Circ Res, 2004. 95(9): p. 937-44.**
197. **Tsunawaki, S., et al.,** ***A novel cytosolic component, p40phox, of respiratory burst oxidase associates with p67phox and is absent in patients with chronic***

granulomatous disease who lack p67phox. **Biochem Biophys Res Commun, 1994. 199(3): p. 1378-87.**

198. Sathyamoorthy, M., et al., ***p40(phox) down-regulates NADPH oxidase activity through interactions with its SH3 domain.*** **J Biol Chem, 1997. 272(14): p. 9141-6.**

199. Kuribayashi, F., et al., ***The adaptor protein p40(phox) as a positive regulator of the superoxide-producing phagocyte oxidase.*** **Embo J, 2002. 21(23): p. 6312-20.**

200. Tsunawaki, S., et al., ***Involvement of p40phox in activation of phagocyte NADPH oxidase through association of its carboxyl-terminal, but not its amino-terminal, with p67phox.*** **J Exp Med, 1996. 184(3): p. 893-902.**

201. Massenet, C., et al., ***Effects of p47phox C terminus phosphorylations on binding interactions with p40phox and p67phox. Structural and functional comparison of p40phox and p67phox SH3 domains.*** **J Biol Chem, 2005. 280(14): p. 13752-61.**

202. Decoursey, T.E. and E. Ligeti, ***Regulation and termination of NADPH oxidase activity.*** **Cell Mol Life Sci, 2005. 62(19-20): p. 2173-93.**

203. Dinauer, M.C., ***Regulation of neutrophil function by Rac GTPases.*** **Curr Opin Hematol, 2003. 10(1): p. 8-15.**

204. Sarfstein, R., et al., ***Dual role of Rac in the assembly of NADPH oxidase, tethering to the membrane and activation of p67phox: a study based on mutagenesis of p67phox-Rac1 chimeras.*** **J Biol Chem, 2004. 279(16): p. 16007-16.**

205. Wersall, J., ***Studies on the structure and innervation of the sensory epithelium of the cristae ampulares in the guinea pig; a light and electron microscopic investigation.*** **Acta Otolaryngol Suppl, 1956. 126: p. 1-85.**

206. Cathers, I., B.L. Day, and R.C. Fitzpatrick, ***Otolith and canal reflexes in human standing.*** **J Physiol, 2005. 563(Pt 1): p. 229-34.**

207. Day, B.L. and R.C. Fitzpatrick, ***The vestibular system.*** **Curr Biol, 2005. 15(15): p. R583-6.**

208. Lim, D.J., ***Morphogenesis and malformation of otoconia: a review.*** **Birth Defects Orig Artic Ser, 1980. 16(4): p. 111-46.**

209. Mann, S., et al., ***The ultrastructure of the calcium carbonate balance organs of the inner ear: an ultra-high resolution electron microscopy study.*** **Proc R Soc Lond B Biol Sci, 1983. 218(1213): p. 415-24.**

210. Ross, M.D. and K.G. Pote, ***Some properties of otoconia.*** **Philos Trans R Soc Lond B Biol Sci, 1984. 304(1121): p. 445-52.**

211. Ornitz, D.M., et al., ***Otoconial agenesis in tilted mutant mice.*** **Hear Res, 1998. 122(1-2): p. 60-70.**

212. Wang, Y., et al., ***Otoconin-90, the mammalian otoconial matrix protein, contains two domains of homology to secretory phospholipase A2.*** **Proc Natl Acad Sci U S A, 1998. 95(26): p. 15345-50.**

213. Verpy, E., M. Leibovici, and C. Petit, ***Characterization of otoconin-95, the major protein of murine otoconia, provides insights into the formation of these inner ear biominerals.*** **Proc Natl Acad Sci U S A, 1999. 96(2): p. 529-34.**

214. Thalmann, R., et al., ***Development and maintenance of otoconia: biochemical considerations.*** **Ann N Y Acad Sci, 2001. 942: p. 162-78.**

215. Cheng, G., Ritsick, D., Lambeth, J.D., ***Nox3 regulation by NOXO1, p47phox, and p67phox.*** **J. Biol. Chem., 2004. 279(33): p. 34250-34255.**

216. **Stec, D.E., Morimoto, S., Sigmund, C.D.,** ***Vectors for high-level expression of cDNAs controlled by tissue-specific promoters in transgenic mice.*** **Biotechniques., 2001. 31(2): p. 256-258.**

217. **Zheng, Q.Y., K.R. Johnson, and L.C. Erway,** ***Assessment of hearing in 80 inbred strains of mice by ABR threshold analyses.*** **Hear Res, 1999. 130(1-2): p. 94-107.**

218. **Karnowski, M., J.,** ***A formaldehyde-glutaraldehyde fixative of high osmolarity for use in electron microscopy.*** **J. Cell Biol., 1965. 27: p. 137A–138A.**

219. **Pozzo-Miller, L., D., Pivovarova, N., B., Connor, J., A., Reese, T., S., Andrews, S., B.,** ***Correlated measurements of free and total intracellular calcium concentration in central nervous system neurons.*** **Microsc. Res. Tech., 1999. 46(6): p. 370-379.**

220. **Osoegawa, K., et al.,** ***Construction of bacterial artificial chromosome (BAC/PAC) libraries.*** **Curr Protoc Hum Genet, 2001. Chapter 5: p. Unit 5 15.**

221. **Anner, R.M., U.E. Nydegger, and P.A. Niescher,** ***[Nitro-blue tetrazolium (NBT) test in the diagnosis of inflammatory diseases].*** **Ther Umsch, 1971. 28(9): p. 601-5.**

222. **Gagnon, L., Bosom, K., Johnson, K.,** ***A new spontaneous mutation on Chromosome 17 in the mouse named head slant (hslt).*** **MGI Direct Data Submission (http://www.jax.org/mmr/hslt.html), 2003.**

223. **Anniko, M.,** ***Development of otoconia.*** **Am. J. Otolaryngol., 1980. 1(5): p. 400-410.**

224. **Sauer, G., Richter, C.P., Klinke, R.,** ***Sodium, potassium, chloride and calcium concentrations measured in pigeon perilymph and endolymph.*** **Hear. Res., 1999. 129(1-2): p. 1-6.**

225. **Anniko, M., Wroblewski, R.,** ***The energy dispersive X-ray microanalysis technique in the study of fluids and tissues of the brain and the inner ear.*** **Histochemistry, 1981. 72(2): p. 255-268.**

226. **Suzuki, H., Ikeda, K., Takasaka, T.,** ***Biological characteristics of the globular substance in the otoconial membrane of the guinea pig.*** **Hear. Res., 1995. 90(1-2): p. 212-218.**

227. **Legan, P.K., Rau, A., Keen, J.N., Richardson, G.P.,** ***The mouse tectorins. Modular matrix proteins of the inner ear homologous to components of the sperm-egg adhesion system.*** **J. Biol. Chem., 1997. 272(13): p. 8791-8801.**

228. **Cohen-Salmon, M., El-Amraoui, A., Leibovici, M., Petit, C.,** ***Otogelin: a glycoprotein specific to the acellular membranes of the inner ear.*** **Proc. Natl. Acad. Sci. U S A., 1997. 94(26): p. 14450-14455.**

229. **Simmler, M.C., Cohen-Salmon, M., El-Amraoui, A., Guillaud, L., Benichou, J.C., Petit, C., Panthier, J.J.,** ***Targeted disruption of otog results in deafness and severe imbalance.*** **Nat. Genet., 2000. 24(2): p. 139-143.**

230. **Sevanian, A., Ursini, F.,** ***Lipid peroxidation in membranes and low-density lipoproteins: similarities and differences.*** **Free Radic. Biol. Med., 2000. 29(3-4): p. 306-311.**

231. **Akiba, S., Nagatomo, R., Hayama, M., Sato, T.,** ***Lipid peroxide overcomes the inability of platelet secretory phospholipase A2 to hydrolyze membrane phospholipids in rabbit platelets.*** **J. Biochem., 1997. 122(4): p. 859-864.**

232. **Balazy, M. and S. Nigam,** ***Aging, lipid modifications and phospholipases--new concepts.*** **Ageing Res Rev, 2003. 2(2): p. 191-209.**

233. **Buege, J.A., Aust, S.D., *Lactoperoxidase-catalyzed lipid peroxidation of microsomal and artificial membranes.* Biochim. Biophys. Acta., 1976. 444(1): p. 192-201.**

234. **Koedood, M., Fichtel, A., Meier, P., Mitchell, P.J., *Human cytomegalovirus (HCMV) immediate-early enhancer/promoter specificity during embryogenesis defines target tissues of congenital HCMV infection.* J. Virol., 1995. 69(4): p. 2194-2207.**

235. **Manfra, D.J., Chen, S.C., Yang, T.Y., Sullivan, L., Wiekowski, M.T., Abbondanzo, S., Vassileva, G., Zalamea, P., Cook, D.N., Lira, S.A., *Leukocytes expressing green fluorescent protein as novel reagents for adoptive cell transfer and bone marrow transplantation studies.* Am. J. Pathol., 2001. 158(1): p. 41-47.**

236. **Geiszt, M., Lekstrom, K., Witta, J., Leto, T.L., *Proteins homologous to p47phox and p67phox support superoxide production by NAD(P)H oxidase 1 in colon epithelial cells.* J Biol Chem., 2003. 278(22): p. 20006-20012.**

237. **Kawahara, T., Ritsick, D., Cheng, G., Lambeth, J.D., *Point mutations in the proline-rich region of p22phox are dominant inhibitors of Nox1- and Nox2-dependent reactive oxygen generation.* J. Biol. Chem., 2005. 280(36): p. 31859-31869.**

238. **Vilhardt, F., et al., *The HIV-1 Nef protein and phagocyte NADPH oxidase activation.* J Biol Chem, 2002. 277(44): p. 42136-43.**

239. **Reeves, E.P., et al., *Killing activity of neutrophils is mediated through activation of proteases by K+ flux.* Nature, 2002. 416(6878): p. 291-7.**

240. **Banfi, B., et al., *A novel H(+) conductance in eosinophils: unique characteristics and absence in chronic granulomatous disease.* J. Exp. Med., 1999. 190(2): p. 183-194.**

241. **Lomonte, B., Angulo, Y., Calderon, L., *An overview of lysine-49 phospholipase A2 myotoxins from crotalid snake venoms and their structural determinants of myotoxic action.* Toxicon, 2003. 42(8): p. 885-901.**

10. Publications

Publications related to the thesis

Péter J. Kiss, Judit Knisz, Yuzhou Zhang, Jonas Baltrusaitis, Curt D. Sigmund, Ruediger Thalmann, Richard J.H. Smith, Elisabeth Verpy, Botond Bánfi. Inactivation of NADPH oxidase organizer 1 results in severe imbalance *Curr Biol.* 2006 Jan 24;16(2):208-13. (IF: 11.033)

Publications not related to the thesis

Stoltz DA, Ozer EA, Taft PJ, Barry M, Liu L, **Kiss PJ**, Moninger TO, Parsek MR, Zabner J. Drosophila are protected from Pseudomonas aeruginosa lethality by transgenic expression of paraoxonase-1. *J Clin Invest.* 2008 Sep 118(9):3123-31. (IF: 16.915)

Szanto I, Rubbia-Brandt L, **Kiss P**, Steger K, Banfi B, Kovari E, Herrmann F, Hadengue A, Krause KH.Expression of NOX1, a superoxide-generating NADPH oxidase, in colon cancer and inflammatory bowel disease. J Pathol. 2005 Oct;207(2):164-76. (IF: 6.213)

Gascon E, Vutskits L, Zhang H, Barral-Moran MJ, **Kiss PJ**, Mas C, Kiss JZ. Sequential activation of p75 and TrkB is involved in dendritic development of subventricular zone-derived neuronal progenitors in vitro. Eur J Neurosci. 2005 Jan;21(1):69-80 (IF: 3.949)

11. Acknowledgements

I thank for my mentors and teachers who taught me techniques, scientific thinking, and helped me becoming a scientist: Drs. Botond Bánfi, Ildikó Szántó, József Kiss, Karl-Heinz Krause, Bill Naussef, Kerepesi Ildikó and Joseph Zabner.

Special thanks to my wife, Judit Knisz, who has helped me through difficult times and always been supporting me. I thank her for the great contribution to the presented work and for critical reading of the manuscript.

I would also like to thank Dr. Gábor Petheõ and Dr. Kate Excoffon for critical reading of the manuscript and for Katherine S. Walters for assistance in Microscopy.

I am thankful for friends in Iowa, especially the Agrawal family, as well as my family and friends in Hungary who have always encouraged and supported me.